Doctoral Dissertation

Pain Facial Expression for Patient Robot based on

Musculoskeletal Pain Inference

September 2021

Doctoral Program in

Advanced Information Science and Engineering

Graduate School of Information Science and Engineering

Ritsumeikan University

LEE Miran

Doctoral Dissertation Reviewed
by Ritsumeikan University

Pain Facial Expression for Patient Robot based on
Musculoskeletal Pain Inference
（筋肉関節痛の推論に基づく患者ロボットの疼痛表現）

September 2021
２０２１年９月

Doctoral Program in Advanced Information Science and Engineering
Graduate School of Information Science and Engineering
Ritsumeikan University
立命館大学大学院情報理工学研究科
情報理工学専攻博士課程後期課程

LEE Miran

リ ミラン

Supervisor: Professor LEE Joo-Ho
研究指導教員: 李 周浩教授

Declaration

I, Miran Lee, declare that I have developed and written the enclosed dissertation entirely by myself and have not used sources, means, or materials without declaration in the text. Any thoughts from others or literal quotations are marked. The thesis has not been used in the same or similar version to achieve academic performance or is being published elsewhere.

- -

Miran Lee

September, 2021

Acknowledgments

Abstract

Pain Facial Expression for Patient Robot based on Musculoskeletal Pain Inference

Miran Lee

Graduate Shool of Information Science and Engineering

Ritsumeikan University

Care and nursing training (CNT) is to develop the ability to effectively respond to the needs by investigating patients' requests and improving trainee' care skills in a caring environment. With the advances in medical and health care systems, it is essential in care and nursing education to train professionals who can competently handle various situations and help the needs of individuals with diseases and care recipients' quality of life in homes, hospitals, and facilities. Although conventional CNT program has been conducted based on videos, books, and role-playing, the best way is to practice on an actual human. However, it is challenging to recruit patients for training continually, and the patients may have experienced fatigue or boredom with iterative testing. As an alternative approach, a patient robot that reproduces various human diseases and provides feedback to trainees has been introduced.

This dissertation introduces a patient robot that can express facial emotions or feelings of pain states like an actual human does in joint care education. The primary three objectives for the proposed patient robot-based care training system are (a) to understand better the effects of care skills by deeper interpretation of the results based on quantitative data obtained from the robot for providing an effective patient robot-based care education system, (b) to infer the pain felt by the patient robot and intuitively provide the trainee with the patient's pain state, and (c) to provide the facial expression-based visual feedback method of the patient robot for care training.

The first objective is to develop the development of the patient robot's upper limb containing a shoulder and an elbow complex. Experts who have experienced for many years in the medical field and students participate in the data acquisition process to collect quantitative data of the patient robot by performing care tasks as range of motion (ROM) exercises. Based on the robot's sensor data, the results are analyzed and interpreted through various perspectives to discuss the effectiveness and feasibility of the patient robot. The second objective is to improve the way of interaction and feedback in which the patient robot provides the current pain state to the trainees by proposing the method for inferring the pain state of the patient robot. The conventional post-analysis is proper to interpret the analysis of parameters associated with the robot's pain and use when investigating the effect of parameters on care training. However, there are limitations in quantitatively evaluating their care skill and automatically recognizing the robot's pain during care education. To overcome the issues, the method of pain inference is suggested. The third objective is to develop a robot's emotion and pain expression by developing a robot's avatar in joint care education. For this objective, tracking the user's emotions in real-time based on the face image is proposed. Consequently, the robot's avatar can express a continuous mood transition and the pain state to the trainees during the care training. The findings of this study are anticipated to provide a new path for the development of advanced patient robots used in the care training environment by reproducing the symptoms of various muscle and joint diseases, such as paralysis, contracture, and muscle weakness. Further, the robot's emotion and pain expression techniques are expected to provide efficient feedback on care training in terms of human-robot interactions.

Table of Contents

List of abbreviations

ANOVA   Analysis of variance.

AU   Action unit.

BF   Big five factors.

CEI   Current emotional intensity.

CNT   Care and nursing training.

ConvNet   Convolutional neural network.

DOF   Degree of freedom.

EEF   Extension and flexion of the elbow complex.

FACS   Facial Action Coding System.

FIS   Fuzzy inference system.

FLPI   Fuzzy logic-based pain intensity.

FLPI-EROM   Fuzzy logic-based pain inference of the ROM exercise of the elbow joint.

FLPI-SROM   Fuzzy logic-based pain inference of the ROM exercise of the shoulder complex joint.

FV   Feature vector.

GH   Glenohumeral joint.

HBPD   Human body properties database.

HPS   Human patient simulation.

IRB   Institutional review board.

M	Mean.
MAE	Mean absolute error.
OECD	Organization for Economic Cooperation and Development.
PCC	Pearson correlation coefficient.
PG	Pain group.
PR	Precision.
PRCT	Patient robot for care training.
PSEN	Pain sensitivity.
PSMA	Pressure signal magnitude of area.
PSPI	Prkachin and Solomon pain intensity.
RC	Recall.
REI	Robot's emotional intensity.
REIP	Robot's personality-based robotic emotional intensity.
RMT	Robot's mood transition.
ROA	Range of angle.
ROI	Range of interest.
ROM	Range of motion.
ROT	Range of torque.
RP	Research problem.
RU-FEmoI2021	Ritsumeikan University-Facial emotional intensity database.
RU-PITENS	Ritsumeikan University-Pain intensity using transcutaneous electrical nerve stimulation database.
SC	Sternoclavicular joint.

SD	Standard deviation.
SED	Elevation and depression of the shoulder complex.
SEF	Extension and flexion of the shoulder complex.
SLM	Lateral and medial rotation of the shoulder complex.
SNPI	Siamese network-based pain intensity.
SPS	Subjective pain score.
TENS	Transcutaneous electrical nerve stimulation.
VAS	Visual analogue scale.

List of Figures

xvii

List of tables

xx

Chapter 1

Introduction

This dissertation considers care training systems for effectively improving care skills during care education and training. The ultimate goal is to make effective care education that allows users to react immediately to robots' actions by continually interacting. This thesis achieves patient robots' development, prediction of pain intensity of robot, tracking of robot's mood transition, and providing feedback that includes the robot's current pain and emotional state to caregivers.

This Chapter describes the essential background, objective, and research problems of the proposed system in this dissertation and reports the contributions to the research findings in detail.

1.1 Background

1.1.1 Care and nursing training

A caregiver is an expert who provides medical treatment or non-medical care to improve care recipients' quality of life in homes, hospitals, and facilities. The role of the caregiver is to support appropriate care and nursing by constantly interacting with the care recipient and helping care recipients maintain a good life by providing treatment methods to perform various activities in their daily lives thoroughly. Care recipients who need the help of a professional caregiver such as a nurse or therapist due to an accident, illness, or aging, can be divided into three main groups: 1) elderly, 2) disabled, and 3) patient, depending on the needs and purpose of care and nursing skills.

1
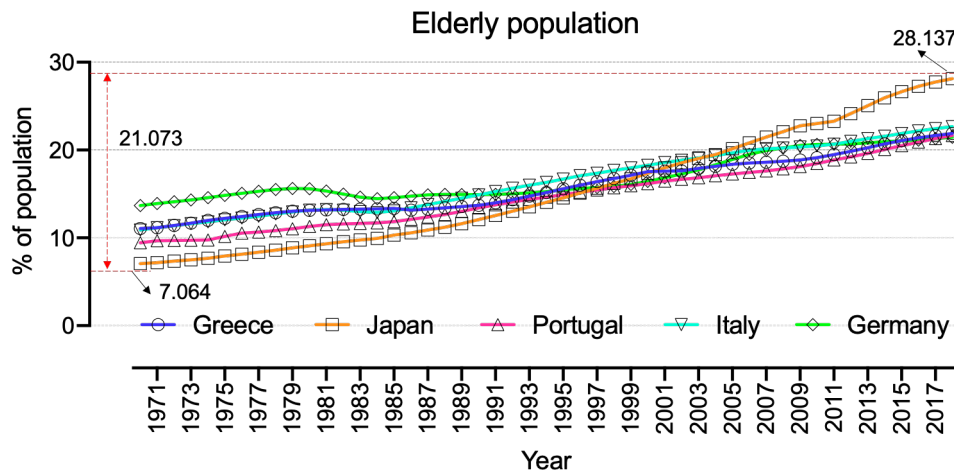
Figure 1.1. Demographic indicators of the elderly population of major countries (Greece, Japan, Portugal, Italy, and Germany) provided by the Organization for Economic Cooperation and Development (OECD) [1]. The elderly population is defined as people aged 65 and over.

- Elderly: According to the Organization for Economic Cooperation and Development (OECD) report, the population of older people in Japan was 12.05% in 1990 and more than doubled to 25.06% in 2013 as shown in **Fig. 1.1** [1]. In this aging society, the role of caregivers becomes crucial, as most older people need routine help daily due to their reduced functional and cognitive capabilities [2]. The caregivers must be trained in an appropriate and accurate training environment to acquire proficient skills to care for the elderly to ensure the comfort and safety of the elderly. Further, the caregivers should continually train their ability to deal with the limited range of joints and muscles' movement and help with stretching exercises periodically to prevent muscle weakness, contracture, and stiffness for the elderly in daily life.

- Disabled: Since disabled individuals have different challenges and needs, such as moving, washing, and cooking, it is necessary to maintain a dignified life based on the support of appropriate care and nursing and independently satisfy various daily activities.

- Patient: Communication with patients is one of the most critical factors in care

and nursing [3]. The nurse needs to resolve the patient's illness based on suitable treatment methods and provide evaluation and support for treatment to establish a positive interaction with the patient. Therefore, nursing for continuous treatment evaluation is also an essential role in terms of patient care.

In terms of various care and nursing environments, an outstanding caregiver must have not only competent skills to provide adequate care and support but also ancillary qualifications such as reliability [4], stability [5], optimism [4], and communication [4, 6] with care recipients as follows:

- Reliability: Skilled caregivers must increase the reliability of their skills by empirically acquiring the required skills of treatment and care.

- Stability: Stable posture and facial expression can reassure the patient and create a comfortable environment when constantly communicating with the patient.

- Optimism: Caregiver with an optimistic disposition can positively change the depression or low moods and anxious psychology of a care recipient.

- Communication: Care recipients may experience pain or stress in care or nursing environments, and caregivers must interact with them based on communication.

To achieve these abilities and qualities, experts or students in care and nursing need to learn and train to reach their superior skills consistently. Care and nursing training (CNT) is to develop the ability necessary to effectively respond to the needs by investigating patients' requests and improving caregivers' skills in a caring environment. In CNT, however, the principal issue is the risk of injury to the subjects during training due to a trainee's ineptitude. Therefore, it is necessary to train experts who can competently manage various situations and meet the needs of individuals with diseases [7] according to medical and healthcare systems' advances.

1.1.2 Human patient simulation

For CNT, students or novices who wish to become professional caregivers or therapists can accumulate theoretical knowledge through the traditional methods (watching videos and reading books) and the empirical methods for hands-on practice as human patient simulation (HPS) as shown in **Fig. 1.2**. HPS can be divided into three areas, such as role-playing, stationary human mannequin, and patient robot, and the definitions and pros and cons can be described as follows:

- Role-playing: Role acting is a method of asking a nursing college student or subjects familiar with the target patient's symptoms to act as a patient. The role-playing method, however, is ineffective because a healthy person cannot accurately simulate a patient's actions suffering from declining muscle strength and paralysis [8].

- Stationary human mannequin: In the late 1950s, a life-sized prototype mannequin was utilized to evaluate the skills of the physical assessment of student nurses [9]. Since then, stationary mannequins are frequently used for training in clinical examinations (e.g., blood pressure measurement, diagnosis using a stethoscope) and intravenous injections. However, there is a limitation in that trainees cannot receive feedback after CNT because the conventional method of HPS, such as stationary mannequins, imitate care-receiver movements or specific diseases and do not contain interaction technology.

- Patient robot: A patient robot is a human-like mannequin (or tool) that effectively provides CNT for gaining skills based on the interaction between humans and the robot. Since it is difficult for student nurses to have opportunities to train care and nursing for real-patient, a patient robot has the robust advantage of benefit from the teaching and learning of their care and nursing skills in a controlled environment [10].

To summary this Section, although there are various suitable methods for using HPS depending on the purpose and target of CNT, the importance of research related to feedback on HPS has been increasing because effective methods for assessing CNT performance, including caregiver and care recipients interactions, are not well defined, and the development of more advanced HPS is required.

Figure 1.2. Different methods for care and nursing training (CNT); textbook of nursing [11], carer's book [12], video [13], role-playing [14], virtual reality (VR) [15], medical mannequin [16], robot in patient transfer [8], and patient robot [17].

1.2 Statement of problem

In CNT, most students aspiring to be caregivers, nurses, or therapists are provided an opportunity for training at the school or institute for a fixed training period. Although they gain experience through conventional methods such as watching videos, reading books, practicing with simulated subjects, the most recommended training method involves practicing on an actual human. However, it is challenging to continually recruit patients for training with ethical and safety concerns in care and nursing methods, and the care-receiver in the CNT program experiences fatigue or boredom with iterative testing. To resolve these concerns of conventional care and nursing education systems, developing a human patient simulation (HPS) for CNT has been inevitable.
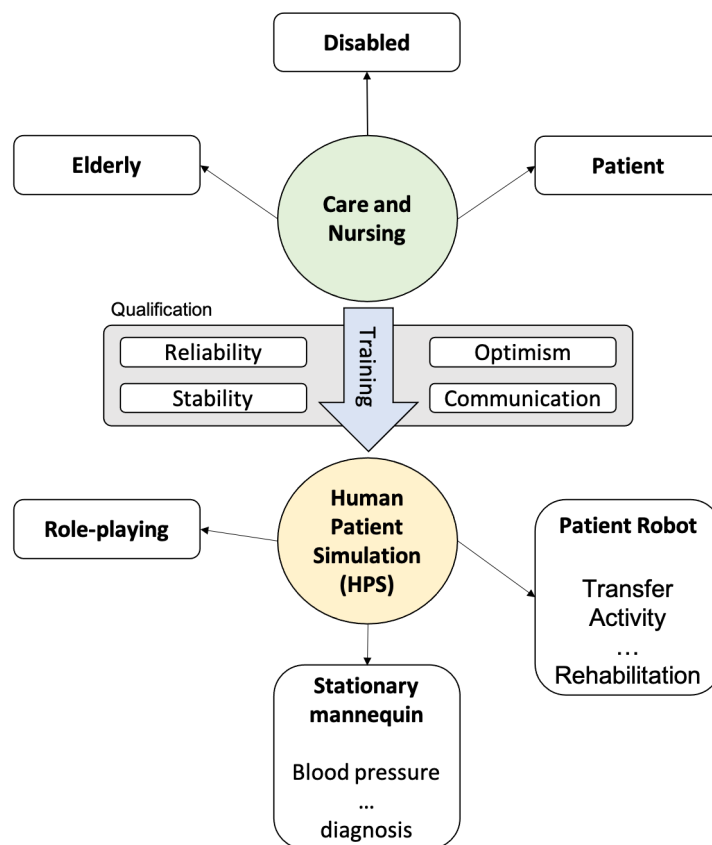
Figure 1.3. Conceptual and motivational mind map to derive the problem's statement in this work.

Fig. 1.3 shows the conceptual and motivational mind map to derive the problem's statement in this dissertation. As explained in Section 1.1.2, HPS can be mainly divided into role-playing, stationary mannequin, and patient robot. One of the main limitations of a stationary mannequin is its insufficient effectiveness in enhancing the care training performance because it is unable to record quantitative data on movements, such as the joint angle, force, speed, duration, and pressure value; thus, evaluating the efficacy of care education for trainees becomes difficult. Besides, the role-playing method that cannot satisfy excellent feedback is ineffective because a healthy person cannot accurately simulate a patient's actions suffering from declining muscle strength and paralysis [8]. On the other hand, the patient robot can be used not only for caregivers to train care and nursing but for therapists to rehabilitate patients with the disease, which are considered helpful in improving their skills, and many studies have been introduced recently [18, 19, 20, 21, 22, 23]. Although a lot of research has been proposed to develop patient robots for various purposes, there remains a need for research to reproduce specific diseases in patients. In particular, since patient robots for CNT reproduce various tasks such as transferring, rehabilitation, and diagnosis, the patient robots that respond to specific tasks must be continuously developed. Also, patient robots have been developed to speak, hear, and breathe and respond actively and passively to joint movements and reproduce symptoms to simulate various situations and activities in humans to help train students [24]. However, it is unclear to get feedback on how well students performed their tasks from the robot's emotion during training. Therefore, a more advanced HPS is required to express current emotions or feelings of pain like a human through text-, alarm-, voice-, and visual-based methods for interaction between users and robots.

Keeping in mind the aforementioned issues and motivation, this dissertation deals with the development of a patient robot that reproduces the patient-specific problematic joint for effectively improving the skills of caregivers and the care training system based on feedback that contains robot's pain and emotional expression for supporting the robot.

7

1.3 Aims and objectives

1.3.1 Aims

To achieve the advanced HPS in CNT, this dissertation introduces the patient robot for care training assistant to reproduce the patient with specific musculoskeletal symptoms. As described above, the advanced feedback system for care training is a significant issue for the proposed care training system. Therefore, this dissertation proposes a patient robot that can express emotions and pain like humans and studies a visual feedback method that allows the user to respond immediately to the robot's emotion and pain state in care training. Furthermore, the proposed integration system consists of several modules such as the care quantitative score estimator, user's facial expression recognizer, patient robot's avatar generator, and provider of the facial expression with pain and emotion is crucial for the development of the proposed system.

The primary aims of this dissertation are (a) to understand better the effects of care skills by deeper interpretation of the results based on quantitative data obtained from the robot for providing an effective patient robot-based care education system, (b) to infer the pain felt by the patient robot and intuitively provide the trainee with the patient's pain state, and (c) provide a novel approach to the facial expression-based visual feedback method of the patient robot for care training to improve the interaction skill of the caregivers.

1.3.2 Objectives

To accomplish the three principal aims of this work, the specific objectives must be attained as follows, and more detailed objectives are specifically addressed in each Chapter.

- To develop an upper limb robot for care education consisting of the shoulder complex and elbow joint.

- To develop a graph-based system for monitoring care training in real-time.

- To reproduce the patient-specific problematic joint using a developed robot.

- To conduct four kinds of ROM exercises (extension and flexion of shoulder complex joint, elevation and depression of shoulder complex joint, lateral and medial rotation of shoulder complex joint, and extension and flexion of elbow joint) using a care assistant robot.

- To evaluate the feasibility of care training assistant robot and monitoring program.

- To investigate the significant differences in care training between students and experts and the effects of continuous and repetitive care education using robots.

- To generate 3D avatars with pain expression by building the database including facial images through pain stimulus expression using transcutaneous electrical nerve stimulation (TENS).

- To develop visual-based feedback of robot based on robotic emotional transition method using modules of care training ability and interaction skill in CNT.

1.3.3 Main research problems

This Section presents the research problems (RPs) to be solved as follows according to the research objectives described above as follow:

- Does the proposed system lead to a more significant effect in the final trial than the initial trial in the care education using robots for users?

- Does the proposed system prove a significant difference in care skills between experts and novices in care education using a robot?

- Do experts with many years of experience participate in care education in the same manner and behavior?

- Do experts differ in quantitative performances when performing the same type of care education (exercise)?

- Does the proposed method provide an assessment of how well the user performs care training according to the guidelines of care in the assessment aftercare training?

- Does the proposed method provide feedback to the user on how well the interaction between the user and robot is performing?

This dissertation describes the proposed system modules by analyzing and interpreting the results for modules' performance and feasibility to achieve the research purposes. In the following Chapters, the specific research problems are suggested, and the observations obtained while solving RPs are presented.

1.4   Statement of contributions

This Chapter describes the contributions of the work. The specific assessment of contributions achieved from the results are described in Chapter 7.

- The proposed patient robot has been proven to potentially improve caregivers' care skills by conducting experiments on ROM exercises in a group of experts and students.

- The results of the study confirmed the feasibility of utilizing the patient robot with pain expression for care training, and it is concluded that the proposed approach may be used to improve care and nursing skills upon further research.

- The proposed patient robot that can effectively improve care skills is proposed, using the robot that reproduces a subject with musculoskeletal disorders, providing more functions than existing methods such as books, videos, and medical mannequins.

- The proposed visual feedback method providing the robot's pain and emotional state expression can help to improve the interacting skills of caregivers.

- The proposed robot's pain and emotion expression system allows the user to respond more immediately to the robot's emotional state or pain than the previous graph-based feedback method.

To summarize, this Chapter outlined the fundamental background related to CNT and the patient robot to improve understanding of the purpose of this work. The paper's main purpose provides a deeper understanding and results in the analysis of the mechanism of the robot for care training to improve the skills of the caregiver effectively and propose a novel approach to the visual feedback method that provide the robot's pain and emotion expression. The dissertation's detailed contributions are explained in detail from the subsequent Chapters by proposing a care training system.

1.5 Organization

This dissertation is organized as follows (**Fig. 1.4**). The literature review works on the human patient simulator and feedback method for care training is done in Chapter 2. To propose the visual-based feedback for care training using that patient robot, the method to develop the patient robot and to reproduce the musculoskeletal problematic symptoms is presented in Chapter 3. Chapter 4 describes the pain inference and expression of patient robot, and in Chapter 5, the robotic emotion generation method for robot's current emotional expression is detailed. Chapter 6 presents an integration system to the care training feedback system that provides an avatar of the patient robot. Finally, some concluding remarks of this dissertation are addressed with future work in Chapter 7.
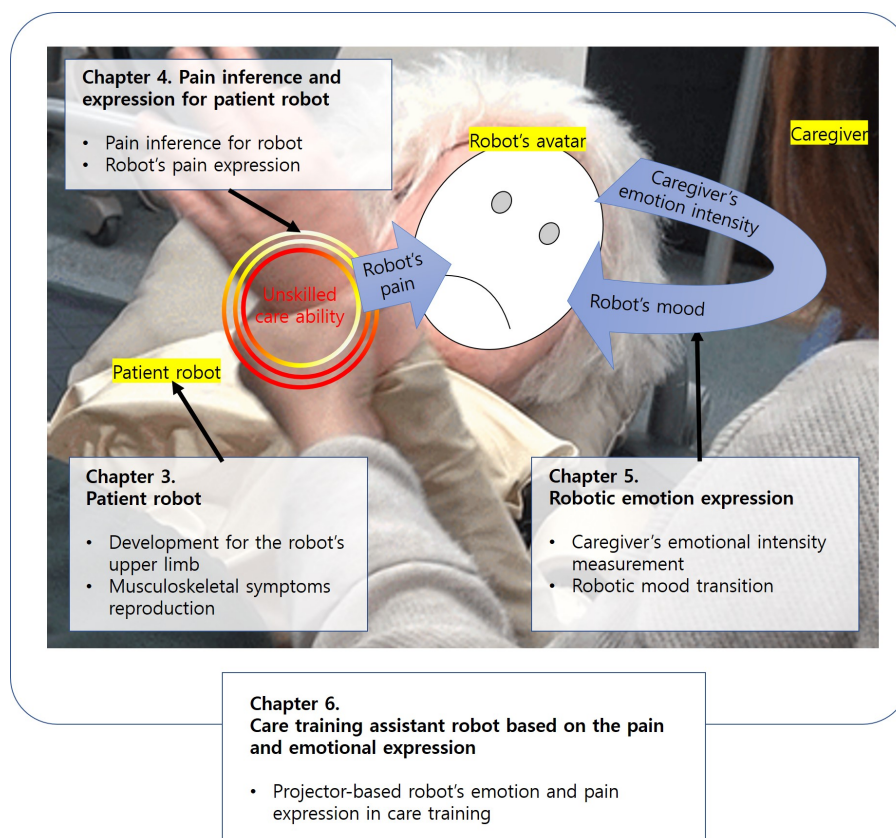
Figure 1.4. A brief summary of the organization of the thesis.

Chapter 2

Literature review

This Chapter's objective is to review the accurate and comprehensive research literature on patient robots, which is the main theme of this dissertation. The literature review of this Chapter will be essential findings to form the fundamental background and motivation for the proposed method in the following chapters and will be a detailed knowledge of the materials for the proposed method.

2.1 Patient robot

A patient robot, computer-controlled patient simulator, was first introduced to augment resident education in the medical field in 1969 [25, 26]. The patient robot presented by Denso and Abrahamson [25, 26] proved that the robot was competent at acquiring skills for anesthesia training through subjective performance improvement. In universities and research institutions, patient robots are extended to demonstrate the various fields for the students' training [27, 28] and are considered helpful in improving the students' skills since the introduction of patient robots.

2.1.1 Patient robot for medical training

Patient robots have been developing according to the purposes they are used, such as surgery, anesthesia, nursing, and care. Wang *et al*. [20] proposed a robot containing arm joints for neurologic examination training to enhance the medical staff's ability. Kitgawa *et al*. [22] presented a human-like patient robot that can express emotions to facilitate training in administering injections. In addition, Takanobu *et al*. [29] proposed the dental patient robot with questionnaire assessment, and Noh *et*

al. [30] presented the WKA-1R robot assisted for evaluating quantitative assessment of airway management. Although robots are used for surgery or clinical diagnosis training since the hands move freely by various tools with both hands, the interaction between the hands and robots or surgical equipment is excessively entangled [31] in surgery; the surgical training system has been developing through virtual and augmented reality [15, 31, 32]. In terms of CNT using a patient robot, however, a training conducts actively or passively movement by applying physical force, such as rehabilitation or regular stretching. A robot for CNT, therefore, that produces sensor data such as joint angle, resistance torque, and pressure may be more suitable than an educational system based on virtual reality or augmented reality.

2.1.2 Patient robot for care and nursing training

Patient robot for care and nursing training (PRCT) can be used for training and improving care ability in interactions with patients or care-receivers, such as treatment, nursing, bathing, transferring, and rehabilitation. One of the critical challenges of using the PRCT in daily life is patient transfer, and the other is rehabilitation. For patient transfer, caregivers commonly perform a task in hospitals, vehicles, and homes to move patients with mobility problems or who need a wheelchair [8]. Patient transfer's complicated tasks include parking a wheelchair, mutual hugging, standing up, pivot turning and sitting down in a wheelchair. As a training system for these tasks, Huang *et al*. [8, 33, 34] proposed the patient robot for transfer and investigate the effect of practice on training skills through robot patient. Besides, PRCT has been proposed to assist patients in sit-to-stand postures by Lin *et al*. [35], and many studies involving training systems for daily life activities using patient robots have been achieving notable outcomes.

In the case of rehabilitation, patients with musculoskeletal disorders may experience the limited movement of muscles and joints due to symptoms such as stiffness, contraction, or weakness of muscles. Thus, caregivers or therapists must periodically ask patients to perform the rehabilitation. The caregivers must practice sufficiently in

14

advance so that they do not stress the joints or skin of a patient with musculoskeletal disorders when performing care or treatment because trainees tend to apply unnecessary force to the joint when doing rehabilitation or stretching for patients. Mouri *et al.* [19] developed the robot hand with disability (contracture) for rehabilitation therapist training by using a distributed tactile sensor that estimates the elbow joint torque of the robot hand (**Fig. 2.1** (a)). Fujisawa *et al.* [18] proposed the upper limb patient simulator for training the practical experiences. Their simulator can reproduce the stiffness of elbow joint to allow trainee to improve the opportunities to stretch of the physical therapy (**Fig. 2.1** (b)).
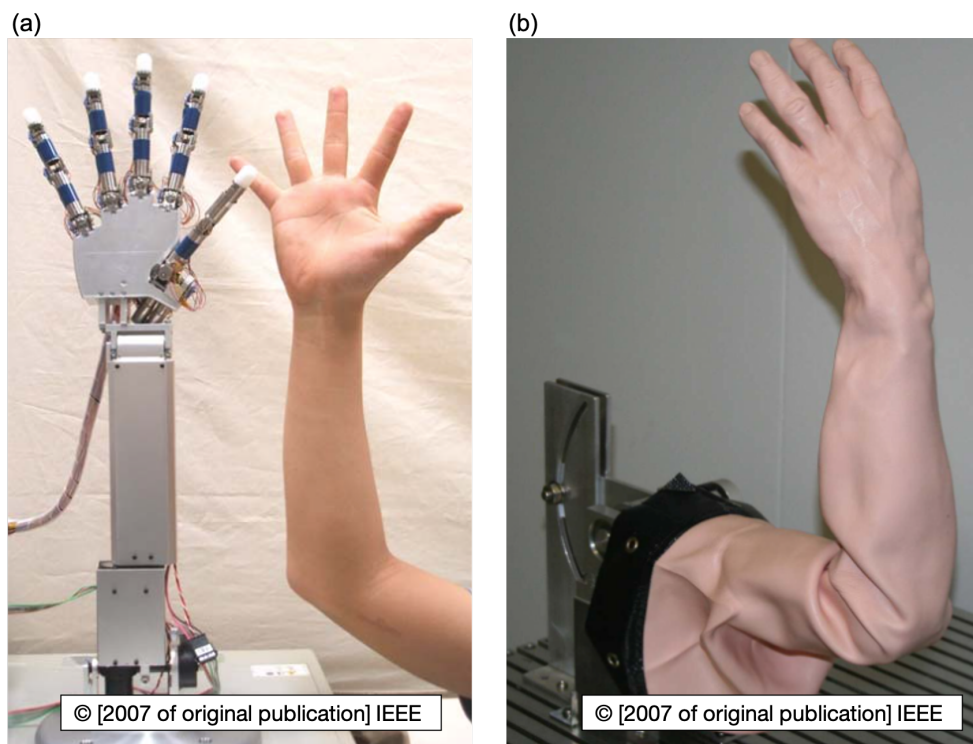
Figure 2.1. Rehabilitation training using patient robots. (a) Robot hand for therapist education [19] ©Reprinted, with permission, from [*Mouri et al.*, Development of robot hand for therapist education/training on rehabilitation, 2007 IEEE/RSJ International Conference on Intelligent Robots and Systems, and 10/2017 of publication] (b) Upper limb patient simulator [18] ©Reprinted, with permission, from [*Fujisawa et al.*, Basic Research on the Upper Limb Patient Simulator, 2007 IEEE 10th International Conference on Rehabilitation Robotics, and 06/2017 of publication].

2.2 Musculoskeletal symptoms

Musculoskeletal disorders of the upper limb contain a variety of symptoms, including disorders of joints, muscles, ligaments, and nerves [36]. Common symptoms of musculoskeletal disorders include aching, stiffness, fatigue, muscle and joint pain that worsens with movement. A general treatment technique to relieve these symptoms in daily life is a range of motion (ROM) exercise or stretching.

2.2.1 ROM exercise

Range of motion (ROM) exercise, which describes physical exercise that is used for improving the movement of joints. This ROM exercise is characterized by the musculoskeletal actions when performing an exercise [37]. ROM exercises in the upper limbs can be performed by the shoulder complex and the elbow joint. There are about nineteen types of ROM movements of the upper limb [38] as shown in **Fig. 2.2**.
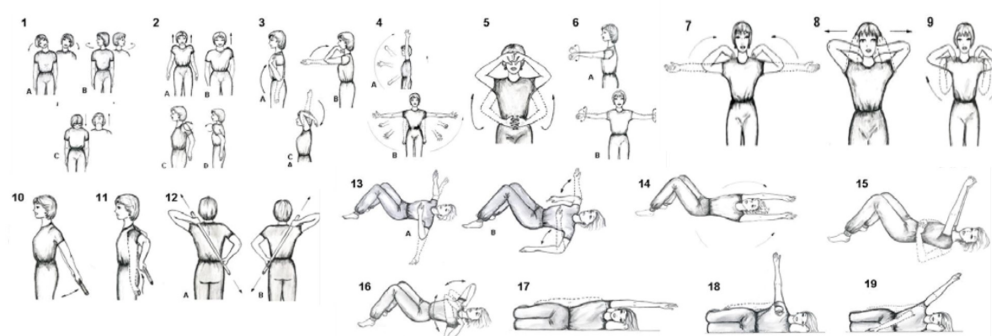
Figure 2.2. Range of motion (ROM) exercises of the upper limb. ©Reprinted, with permission, from [*MMF et al.*, Efficacy of shoulder exercises on locoregional complications in women undergoing radiotherapy for breast cancer: clinical trial, Brazilian Journal of Physical Therapy, and 11/2008 of publication].

2.2.2 ROM exercise effects

Many studies have reported that ROM exercise is effective in preventing movement limitation in patients with musculoskeletal disorders [39, 40, 41]. Observing the quantitative results of the reported data, Kim *et al.* [40] reported passive ROM exercise for upper extremities in 37 patients with acute stroke, and the results of the work showed a significant increase in range of motion for four weeks compared to initial exercise for two weeks as shown in **Table 2.1**. At two weeks, the average effect of all ROM exercises was 2.25° in the experimental group (patients with stroke) and 0.42° in the control group (healthy group). On the other hand, in the results of four weeks, it can be seen that the ROM effect was significantly improved to 4.27° in the experimental group and 2.05° in the control group.

As a result of reliably supporting the aforementioned result, Ono *et al* [41] demonstrated the positive effects of ROM exercise on rats with denervation and joint contracture in an *in vivo* experiment (**Fig. 2.3**). Their results indicated that passive ROM exercise prevents the expansion of contracture caused by neglect and denervation and may help maintain flexibility of myogenic and atherogenic limitations. In changes in ankle dorsiflexion ROM, the rat models exposed to sciatic nerve resection (reduced muscle stiffness and muscle strength) and joint fixation recovered muscle strength after one week of ROM exercise, with a difference of 6° between the control and ROM exercise group and 19° between the control and non-ROM exercise groups. These findings of these studies suggest the importance and necessity of regular ROM exercise in musculoskeletal patients in daily care and nursing activities.

Table 2.1. Comparison of range of motion of affected shoulder and elbow joint. *Exp* and *Cont* indicate the experimental and control group. Participants in the experimental group were patients with stroke. All participants performed passive ROM exercise for 2 and 4 weeks (abbreviated as *wks*). Table adapted from *Kim et al* [40].

Variables (degree)		Baseline	After 2wks	After 4 wks
		Mean (Standard deviation)		
Shoulder				
Flexion	Exp (n=19)	114.1 (13.0)	116.7 (12.8)	119.0 (12.6)
	Cont (n=18)	109.1 (20.2)	109.8 (20.7)	111.1 (21.1)
Extension	Exp (n=19)	25.2 (5.2)	27.1 (4.9)	29.5 (5.3)
	Cont (n=18)	31.2 (4.7)	31.3 (4.7)	31.9 (4.8)
Abduction	Exp (n=19)	94.2 (12.0)	96.3 (12.1)	98.4 (12.5)
	Cont (n=18)	92.7 (13.0)	93.0 (13.1)	94.2 (13.4)
Internal rotation	Exp (n=19)	51.3 (19.8)	53.8 (19.5)	55.6 (19.6)
	Cont (n=18)	57.7 (14.8)	58.3 (14.8)	58.8 (15.2)
External rotation	Exp (n=19)	44.8 (24.9)	46.7 (25.3)	48.6 (25.5)
	Cont (n=18)	35.0 (18.2)	35.4 (18.3)	36.0 (18.3)
Elbow				
Flexion	Exp (n=19)	95.2 (35.3)	97.7 (35.3)	99.3 (35.1)
	Cont (n=18)	103.6 (16.7)	104.0 (16.9)	105.4 (16.8)

Ankle fixation

ROM exercise

ROM measurement
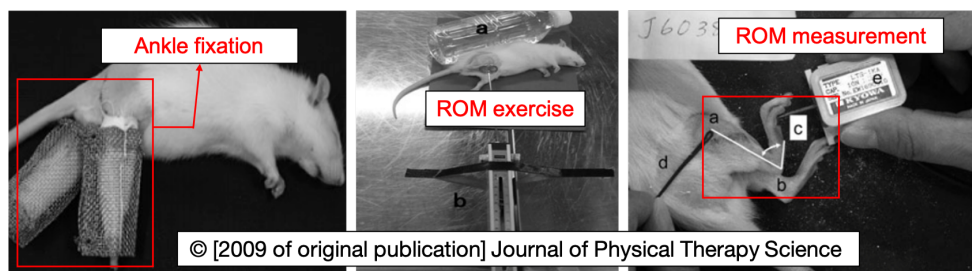
Figure 2.3. Experiment for ROM effects in rat model. Figure adapted from [41]. ©Reprinted, with permission, from [*Ono et al.*, The Effect of ROM Exercise on Rats with Denervation and Joint Contracture, Journal of Physical Therapy Science, and 07/2009 of publication].

2.2.3 Musculoskeletal symptoms reproduction

Yamazaki and Tanaka [42] proposed a method to reproduce the skeleton simulating the resistance characteristics of human's joints. In [42], an exponential function-based prediction method has been proposed to reproduce the resistance nonlinear characteristics of joints, as shown in **Eq. 2.1**.

$$T(\theta) = e^{(p_1(\theta - p_2))} - e^{(p_3(p_4 - \theta))}. \tag{2.1}$$

where $T(\theta)$ is the resistance torque (Nm), θ is the joint angle (degrees), p_2 and p_4 are the coefficients indicating the position where the resistance torque increases rapidly, and p_1 and p_3 are the coefficients indicating the degrees of increase in the resistance torque in the range of movement (**Fig. 2.4**).
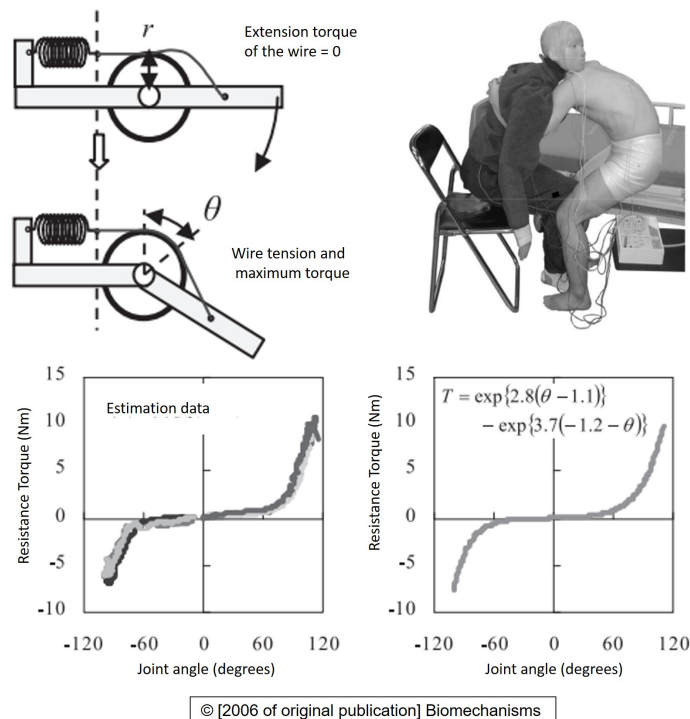
Figure 2.4. Musculoskeletal symptoms reproduction. Figure adapted from [42] ©Reprinted, with permission, from [*Yamazaki and Tanaka. Development of a Human Joint Imitated Dummy, Biomechanisms, and 01/2006 of publication*].

2.2.4 Limitations

Although the studies show that greater attention is being paid to patient simulator robots, simulators for human care training are still insufficient. Besides, although simulated robots have been developed in many studies, the development of a human-robot interaction system in which simulated robots can directly interact with humans is still lacking. The human-simulated robot interactions for care education can be developed based on text-, alarm-, voice-, and visual-based methods. However, the simulated robot for CNT still relies on the post-evaluation using statistical analysis, and a more advanced feedback method is required for the interaction between users and robots.

2.3 Robot's pain and emotion expression

This Section describes the importance and necessity of expressing pain and emotions in the patient robots. The full advantages of patient robots over the role of static medical mannequins cannot be proved unless it provides feedback on pain, stress, and emotions to the caregivers when the patient robot is applied to an actual training environment. To achieve effective CNT feedback, it is important for care and nursing training to design patient robots that can express emotions or feel pain like humans through visual feedback. The robust feedback methods that robots can provide to learners can be based on visual information and sounds. Among them, visual-based feedback is the most effective method in terms of practice for caregivers because the caregivers should periodically investigate whether the patient is feeling pain or not. In particular, it is imperative to observe painful expressions on the patient's face because the patient may experience a burden in communication with caregivers.

2.3.1 Relationship between pain and emotion

According to [43], the relationship between pain and emotions can be presented in several potential theories, which are highly complicated and ambiguous. Basically, pain is a sensory and emotional experience, and although pain may lead to unpleasantness, it may be defined separately from emotions. However, another concept of this relationship is that pain implicitly contains a sensory, emotional composition, cognition, and experiential and external factors, and it is challenging to consider to completely separate pain and emotion. On the other hand, pain implies a vertical relationship between pain and emotion because it can be conceptualized as a type of emotional categories such as fear or anger. Besides, the relationship between pain and emotion can be defined as a horizontal intersecting relationship, and there are many more potential theories to define this relationship [44, 45, 46].

2.3.2 Robot's pain

Pain is an immediate response that protects the human body from tissue damage and can be observed as an absolutely subjective measure. When most humans are subjected to physical pressure from external factors, most humans usually express pain through facial expressions, voices, and physical responses.

In 2011, the realistic child robot *Affetto* was presented by Ishihara *et al.* [47], which is to understand and interact between the caregiver and child to support the child's development. *Affetto* is able to feel touch or hit by detecting changes in pressure from synthetic skin [48]. Based on this pressure sensation, *Affetto* is being developed as a robot capable of expressing pain and emotions with a painful nervous system. In this way, applying the pain response system to a robotic system makes it possible to build a robotic system that can feel pain like an actual human when most humans are subjected to physical pressure from external factors.

2.3.3 Robotic facial expression

The intelligent robotic facial expressions using emotional processing are more reliable, coherent, and human-like [49], forming constant and more profound interactions because the emotional processing heightens strongly the robot's empathy and learning abilities with people [50]. Typically, human emotions can be expressed in three axes, including pleasure, arousal, and dominance, that Mehrabian and Russell [51] developed to evaluate experience, as shown in **Fig. 2.5** (a). Using this relationship between pleasure and arousal axis, Russell [52] coordinated several basic human emotions, such as anger, disgust, fear, happiness, sadness, surprise, and neutral, into two-dimensional map as shown in **Fig. 2.5** (b).
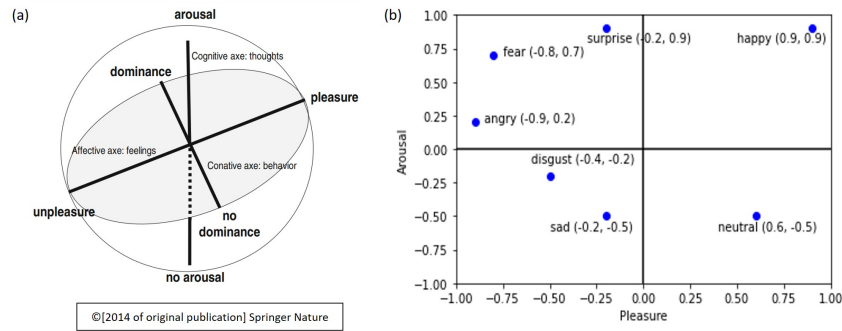
Figure 2.5. Area of human emotions. (a) Three dimensional model as tripartite view of experience [53] ©Reprinted, with permission, from [*Bakker et al.*, Pleasure, Arousal, Dominance: Mehrabian and Russell revisited, Current Psychology, and 06/2014 of publication] (b) Pleasure (x-axis) and arousal (y-axis) axis for human emotional state.

In recent studies, the robot's emotions depend on human facial expressions, texts, or voices, and research on *Robotic Mood* in which the robot's emotions continuously change according to the current emotional state of humans has been actively pursuing. In [22] and [54], the emotional model of the patient robot was proposed for injection training. The proposed model was designed based on emotional fluctuation by chaos theory, and the robot expressed four emotions—normal, smile, angry, and pain—using robotic head. These emotions are deeply related to personality, and the robot have different personalities in behavior and emotional response [55]. Therefore, studies on the emotional response according to the personality of the robot were also conducted. In [56], a robotic mood transition with personality was proposed for autonomous emotional interaction with humans, and the questionnaire of their experiment showed positive and feasible evaluation of responsive robotic facial expressions. Masuyama *et al.* [57, 58] claimed that the relationship between emotion and personality are influential factors in communication and proposed the robotic emotional model with the human's personality factors based on the pleasant and arousal scaling. Likewise, the research on robotic emotions can further improve the user's satisfaction in the human-robot interaction system and can lead to a positive effect of receiving more feedback from responsive robots.

2.4 Summary

With the advances in medical and health care systems, it is essential in care and nursing education to train professionals who can competently handle various situations and meet the needs of individuals with diseases [7]. To improve care and nursing skills, most students aspiring to be caregivers, nurses, or therapists are provided an opportunity for training at the school over a given period. Although they gain experience utilizing watching videos, reading books, and practicing with simulated subjects, the most effective way is to practice with an actual human. However, it is challenging to recruit patients for care and nursing programs continually, and the patients may have experienced fatigue or boredom with iterative testing. Therefore, a novel approach to the care and nursing training system is required to resolve the existing methods' issues effectively. The patient robot imitates an actual human's behavior and activity [23, 59] and can be used for care training and improving nursing skills in interactions with patients or care-receivers, such as bathing, transferring, and rehabilitation [60, 61, 62]. Although many studies have proposed the patient robot, however, the care training studies depend on the statistical or empirical techniques that can analyze results manually. These methods are proper for analyzing each parameter and easy to use when investigating the effect of parameters on care training. Consequently, it is difficult for trainees to evaluate their treatment quantitatively in a real-time system, and there is a limitation in calculating the final score automatically after finishing care education. Further, the post-analysis method has a limitation in that it is difficult to recognize the emotional state, pain, or stress that the robot feels during care education. Keeping in mind the aforementioned motivation, it is crucial for a more advanced HPS system to develop patient robots that can express current emotions or feelings of pain like an actual human through text-, alarm-, voice-, and visual-based methods for interaction between users and robots. While several studies have demonstrated the advanced patient robot, there remains an opportunity to improve how robots provide effective feedback to caregivers and how robots interact with caregivers in care education.

24

Chapter 3

Care training assistant robot

In CNT, students lack methods for acquiring the necessary skill and experience. Besides, they lack sufficient opportunities to practice on actual human beings. This chapter, therefore, presents a patient robot with the musculoskeletal symptom that supports efficient care education for caregivers to achieve improved care skills, interprets the results to prove the necessity and feasibility of the patient robot developed in this chapter, and discusses the results. First and foremost, this study aims to develop a patient robot with a shoulder (the glenohumeral joint and sternoclavicular joint) and elbow complex and a care training monitoring program. By performing care tasks as range of motion (ROM) exercises (extension and flexion, elevation and depression, and lateral and medial rotation of the joint) in care education using a patient robot, four experts who have experienced for many years in the medical field, participated in the data acquisition process to collect quantitative data of the patient robot. Based on this information, the results are analyzed and interpreted through various perspectives to investigate and discuss the effectiveness and feasibility of the patient robot. This study is anticipated to provide a new pathway for developing advanced patient robots used in care training environments by imitating the symptoms of various muscle and joint diseases such as palsy, contracture, and muscle weakness.

3.1 Motivation

The examination of the correlation between simulated robots and actual humans can help evaluate simulated robots' applicability. Kim *et al.* [63] presented a haptic elbow spasticity simulator and compared the robot and in-person questionnaire results for improving the reliability of clinical assessment. Based on their results, they concluded that their proposed haptic recreation of spasticity has the potential to be used as a training tool for standardizing and enhancing the reliability of clinical assessment. Huang *et al.* [8, 34] proposed a robot patient for nursing skills training during stand-up and sit-down actions on a wheelchair during patient transfer, in addition to performing relevant experimental tests. Their results revealed that the robot patient could successfully simulate the limb actions of a patient according to the operations performed by the nursing teachers and was suitable for nursing-skill training.

Caregivers to the patient with musculoskeletal symptoms should continually develop their ability to deal with the limited range of movement of joints and muscles and assist in stretching exercises periodically to prevent the muscle weakness, contracture, and/or stiffness of patients. As mentioned in Chapter 2, the passive range of motion (ROM) exercise is a type of physical exercise that is used for improving the movement of joints, which is one of the most important tasks in care and nursing because the patients may experience limited joint movement in daily life due to the musculoskeletal symptoms. However, the principal issue in caregiving training is the risk of injury to the patient during the training due to a trainee's inexperience. In addition, although robots for various purposes with specific diseases have been proposed to be used for the betterment of care and nursing education, there are still not enough research and well-established training systems to develop patient robots that mimic the musculoskeletal diseases of the elderly. To resolve these issues, a patient robot is presented as a method to improve the care abilities of caregivers or students effectively.

3.2 Objectives and research problems

3.2.1 Specific objectives

The objectives of the care training assistant robot introduced in this Chapter to achieve the goals are as follows.

- To develop an upper limb robot for care education consisting of the shoulder complex and elbow joint and reproduce the patient with musculoskeletal symptoms.

- To develop a care education system for monitoring care training in real-time.

- To conduct four kinds of ROM exercises using the patient robot.

- To investigate the significant differences in care training between students and experts and the effects of continuous and repetitive care education using robots.

3.2.2 Research problems

In order to achieve the goals of the proposed patient robot in this Chapter, the research problems are as follows:

- **RP 3.1)** Are there any statistically significant differences between expert and student groups in care training using the patient robot?

- **RP 3.2)** Do experts with many years of experience participate in care education in the same manner and pattern?

- **RP 3.3)** Does the proposed patient robot have sustainability and feasibility in the future?

3.3 Requirements

3.3.1 Target subjects

In the study of this Chapter, the patient robot will be designed for the following conditions by considering the medical symptoms of *elderly-specific problematic movements* of the upper limb joint. Here, the *specific problematic movements* means that the current range of motion of the joint is more limited than that of the past due to the stiffness, and several experts have determined the range of motion of the patient robot during the development process.

3.3.2 Target tasks in care training

The patient robot in this study aims to be developed to educate passive ROM exercises in the care education environment. These ROM exercises are frequently performed for the rehabilitation of people suffering from musculoskeletal diseases. In the several ROM exercises mentioned in Section 2.2.1, the main ROM exercises are the extension and flexion of the shoulder complex joint (SEF), elevation and depression of the shoulder complex joint (SED), lateral and medial rotation of the shoulder complex (SLM), and extension and flexion of the elbow joint (EEF). In the SED exercise, elevation and depression represent the upward and downward movement of body structures, respectively; for example, the depression of a sternoclavicular joint corresponds to the arm moving vertically downward. The SEF exercise constitutes increasing and decreasing the angle between the two bones connected by the glenohumeral joint [64]. The SLM exercise refers to the lateral and medial arm rotations of the humeral around its longitudinal axis. A brief explanation is as follows:

- SEF: The caregiver holds the patient's wrist with one hand and the shoulder with the other, bending the patient's arm straight to the tip of the shoulder (**Fig. 3.1 (a)**).

- SED: The caregiver holds the patient's shoulder with one hand and the elbow with the other, moving the shoulders upwards and downwards (**Fig. 3.1** (b)).

- SLM: The caregiver holds the patient's elbow in one hand, the forearm in the other hand, and rotates the arm in the patient's shoulder joint's lateral- and medial axis (**Fig. 3.1** (c)).

- EEF: The caregiver holds the patient's wrist with one hand and the shoulder with the other, bending the patient's arm based on the elbow (**Fig. 3.1** (d)).
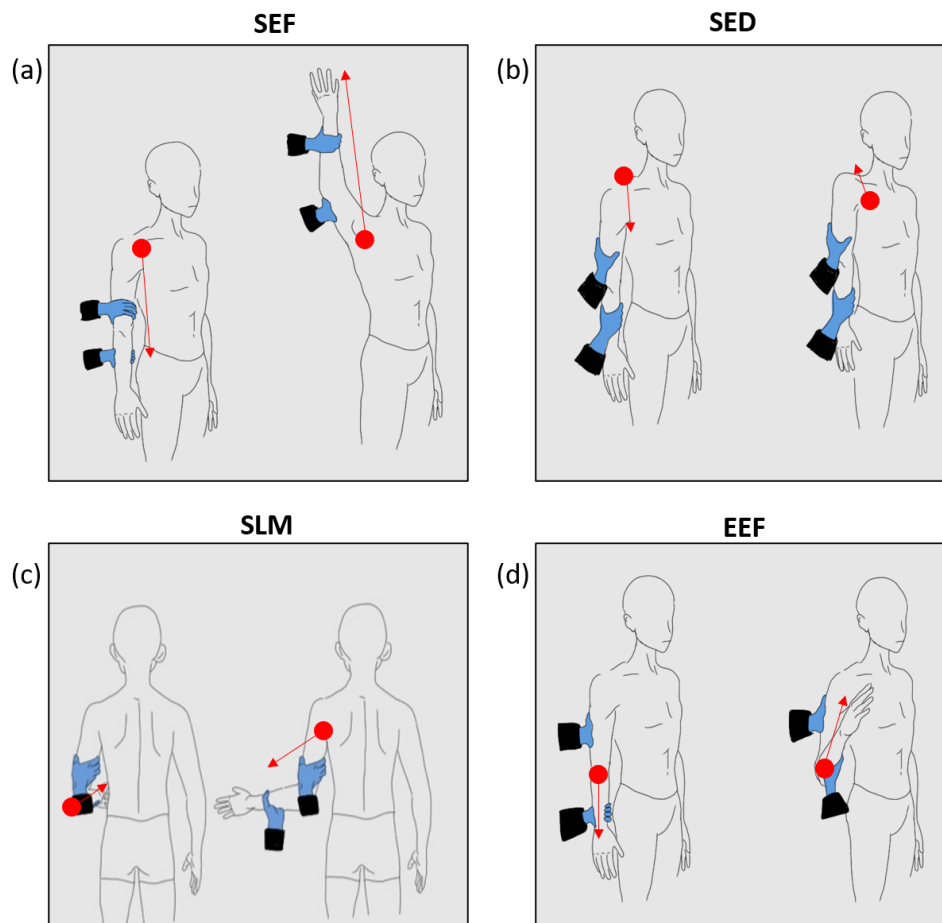
Figure 3.1. Range of motion (ROM) exercises of the upper limb (a) SEF: shoulder extension and flexion (b) SED: shoulder elevation and depression (c) SLM: shoulder lateral and medial rotation (d) EEF: elbow extension and flexion.

The positive effects of these periodic ROM exercises in patients with musculoskeletal disorders are demonstrated in Section 2.2.2. The patient robot in this Chapter is used for four kinds of ROM exercises for care training by reproducing the joint movements of the patient target mentioned above.

3.3.3 Target joints and kinematics

To perform care training for the four ROM exercises, SEF, SED, SLM, and EEF, the patient robot requires joints of the shoulder complex and the elbow complex, as shown in **Fig. 3.2**. The shoulder complex includes the sternoclavicular (SC) joint and the glenohumeral (GH) joint; the SC joint is located where the clavicle and sternum meet. The GH joint indicates the joint where the glenoid cavity and the head of the humerus are connected. On the other hand, the elbow joint is a complex consisting of the humerus and the radius and ulna of the arm.

The upper extremity kinematics for the four ROM movements can be described **Fig. 3.3**, and **Fig. 3.3** (a) shows the overall structure and mechanism of the upper extremity joints. The elbow complex consists of the rotational motion based on the z_1 axis in three orthogonal joints (**Fig. 3.3** (b)). The glenohumeral joint of the shoulder complex consists of a spherical joint and can be disassembled into three orthogonal rotation joints (**Fig. 3.3** (c) and (d)). This joint rotates lateral and medial direction based on the y_2 axis (**Fig. 3.3** (c)), and performs vertical movement based on the z_2 axis (**Fig. 3.3** (d)). Finally, the clavicle joint, which is contained in the sternoclavicular joint, rotates based on the x_3 axis (**Fig. 3.3** (e)).
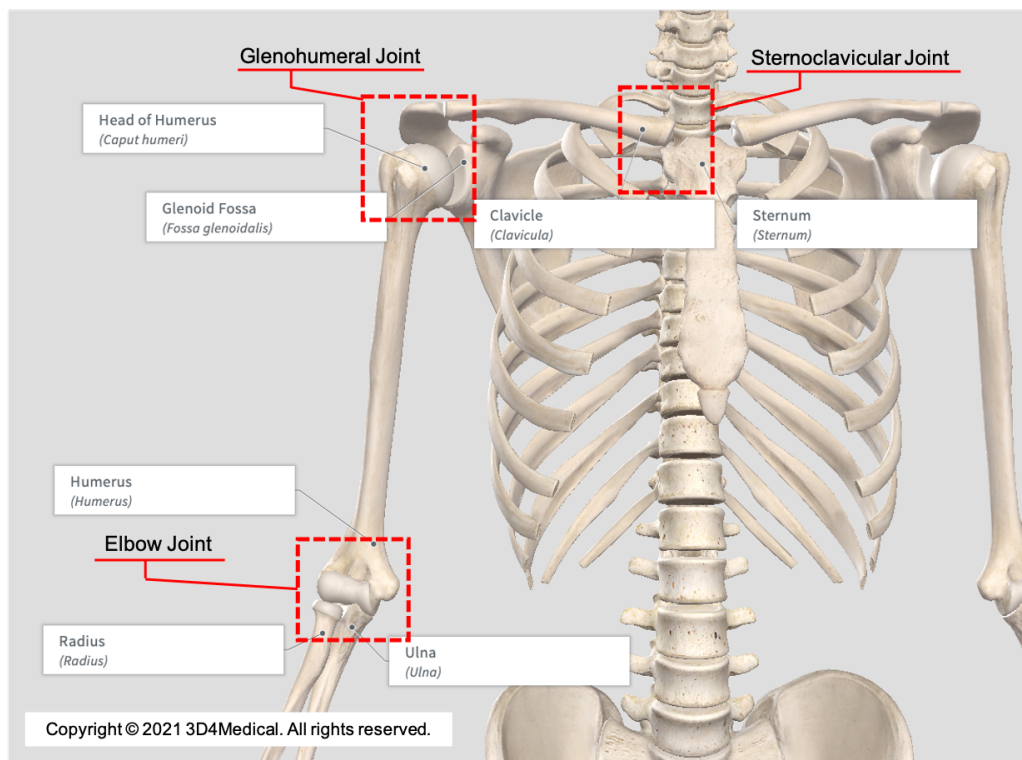
Figure 3.2. The bones of the shoulder complex and elbow complex. A picture of the anatomy is provided in *Complete Anatomy* [65]. The sternoclavicular joint is located where the clavicle and sternum meet. The glenohumeral joint is located where the glenoid cavity and the head of the humerus meet. The elbow joint is a complex consisting of the humerus and the radius and ulna of the arm.
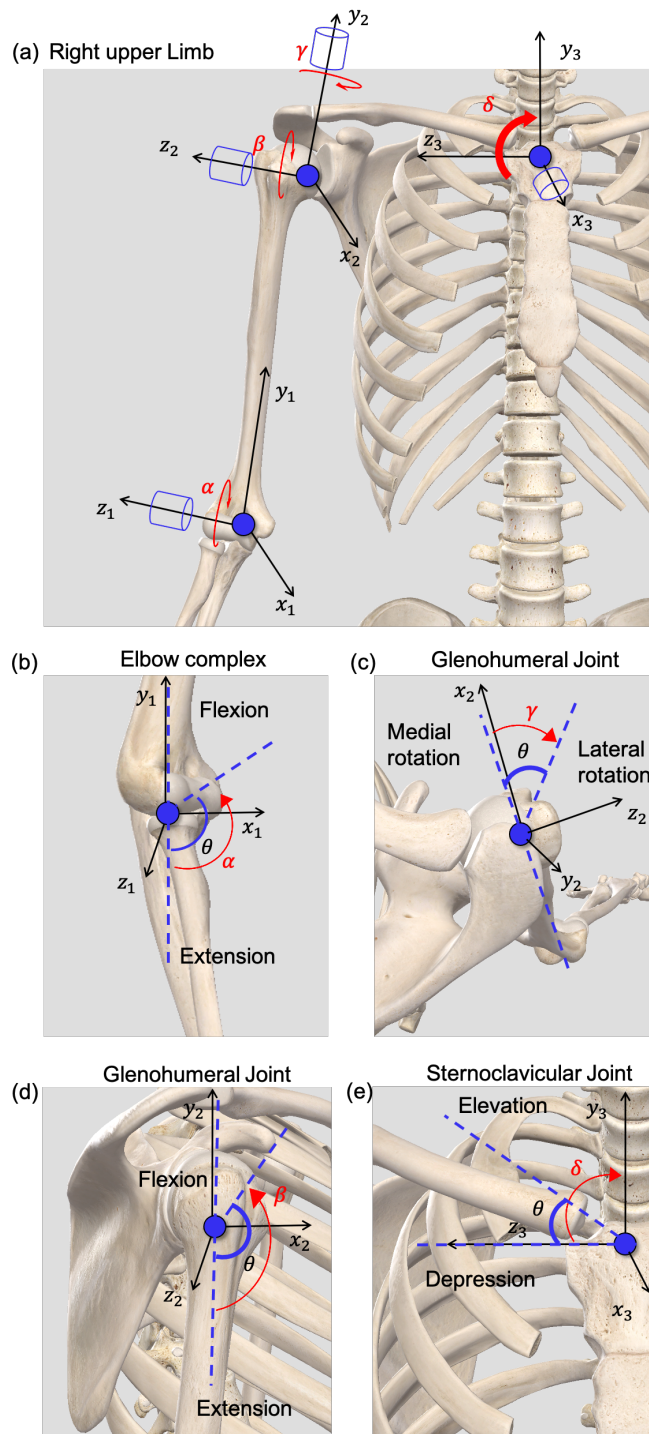
Figure 3.3. Upper limb kinematics (a) Right upper limb (b) Extension and flexion of elbow complex (c) Lateral and medial rotation of glenohumeral joint (d) Extension and flexion of glenohumeral joint (e) Elevation and depression of sternoclavicular joint. θ indicates the range of angle of each joint.

3.4 Hardware configuration of the patient robot

3.4.1 Specification

As explained in Section 3.3.1, the patient robot developed in this study was determined for the elderly with joint problems, and the robot body size of the elderly person was set based on Human Body Properties Database (HBPD) [66] in Japan and was set to the average size of an elderly person older than 65 years. As shown in **Table 3.1**, based on the HBPD, the lengths of the upper arm and the forearm, as well as the circumferences of the upper arm and the forearm, together with the weight of the robotic elbow joint, were set to 288 mm, 285 mm, 220 mm, 240 mm, and 0.35 kg, respectively.

Table 3.1. Size of the joints of the actual human and the patient robot.

	Human [66] (mm)	Robot (mm)
Upper arm length	289	170
Upper arm circumference	280	285
Forearm length	225	220
Forearm circumference	242	240

3.4.2 Joint configurations

The joint configuration of the robot is shown in **Fig. 3.4**, which has totally six joints: three parts of glenohumeral (GH1), (GH2) and (GH3); two parts of sternoclavicular (SC1) and (SC2); as well as the elbow joint.

The robotic joints of glenohumeral (GH) and sternoclavicular (SC) were combined into the shoulder complex robot. These joints were designed based on the forceless joint because the elderly robot does not need to move actively during the care training. The robotic GH and SC joints (GH1, GH2, GH3, SC1, and SC2) were

designed using six *Dynamixel XM-430-W350-R* (Robotis Inc., Seoul, South Korea) servo motors (**Fig. 3.4** (a)). The *Dynamixel XM-430-W350-R* has the main feature of a robot exclusive actuator with integrated motor, reduction gearhead, controller, driver, and network in one module (**Fig. 3.4** (b)). In addition, two 6-axis force sensors *PFS030YA301* (Leptrino Inc., Nagano, Japan) was used to measure the torque acting at the robotic joints (**Fig. 3.4** (c)).
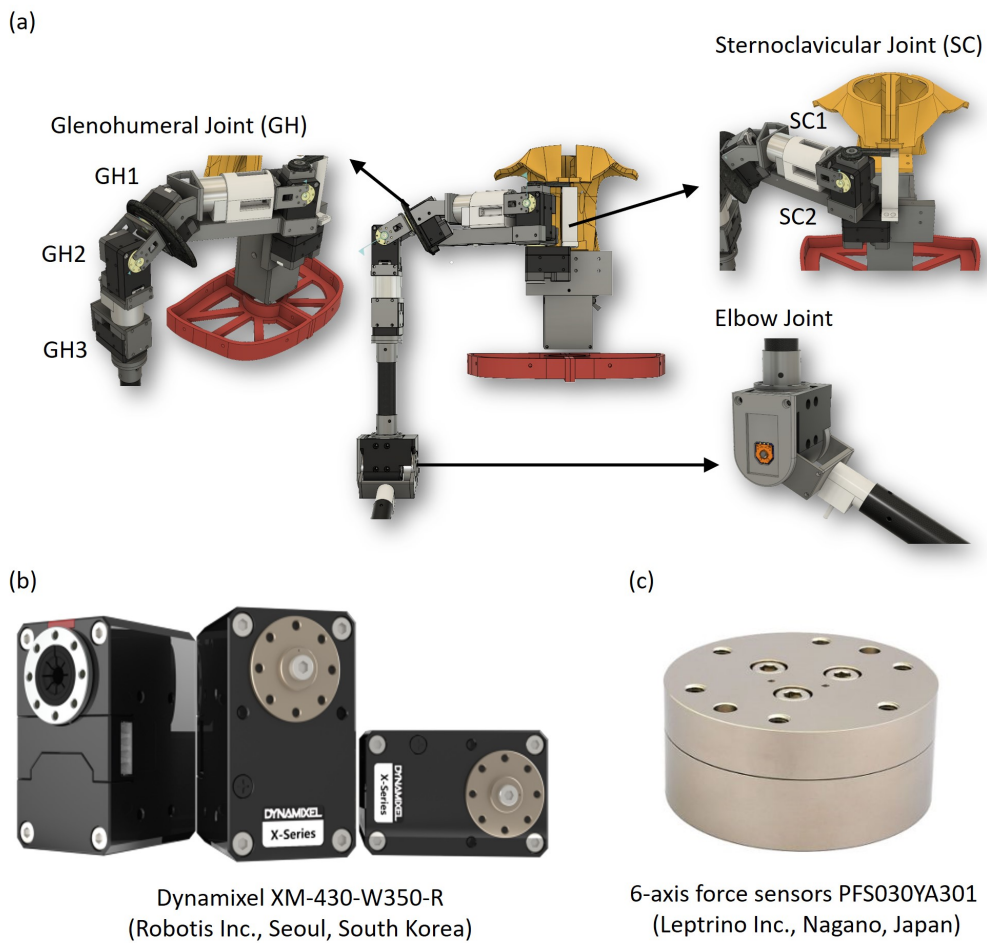
Figure 3.4. Hardware configuration of the shoulder complex (a) Joint design (b) Servo motor Dynamixel XM-430-W350-R (Robotics Inc., Seoul, South Korea) (c) Six-axis force sensors PFS030YA301 (Leptrino Inc., Nagano, Japan).

Fig. 3.5 (a) shows the 3D design, using *Autodesk Fusion* 360 ®, of the elbow complex. It includes a carbon frame with components such as a position sensor, a force sensor, a servo motor, and pressure sensors (**Fig. 3.5** (b)). The *MX-28* (Robotis Inc., Seoul, South Korea) was selected as a servomotor, which is utilized for actuation of the elbow joint. This motor supports low weight (72 g) and has an operating range of 360°. One of the purposes of using the *MX-28*, which provides position and speed proportional–integral–derivative controller, was that the user could control the position and speed in real-time [67]. Additionally, the 6-axis force sensor *CFS018CA201U* (Leptrino Inc., Nagano, Japan) was used for measuring the torque of the robotic joint. The position angle sensor *SV01L103AEA11T00* (Murata Electronics Co., Ltd., Kyoto, Japan) and four pressure *FlexiForce A201* (Tekscan, Inc., MA, USA) sensors were used for obtaining the angle and pressure values of the elbow joint of the robot, respectively.

In the case of the ROM exercise of the elbow joint, when undergoing the care and nursing training, caregivers may grip the wrist of the patient and there is a possibility of straining the wrist of the patient as shown in **Fig. 3.5** (c). Therefore, the pressure sensors attached to the wrist of the elbow joint can provide feedback on the gripping pressure. As shown in **Fig. 3.5** (d), four pressure sensors were attached to the wrist of the elbow joint robot: radius (P1), outside of the wrist (P2), ulna (P3), and inside of the wrist (P4). The position angle sensor and four pressure sensors embedded in the elbow joint are obtained through custom hardware boards (**Fig. 3.5** (e)) and then transmitted to a computer. The torque data from force sensor are transmitted to the computer. The sampling rate of all sensors is set to 100 Hz.
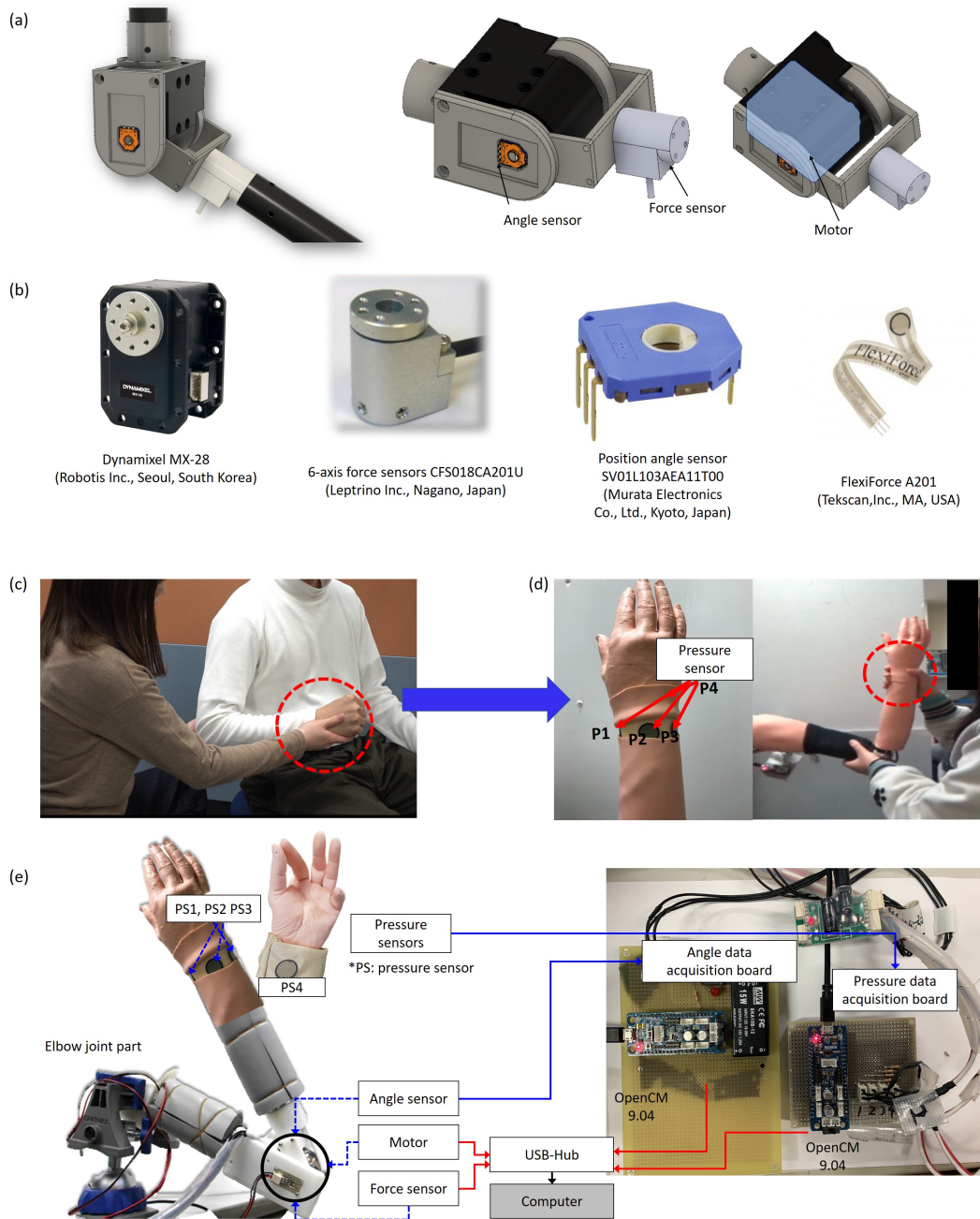
Figure 3.5. Hardware configuration and design of the elbow complex containing pressure sensors (a) Joint design (b) Sensors: in order from left to right, servo motor Dynamixel MX-28 (Robotics Inc., Seoul, South Korea), six-axis force sensors CFS018CA201U (Leptrino Inc., Nagano, Japan), position angle sensor SV01L103AEA11T00 (MurataElectronics Co., Ltd., Kyoto, Japan), and FlexiForce A201 (Tekscan, Inc., MA,USA) pressure sensors (c) ROM exercise of the elbow joint (d) Position of pressure sensors (P1: radius; P2: outside the wrist; P3: ulna; and P4: inside the wrist) (e) Hardware design.

The elbow joint of patient robot can switch between active rotation (to enable the elbow to be moved actively) and passive rotation (to enable the elbow to be moved passively) by connecting the clutch and the motor. In passive rotation, as the rotating part of the motor and the elbow joint part of the forearm are separated from each other, power is not transmitted at all and the forearm can only be moved by an external force. In the active state, it is possible to transmit power by fixing the rotating part of the motor and the elbow joint part of the forearm with screws. However, since switching between active and passive states is not required while the robot is imitating a symptom in this study, it was determined that there would be no influence even when it is switched manually.

The exterior of the shoulder complex was designed using 3D CAD (Autodesk, Fusion 360, CA, USA) and created with a 3D printer (Zortrax S.A Inc., Lubelska, Poland), whose material was applied based on acrylonitrile butadiene styrene copolymer for robust durability (**Fig. 3.6** (a)). On other hand, the exterior of elbow joint which was sheathed in artificial skin to make it look more human. To provide the tactile feeling of a human being, a urethane sponge was placed under the artificial skin (**Fig. 3.6** (b)).

(a)

(b)

Figure 3.6. Pictures of exterior design of the patient robot with artificial skin (a) Shoulder complex (b) Elbow complex.

3.5   Mechanism

3.5.1   Mechanical design

Fig. 3.7 (a) shows the movement of the shoulder complex joint and the servo motor of the GH joint used to control the extension-flexion (SEF) and lateral-medial rotation (SLM) of the robotic GH joints. In addition, the robotic SC joints were developed, whose elevation–depression (SED) was controlled with the SC joint as the rotation axis. **Fig. 3.7** (b) shows the mechanism of the elbow joint robot and demonstrates the performance of movement of EEF of the joint by the elbow joint of patient robot.
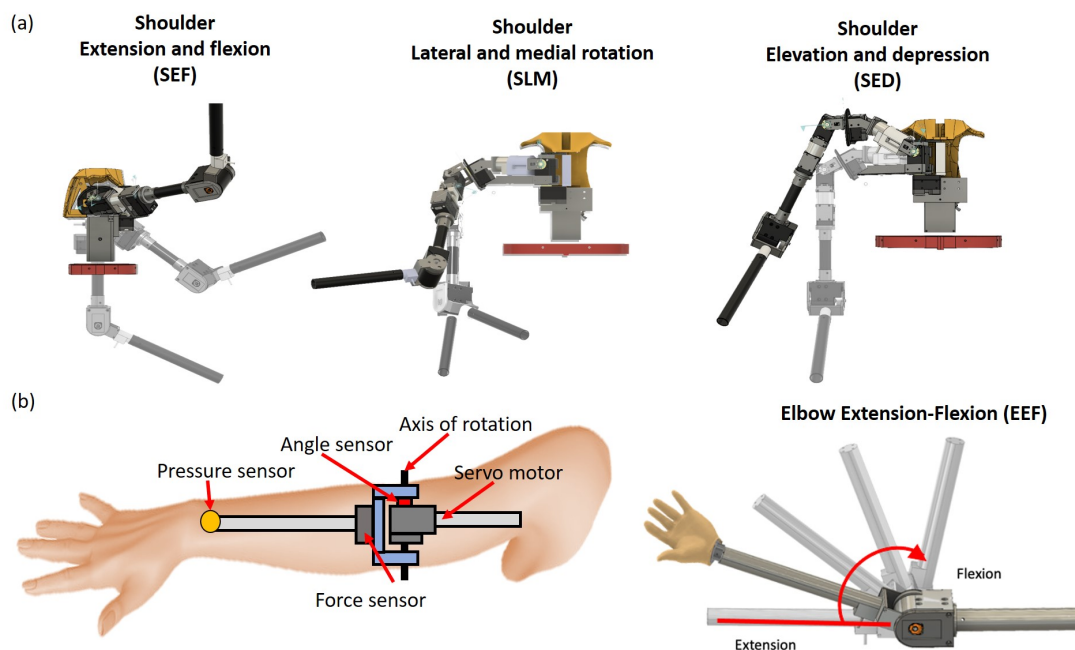
Figure 3.7. Mechanism of the patient robot (a) Shoulder complex (b) Elbow complex.

3.5.2 Symptom reproduction

To mimic the movement of the actual human joints, Yamazaki and Tanaka [42] proposed the **Eq. 3.1** of resistance torque by fitting four parameters as p_1, p_2, p_3, and p_4.

$$T(\theta) = e^{(p_1(\theta - p_2))} - e^{(p_3(p_4 - \theta))}. \tag{3.1}$$

where $T(\theta)$ represents the resistance torque $(N \cdot m)$ of the joint of the patient robot. Parameters p_1 and p_3 determine the degree of resistance torque at the end of the range of the joint angle, whereas p_2 and p_4 are coefficients that designate the joint angle range and can determine the timing at which the onset of the resistance torque can be perceived. The parameters of p_1 and p_3 are coefficients that determine the extent of resistance torque increases in the end-feel, whereas the parameters p_2 and p_4 are coefficients indicating the position where the end-feel begins. To have the robot imitate a patient with joint-specific problematic movements, the range of joint movement of a patient with limited range of motion was reproduced based on the opinions of the experts (caregivers) who participated in this experiment. The angle at which feeling of resistance begins was set from θ_{start} to θ_{end} as shown in **Table 3.2**.

Table 3.2. Determination of the parameters for resistance torque.

	Range of limited angle (degrees)		Parameters			
	θ_{start}	θ_{end}	p_1	p_2	p_3	p_4
SEF	-15	100	2.8	2.0	2.4	0
SLM	-10	10	0.75	-0.3	0.3	0
SED	-10	5	0	0	1.3	0
EEF	100	105	10.5	2.1	8.5	1.6

Note: SEF, SLM, SED, and EEF indicate the extension and flexion of the shoulder complex, the lateral and medial rotation of the shoulder complex, the elevation and depression of the shoulder complex, and the extension and flexion of the elbow complex, respectively.

In **Fig. 3.8**, a graph of the resistance torque with respect to varying joint angles were represented. By changing p_1 and p_3, the slope of the graph changed. The **Eq. 3.1** of resistance torque was applied to the proposed patient robot.
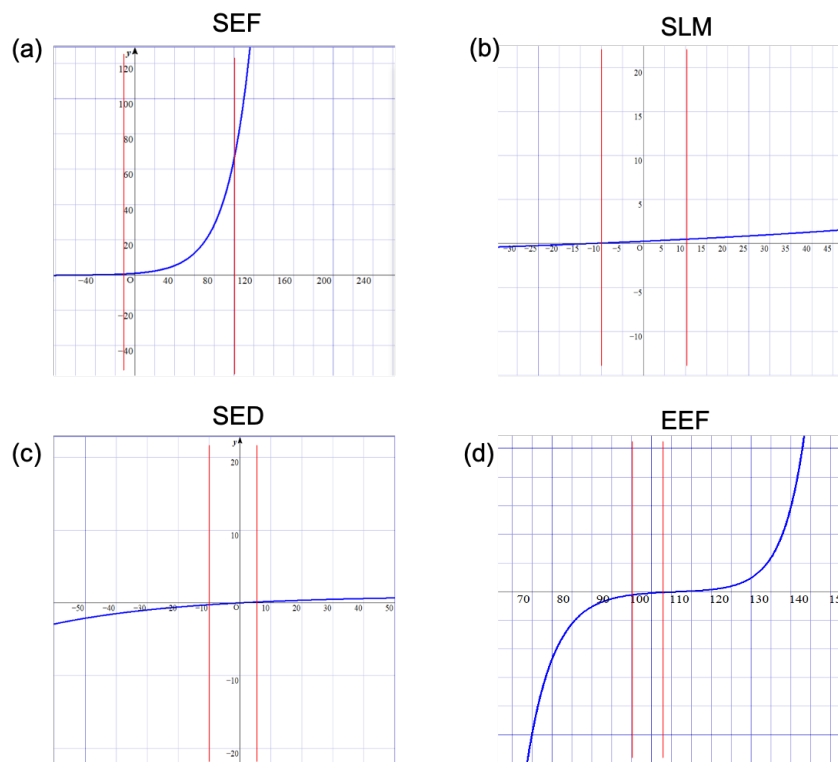
Figure 3.8. Resistance torque graph of joint resistance torque (y-axis) with respect to joint angle (x-axis): (a) SEF (b) SLM (c) SED (d) EEF.

3.6 Interface

For the monitoring of care training in real-time, the custom program using Python was developed as shown in **Fig. 3.9**. Firstly, the patient robot is connected to the computer by serial communication, and the data from both the force sensor (unit: *Nm*) and angle sensor (unit: degrees) are input simultaneously to the computer. In the control window as shown in **Fig. 3.9** (a), there are four parameters as k_1, k_2, k_3, and k_4 are the parameters for determining the resistance torque (The parameters k_1, k_2, k_3, and k_4 are the same as the parameters p_1, p_2, p_3, and p_4, respectively, in **Eq. 3.1**). In addition, the function to predefine (refer to **Table 3.2**) the maximum and minimum angle to limit the range of joint angle was included.

In **Fig. 3.9** (b), the quantitative data are input from three kinds of sensors such as angle, force, and pressure (the pressure value is obtained using only the elbow complex). On the left side, torque ($N \cdot m$) and angle (degrees) are represented as one-dimensional graphs, and on the right side, the values of four pressure sensors are represented as a circle graph. The orange line of the graph on the left represents the ROM exercise graph obtained from an expert in advance, and is referred to as a guideline. The novices can learn the range of the patient's motion based on this guideline and intuitively check the pressure the patient robot feels on its wrist through the pie graph that appears on the right screen. As described in **Fig. 3.5** (d) and (e), P1 (radius), P2 (outside of the wrist), P3 (ulna), and P4 (inside the wrist) of the pressure sensor of the robot's wrist are attached to the fixed positions, respectively. Accordingly, the pressure value is expressed on the pie graph. As shown in **Fig. 3.9** (c), when the pressure sensor is activated, it can be seen that the corresponding circle point moves outward in the pie graph. **Fig. 3.9** (c) shows the screenshot of obtaining the quantitative data in real-time when care training is performed. The pressure value on the right screen represents the magnitude of the torque in a one-dimensional line from a small circle to a large circle when pressure is detected.
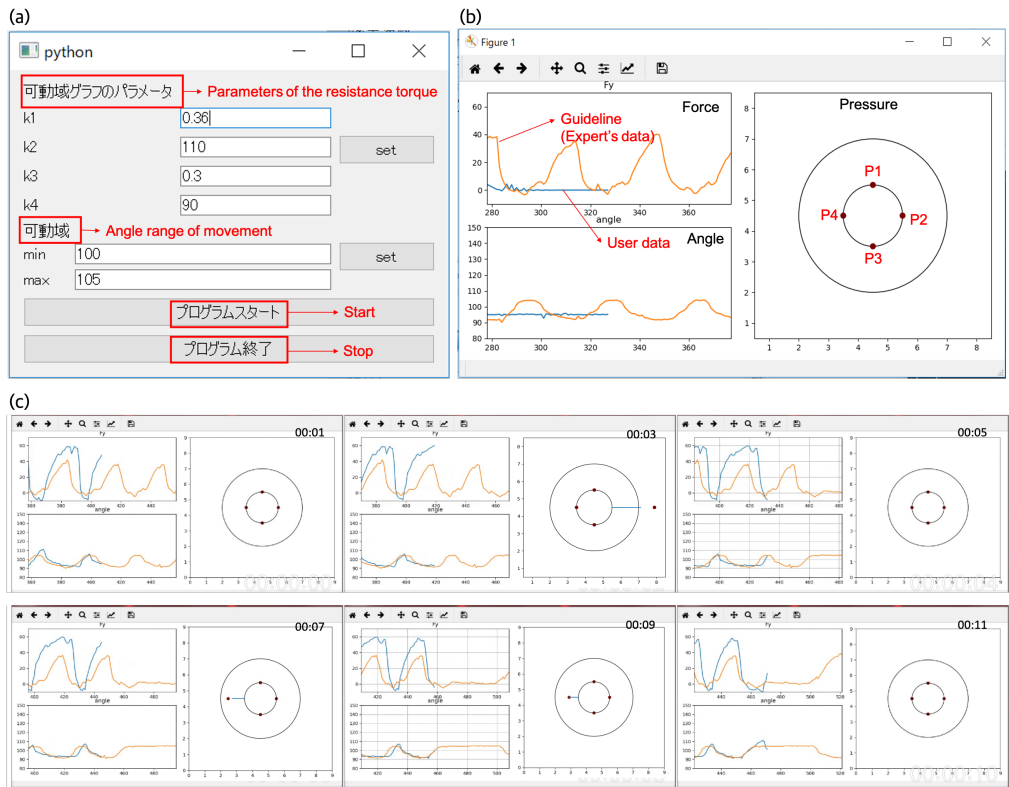
Figure 3.9. Care training monitoring program (a) Control UI; (b) Care training UI, and (c) Examples of obtaining the quantitative data in real-time when care training.

3.7 Experiment and results

3.7.1 Purpose

The purpose of this experiment aims to investigate the effects of using the patient robot for care training. Even though experts have many experiences, care and rehabilitation are carried out empirically and subjectively. Thus, a system is needed to quantitatively evaluate the care skills. Here, this Chapter investigates the contribution of the patient robot used in care training, including the ability to simulate the joints based on the movement range of the patient with musculoskeletal disease, and its applicability to technical training. Moreover, experiments were carried out by experts to confirm the necessity of the care training assistant robot in care education. The issues are discussed to resolve the research problems presented in Section 3.2.2 and to find the observations.

3.7.2 Participants

Eight subjects participated in the evaluation of the care training using the patient robot. Experts were caregivers who took care of the patient for at least two years in the rehabilitation center and the hospital, and a more detailed information of the expert's experience is described as shown in **Table 3.3**. The remaining four trainees (two male and two female) were students in Ritsumeikan University, who had no experience in care to the patient. All subjects agreed to participate by signing a consent form, while researchers tried to ensure their safety. Furthermore, the entire experimental procedure was approved by the institutional review board (IRB) of the Ritsumeikan University (BKC-2018-059).

Table 3.3. Experience and skill of the experts in this experiment.

Expert	Experience and skill	Gender
Expert #1	- Experience in care, nursing, and orthopedics	Male
Expert #2	- Experience in ROM exercise - Physical therapist in a hospital	Female
Expert #3	- National therapist certification - Experience in ROM training for the patients	Female
Expert #4	- Nursing care specialist	Female

3.7.3 Experimental setup and procedures

Fig. 3.10 (a) shows the flowchart of the experiment for the feasibility of the patient robot's capabilities in the three stages of care training—generation of expert's guideline, performing care training of the user's learning skill in accordance with the guideline, and evaluating user's care skill—was investigated by experiments. The investigation was performed to check if there was a correlation between the experts and students through sensor data obtained when trainees with no care experience performed the range of motion (ROM) training using the patient robot. **Fig. 3.10** (b) depicts the flowchart of the protocol and is detailed below:

- The expert first performs ROM exercises using the patient robot and explains the ROM training to the students.

- The students watch the video of the expert performing the ROM training using the patient robot.

- In pre-evaluation, each student performs the ROM training with the patient robot, and the quantitative data of the robot is measured simultaneously.

- After pre-evaluation, all students practice the ROM training for 30 minutes using the patient robot with measured data from the expert displayed on the practice

system.

- In the post-evaluation, each student performs the ROM training and the data is measured again.
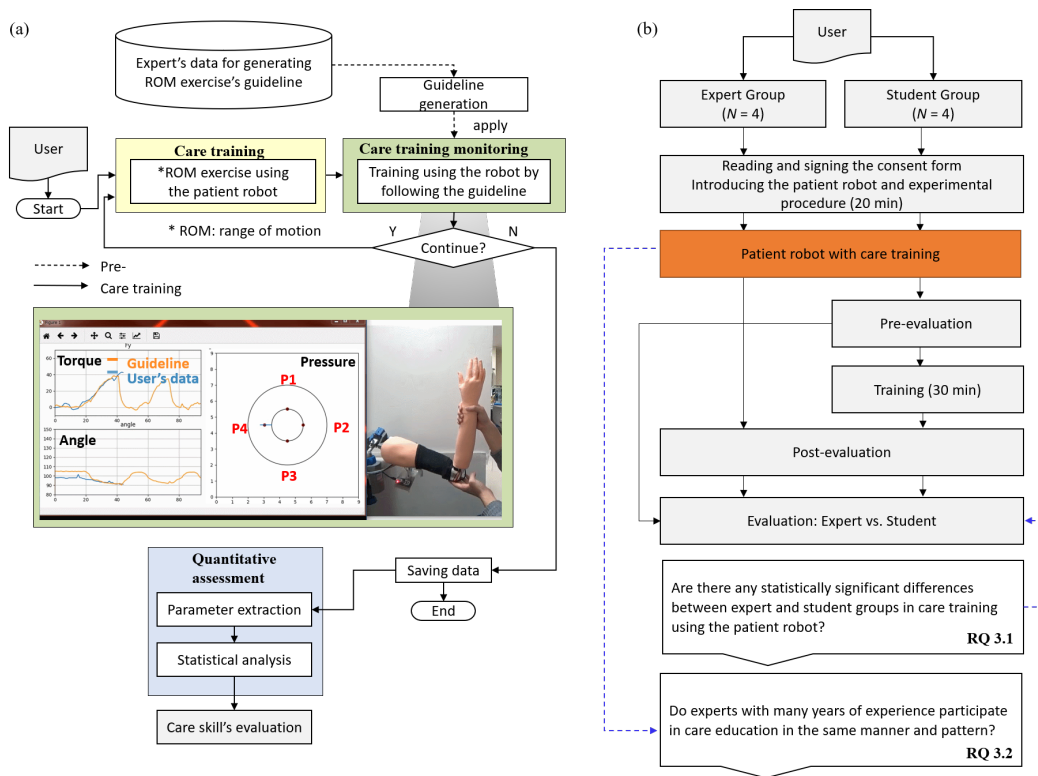
Figure 3.10. The flowchart of experiment (a) Procedure (b) Protocol.

All participants performed the experiment consisting of four kinds of ROM exercises—SEF, SED, SLM, and EEF—as shown in **Fig. 3.11** (a). In the order of SED, SEF, and SLM, and in certain cases, were performed with the robot lying on the bed, based on particular instructions [68, 69], the EEF exercise is performed with the robot's elbow joint fixed to the desk. The sensor data were obtained from the angle, torque, pressure sensors as shown in **Fig. 3.11** (b). The ROM exercises were performed for a total of three-set with each set of ten reps (**Fig. 3.11** (c)), and **Fig. 3.11** (d) is an example showing one trial (rep) of ROM exercise in SEF.

46
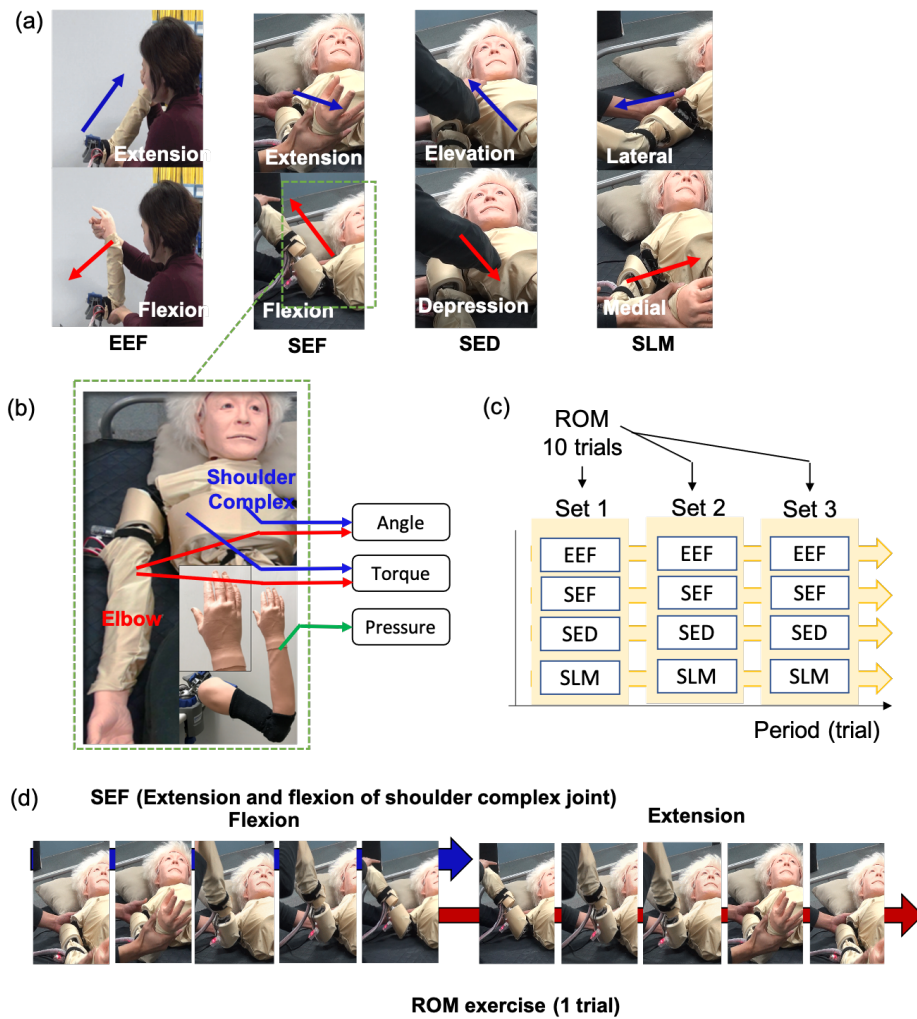
Figure 3.11. Experimental procedure of range of motion (ROM) exercises using the patient robot (a) ROM exercises: elevation and depression of the shoulder complex (SED), extension and flexion of the shoulder complex (SEF), lateral and medial rotation of the shoulder complex (SLM), and extension and flexion of the elbow complex (EEF) (b) Data acquired from sensors attached to joints (c) Description of the entire procedure (d) an example of a trial of the ROM movement.

3.7.4 Result of elbow ROM exercise

This assessment examines the effectiveness of care training using the patient robot in elbow ROM exercise, *i.e.*, EEF, for expert and student groups and aims to discuss quantitative results and differences between the two groups.

Fig. 3.12 depicts the quantitative data (i.e., the elbow joint angle, torque, and pressure data) obtained from the output of the elbow joint of the patient robot. **Fig. 3.13** shows the curve graph of the range of angle (ROA) and range of torque (ROT) in elbow exercise (EEF). For pre-evaluation, the size of both the angle and torque from student group (pre-test) were larger than those of experts (ground-truth). The values of angle and torque in each ROM cycle from the experts were constant (minor standard deviations), while there were large variations in the values from the students.
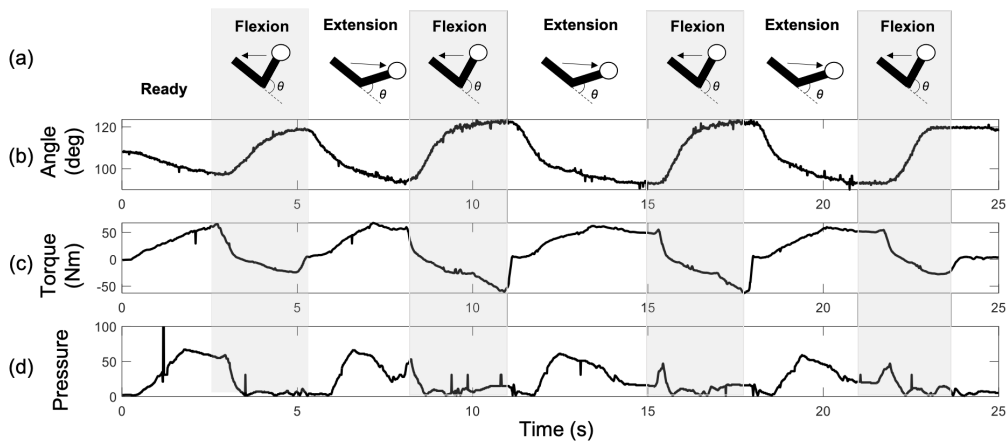
Figure 3.12. Example of quantitative data output from the robot's elbow joint in extension and flexion exercise (EEF) (a) Robot's elbow kinematics (b) Elbow joint angle (c) Torque (d) Pressure data.
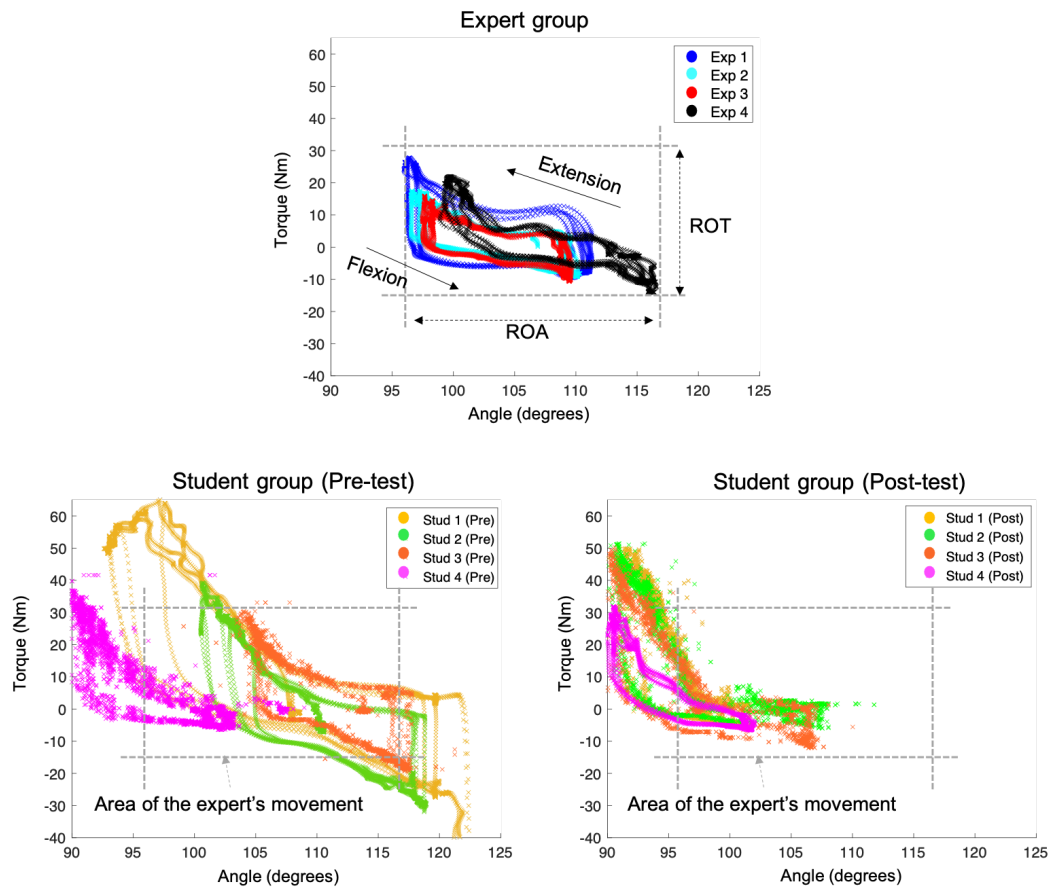
Figure 3.13. The graph of robot's data obtained from experts and students during elbow ROM exercise (EEF) training. ROT and ROA indicate the range of torque and angle value, respectively.

In addition, the graph of the expert shows a clear and constant pattern, and as the angle changes from about 95 to 115 degree, the force torque changes from 30 to -20 Nm. However, in the graph of student #1 (Stud #1 (Pre)), it is observed that the angular change is large, ranging from about 90 to 125 degree, and the force torque changes from about 95 to -40 Nm. These results show that considerable force is applied to the robot's elbow joint because the Stud #1 is male, and it is evident that there are marked variations in both the angle and force values. To interpret one more result, in the graph of student #2, the force torque varies from about 42 to -38 Nm while the angle varies from about 105 to 123 degree. Consequently, both the results of ROM from the

student group were higher than those of the expert group. This result emphasizes that there may be a negative impact on the elbow joint of a patient in the care environment. In the post-evaluation, the results of ROM for both Stud #1, Stud #2, and Stud #3, were significantly lower than the results of pre-evaluation. Based on the results, the angle and force torque of Stud #1 varied from about 87 to 105 degree and from 56 to -15 Nm respectively, and the angle and torque of Stud #2 varied from 84 to 115 degree and from 57 to -15 Nm respectively.
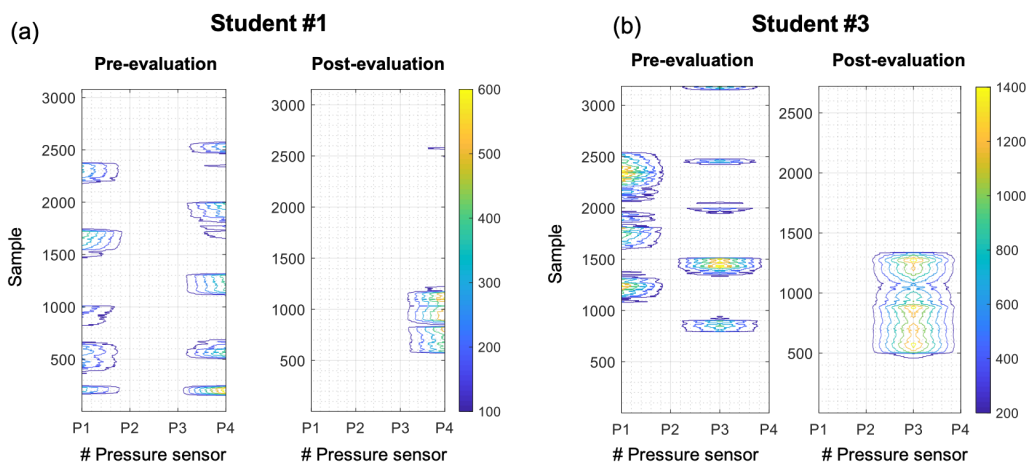
Figure 3.14. Example of contour of pressure values from pre- and post-evaluation of (a) Student #1 and (b) Student #3. P1: radius; P2: outside of the wrist; P3: ulna; and P4: inside the wrist. The rest of the participants in the experiment had little or no pressure sensor value.

Fig. 3.14 (a) and (b) shows the example of contours of the pressure data obtained from Stud #1 and Stud #3, respectively. In the contour, the x-axis represents the indices of pressure sensors, including P1 (radius), P2 (outside the wrist), P3 (ulna), and P4 (inside the wrist). The pressure data from the four pressure sensors by the experts was almost zero because they could control the force applied while gripping the wrist of the robot during the ROM exercise. For Stud #2 and Stud #4, the pressure value was almost zero. As shown in **Fig. 3.14**, in the pre-evaluation, the values of both P1 and P4 are high for each time the ROM training is performed. The results show

that Stud #1 applied pressure on the pressure sensor of the robot's elbow joint during ROM training. However, from results of post-evaluation, it is evident that pressure values only appear twice in P4 and the remaining pressure sensors are not generating any values. In the contours of Stud #3, the values in P1 and P3 appear for each cycle of the ROM training. For the post-evaluation, the pressure value of P3 is represented but the other pressure sensors are not presenting any values. Based on these results, it can be concluded that Stud #1 and Stud #3 did not apply excessive force on the pressure sensors attached to the patient robot's elbow joint after practicing the ROM exercise. These result denotes that when performing passive ROM training, the exercise helps the caregiver develop the ability not to apply force on the wrist of the patient.

Fig. 3.15 depicts the comparison results of ROM training from the experts, students (pre-test), and students (post-test). For the comparison result of the robot's elbow angle, there were statistically significant differences in all groups ($p<0.0001$, analysis of variance (ANOVA) test). In particular, it can be seen that the average angle of the student group's post-test (mean (M)=96.97, standard deviation (SD)=4.73) was shifted close to about 96 degrees compared with that of the pre-test (M=105.31, SD=8.86) ($p<0.01$, z=75.18, Kruskal-wallis test), but the deviation of the angle decreased, resulting in a decrease in the range of motion of the robot elbow joint. Similarly, in case of the torque result, it was confirmed that the deviation in the post-evaluation (M=11.63, SD=16.86) was significantly reduced compared to the pre-evaluation (M=6.57, SD=21.55) ($p<0.01$, z=21.04, Kruskal-wallis test). In the results as shown in **Fig. 3.15**, there was a well-marked difference between the pre-and post-evaluation of the pressure sensor's results ($p<0.0001$, z-value=45.10, Kruskal-wallis test). In the pre-evaluation, the mean of pressure signal magnitude of area (PSMA) was 6.18 (10.90), decreased significantly to 1.32 (5.28) at the post-evaluation.
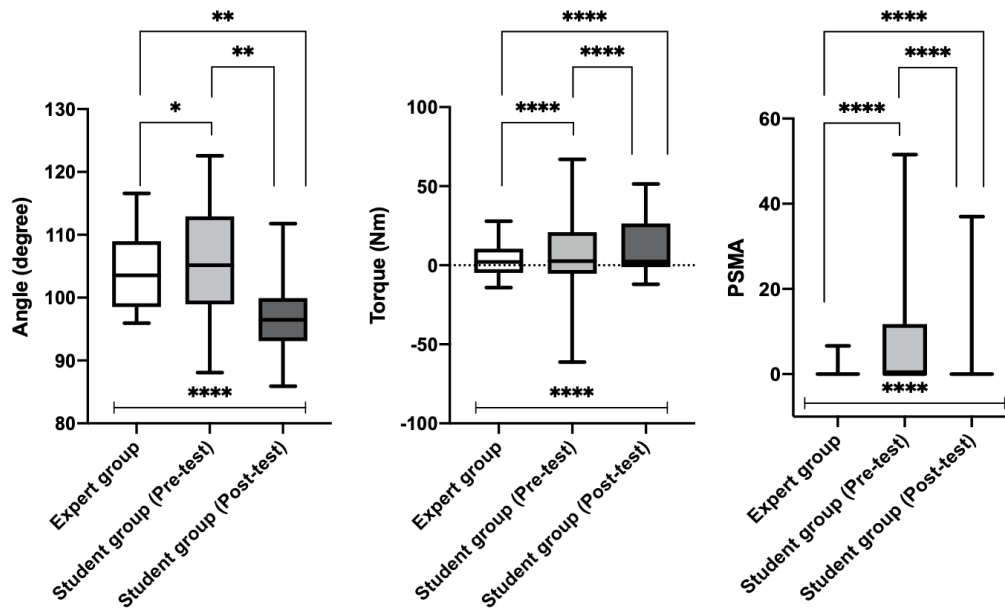
Figure 3.15. Comparison results of the elbow ROM exercise (EEF) among groups (experts vs. students (pre-test) vs. students (post-test)). PSMA means the pressure signal magnitude of area. The asterisk below the bar-graph indicates the statistical result using the ANOVA test among three groups, and the asterisk above the bar-graph indicates the statistical results using the Dunn's multiple comparison test between the two groups. The significance level was set at $\alpha = 0.05$. The asterisk (*), two asterisk (**), and four asterisk (****) indicate statistical significance at $p < 0.05$, $p < 0.01$, and $p < 0.0001$, respectively.

3.7.5 Result of shoulder ROM exercises

This assessment examines the effectiveness of care training using the patient robot in shoulder ROM exercises with SEF, SED, and SLM for expert and student groups and aims to discuss quantitative results and differences between the two groups. **Fig. 3.16** illustrates an example of obtaining quantitative data of the robot from the shoulder ROM exercises by Exp #1. **Fig. 3.16** (a) is the sensor data of the robot acquired in the SEF motion. To interpret the raw data's graph, when the shoulder is extended from flexion to extension based on the GH2 joint of the shoulder complex in SEF exercise, the GH2's angle increases from 0 to roughly 120 degrees, whereas the SC1's angle decreases from 0 degrees to about -50 degrees. From this data, it can be observed that the GH2 and SC1 joints move simultaneously in the extension of the SEF, and it can be confirmed that the force sensor located in the GH also outputs a constant torque according to the extension movement. **Fig. 3.16** (b) is a graph of data output in the SED exercise. The elevation movement of the SED causes the robot's shoulder to move in the vertical direction based on the SC1 joint. Here, the SC1 joint has a range of motion between approximately from roughly -20 degrees to 15 degrees, and the GH2 joint is also involved at the same time. In the case of torque, it was output from about 10 to -20 Nm based on the SC joint. Finally, in SLM (**Fig. 3.16** (c)), the GH3 joint's range of motion increased from about -100 to 10 degrees in the lateral rotation movement, and the movement of the GH1 joint was also observed very finely. On the other hand, it was observed that the values of the torque sensors of SC and GH were output in a similar pattern. Although the results of the graphs mentioned above were limited to the example of Exp #1, the range of motion (angle) of each ROM exercise was similar, but there was a slight difference in the range of torque, the ROM cycle's duration, and the interval both of two ROM movements. Based on these quantitative data, the results were analyzed to evaluate the necessity and the feasibility of the proposed patient robot for the care education.
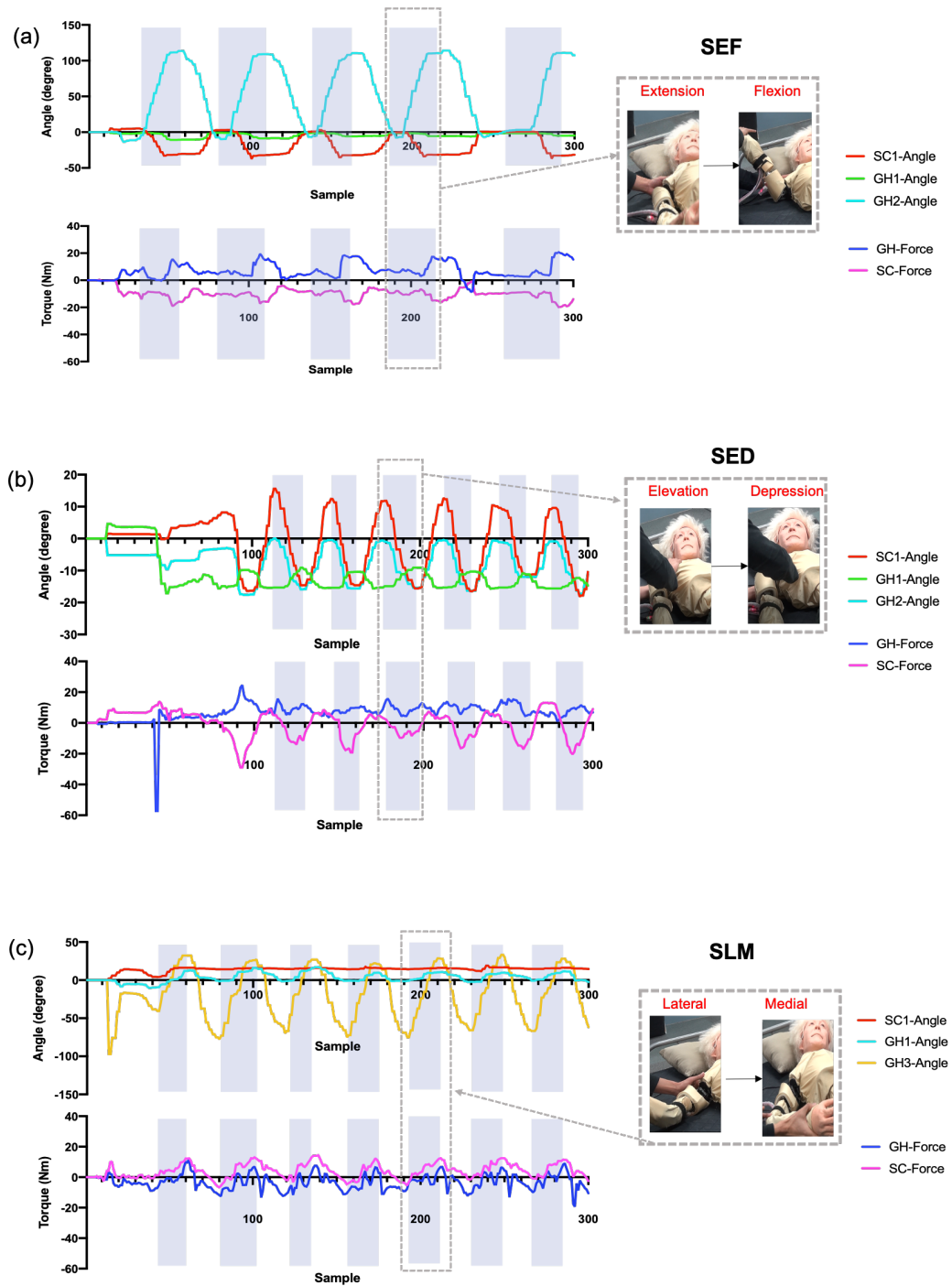
Figure 3.16. Example of quantitative data output from the robot's shoulder complex in (a) Extension and flexion exercise (SEF), (b) Elevation and depression (SED), and (c) Lateral and medial rotation (SLM). GH and SC indicate the glenohumeral and the sternoclavicular joint, respectively.

The experts and students perform the SEF exercise based on the grip positions as shown in **Fig. 3.17** (a), and **Fig. 3.17** (b) illustrates the mechanism of the shoulder complex in SEF exercise. In **Fig. 3.17** (c), the movements performed by the expert group were almost the same as each other. When student #4 (Stud #4) performed the exercise in the pre-test, however, the joint angles were not constant in the time domain, because Stud #4 did not perform a complete movement from flexion to extension, *i.e.*, a contraction was performed again after a slight joint relaxation.
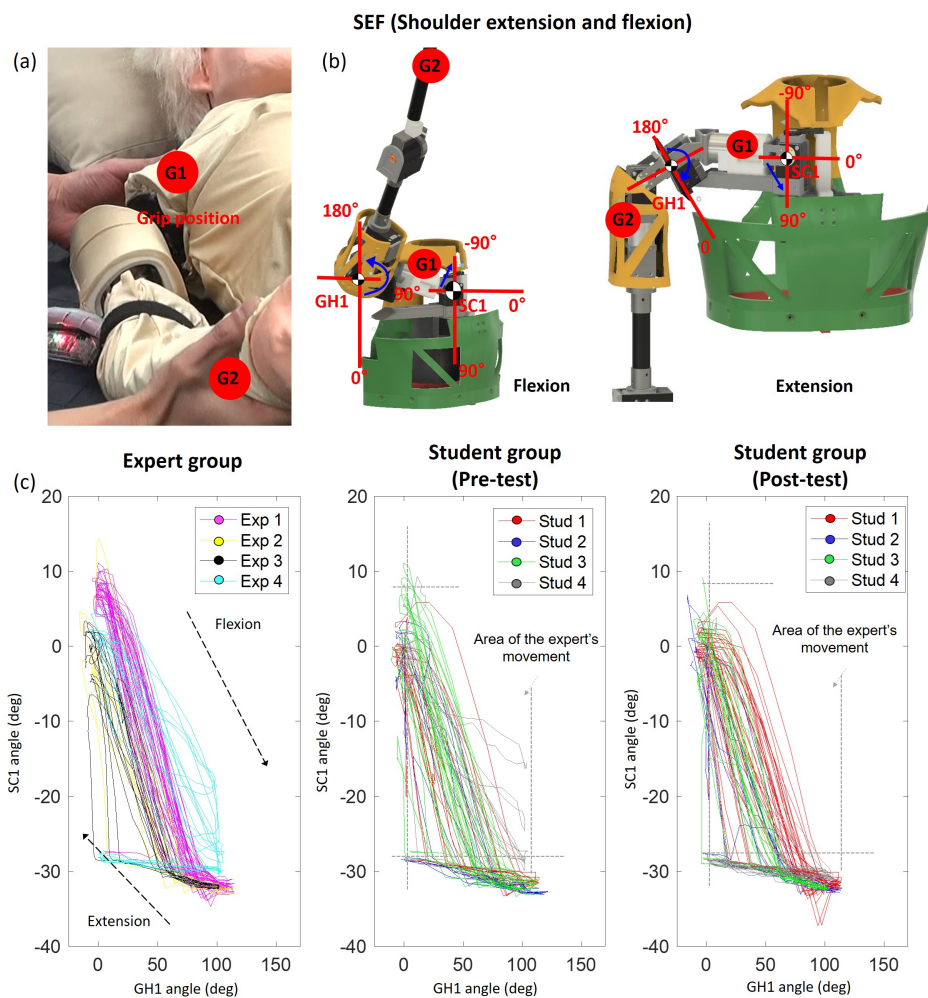
Figure 3.17. Graph of sternoclavicular (SC) and glenohumeral joints (GH) in extension and flexion (SEF) exercise: (a) Grip positions (b) Mechanism of SEF exercise (c) Angle curves between SC1 and GH1 joints.

For the SED exercise, the experts and students perform the exercise based on the grip positions shown in **Fig. 3.18** (a). The robot's shoulder complex moved based on GH2 and SC1 (**Fig. 3.18** (b)), and **Fig. 3.18** illustrates a graph of the SC1 and GH2 joints in SED exercise. In the SED exercise, the joint movements of SC1 and GH2 were clearly represented, in which, the experts performed each cycle of SED exercise in constant motion range. However, the student group in the pre-test differed slightly in the motion range of the joints.
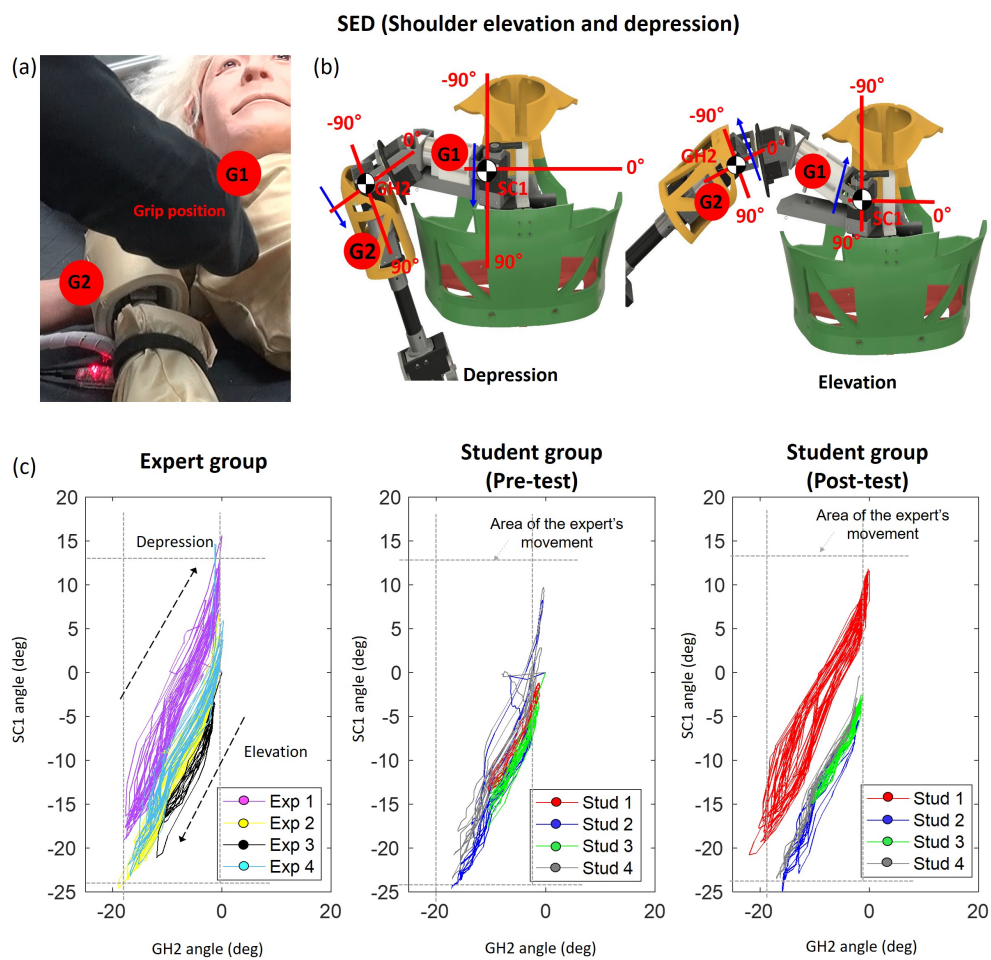
Figure 3.18. Graph of sternoclavicular (SC) and glenohumeral joints (GH) in elevation and depression (SED) exercise. (a) Grip positions (b) Mechanism of SED exercise (c) Angle curves between SC1 and GH2 joints.

In the SLM, the participants performed the exercise by holding the shoulder and wrist of the robot (**Fig. 3.19** (a)), and the robot's joint moved as the mechanism in **Fig. 3.19** (b). In **Fig. 3.19** (c), a graph representing the SLM exercise based on the GH1 and GH3 joints was presented. In the SLM exercise, the results of all students were significantly different. The Stud #1 and Stud #3 had relatively a constant joint angle amplitude and period for each motion cycle. However, the angle range of the GH1 joint of Stud # 2 and Stud # 4 was more extensive compared to the expert group, and it can be suggested that the joint of GH1 was moved excessively when the joint was rotated relative to GH3.
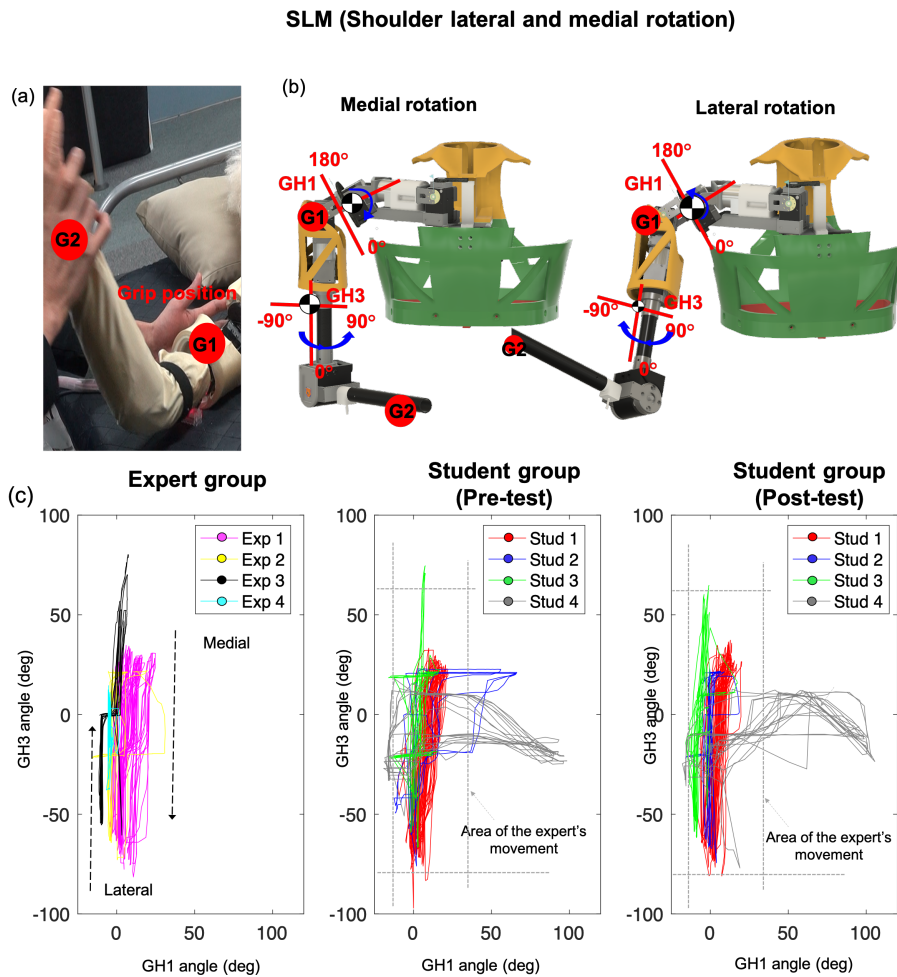
Figure 3.19. Graph of the glenohumeral joints (GH) in lateral and medial rotation (SLM) exercise. (a) Grip positions (b) Mechanism of SEF exercise (c) Angle curves between GH1 and GH3 joints.

Fig. 3.20 shows the statistical analysis of the robot's data obtained in all shoulder ROM exercises. The joint angle and torque data obtained were statistically significant in most three groups due to differences in individual's care techniques and skills.
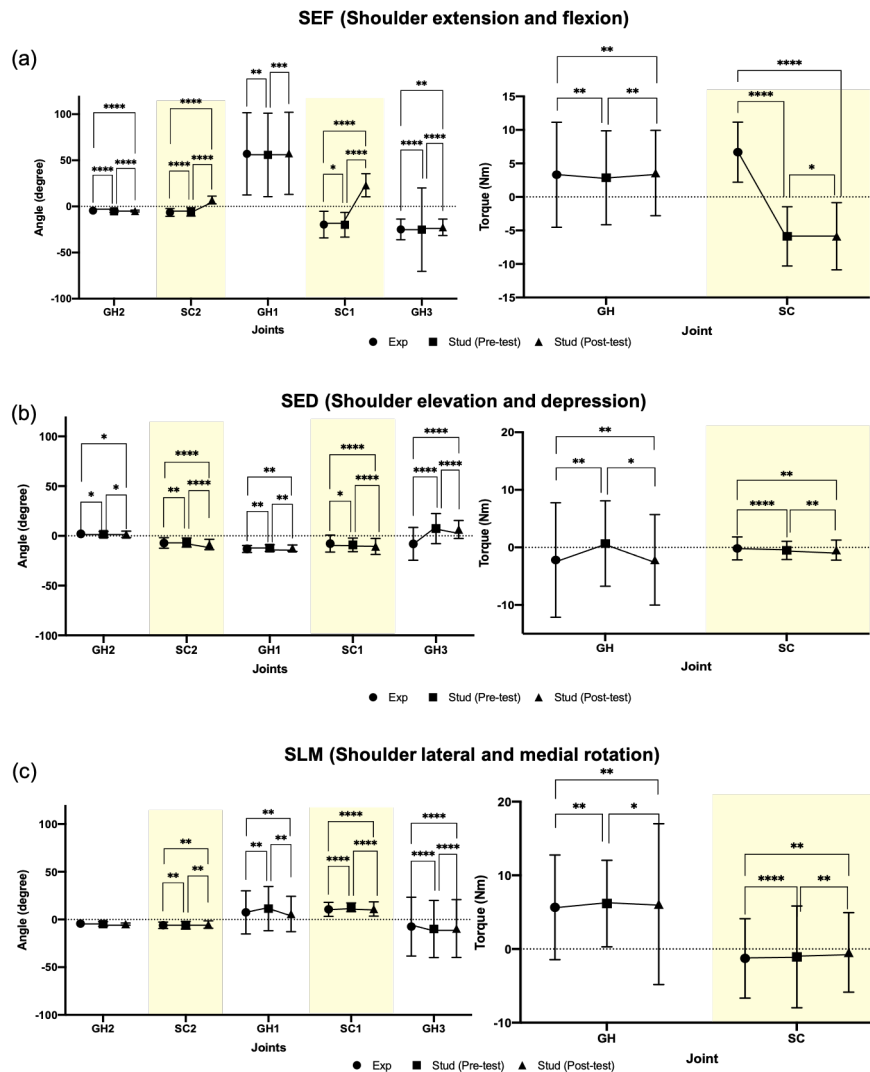
Figure 3.20. Statistical analysis of the quantitative data of the patient robot in shoulder ROM exercises (a) Extension and flexion (SEF) (b) Elevation and depression (SED) (c) Lateral and medial rotation (SLM). The asterisk above the graph indicates the statistical result using the Dunn's multiple comparison test between the two groups. The significance level was set at $\alpha = 0.05$. The asterisk (*), two asterisk (**), and three asterisk (***), and four asterisk (***) indicate statistical significance at $p < 0.05$, $p < 0.01$, $p < 0.001$, and $p < 0.0001$, respectively.

58

Based on the interpretation of the results mentioned above, the observation can be suggested in **RP 3.1** as follows:

- **Observation 3.1)** There was a statistically significant difference between the expert and student groups in the ROM exercises using the patient robot. In particular, the EEF exercise showed notable results demonstrating the effectiveness of care training using the patient robot in the pre-and post-evaluation of the student group.

3.7.6 Results of care skills in the expert group

This evaluation investigates whether skilled professionals conduct care tasks with the same care skills or not (**RP 3.2**). Moreover, the additional assessment examines whether experts with many years of experience in the care environment perform care tasks with the same methods and skills and examines the quantitative results of their care education performance (**RP 3.3**).

Table 3.4, **Table 3.5**, and **Table 3.6** show the results of the statistical analyses based on several parameters in SED, SEF, and SLM exercise, respectively. To statistically evaluate the acquired data, all the eleven parameters were extracted: the maximum parameters consist of the angle of SC1 (MAX-SC1), SC2 (MAX-SC2), GH1 (MAX-GH1), GH2 (MAX-GH2), and GH3 (MAX-GH3); The minimum parameters contains of the angle of SC1 (MIN-SC1), SC2 (MIN-SC2), GH1 (MIN-GH1), GH2 (MIN-GH2), and GH3 (MIN-GH3); and the interval between consecutive cycles (INTV). Based on these parameter, an ANOVA test was conducted to analyze statistically significant differences among the experts.

Table 3.4. Comparison of results of parameters from all experts in SED exercise.

	Exp 1	Exp 2	Exp 3	Exp 4	*p*-value
MAX_SC1	12.58 (1.91)	0.34 (2.89)	-4.84 (1.27)	4.92 (2.24)	<0.01
MAX_SC2	5.51 (2.16)	6.59 (1.56)	2.59 (0.59)	4.21 (0.41)	<0.05
MAX_GH1	3.16 (2.11)	-1.57 (0.59)	-6.09 (1.13)	-13.2 (2.16)	<0.01
MAX_GH2	-0.42 (0.25)	-1.22 (0.54)	-1.66 (2.59)	3.18 (3.12)	<0.05
MAX_GH3	2.14 (0.42)	-1.56 (0.35)	14.56 (1.93)	0.51 (2.54)	<0.01
MIN_SC1	-15.84 (0.77)	-21.12 (3.26)	-17.66 (5.98)	-11.35 (6.31)	<0.01
MIN_SC2	-17.11 (2.59)	-24.56 (5.69)	-22.09 (3.78)	12.44 (3.22)	<0.01
MIN_GH1	-18.26 (1.59)	-16.89 (2.36)	-16.12 (4.59)	-13.24 (4.26)	=0.148
MIN_GH2	-16.36 (0.74)	-15.76 (2.43)	-10.98 (0.62)	-10.24 (0.73)	<0.01
MIN_GH3	-30.15 (0.59)	-22.09 (2.46)	0.59 (0.05)	-21.34 (9.51)	<0.01
INTV	2.26 (2.27)	2.33 (0.32)	4.81 (0.62)	3.31 (3.15)	<0.01

Note: MAX, MIN, and INTV indicate the maximum, minimum, and interval value, respectively. SC and GH mean the sternoclavicular and glenohumeral joint.

Table 3.5. Comparison of results of parameters from all experts in SEF exercise.

	Exp 1	Exp 2	Exp 3	Exp 4	*p*-value
MAX_SC1	3.44 (1.78)	-23.6 (8.18)	-1.24 (2.33)	0.68 (1.61)	****
MAX_SC2	0.56 (0.59)	0.98 (0.56)	0.46 (0.12)	0.16 (0.55)	=0.215
MAX_GH1	111.65 (2.14)	72.06 (2.89)	101.32 (0.75)	102.44 (0.95)	***
MAX_GH2	0.59 (0.55)	1.26 (1.56)	2.56 (0.09)	1.59 (0.14)	**
MAX_GH3	0.67 (0.15)	0.84 (0.59)	0.59 (0.06)	2.59 (1.46)	**
MIN_SC1	-35.2 (2.19)	-32.86 (0.32)	-32.42 (0.11)	-25.74 (5.65)	**
MIN_SC2	0.99 (0.05)	-20.13 (1.35)	-5.69 (1.54)	-10.59 (2.54)	****
MIN_GH1	-6.86 (2.51)	24.74 (32.37)	-7.51 (3.17)	-5.06 (2.3)	****
MIN_GH2	0.59 (0.16)	-20.56 (8.56)	0.81 (0.56)	-2.46 (1.33)	***
MIN_GH3	-79.59 (21.59)	-65.11 (21.56)	-20.59 (8.59)	-78.59 (16.59)	***
INTV	3.91 (0.71)	2.64 (4.91)	2.61 (1.62)	1.61 (6.23)	=0.312

Note: Abbreviations are as described in **Table 3.4**.

Table 3.6. Comparison of results of parameters from all experts in SLM exercise.

	Exp 1	Exp 2	Exp 3	Exp 4	*p*-value
MAX_SC1	20.56 (5.95)	22.15 (11.25)	15.46 (11.21)	17.59 (10.59)	****
MAX_SC2	0.51 (0.12)	0.89 (1.56)	2.16 (0.56)	7.56 (2.64)	**
MAX_GH1	12.62 (3.62)	5.61 (1.21)	11.8 (4.17)	35.08 (2.9)	****
MAX_GH2	2.21 (2.13)	0.75 (0.54)	0.56 (2.16)	0.51 (0.55)	*
MAX_GH3	27.64 (4.01)	21.86 (0.72)	44.16 (26.26)	10.7 (1.29)	****
MIN_SC1	0.12 (0.65)	0.16 (0.13)	1.26 (0.05)	0.11 (1.62)	*
MIN_SC2	1.26 (0.11)	-1.59 (0.59)	2.59 (1.56)	2.56 (2.32)	*
MIN_GH1	-1.98 (0.44)	-0.58 (5.87)	-11.22 (5.42)	-17.32 (1.42)	****
MIN_GH2	0.99 (0.94)	-18.46 (11.54)	-8.56 (4.13)	-18.56 (4.59)	****
MIN_GH3	-72.72 (4.58)	-65.94 (53.53)	-55.94 (10.42)	-32.3 (1.2)	****
INTV	2.51 (0.39)	1.95 (3.57)	5.91 (3.97)	5.8 (0.75)	****

Note: Abbreviations are as described in **Table 3.4**.

In **Table 3.4**, all parameters except MIN-GH1 (p=0.148) were observed to show significant differences between experts in SED exercise. For the SEF exercise (**Table 3.5**), it was observed that most parameters except MAX-SC2 (p=0.215) and INTV (p=0.312), were exhibited significant differences among the experts. In **Table 3.6**, all parameters showed significant differences among experts in SLM exercise. **Fig. 3.21** depicts the radar charts of the parameters in shoulder ROM exercises.
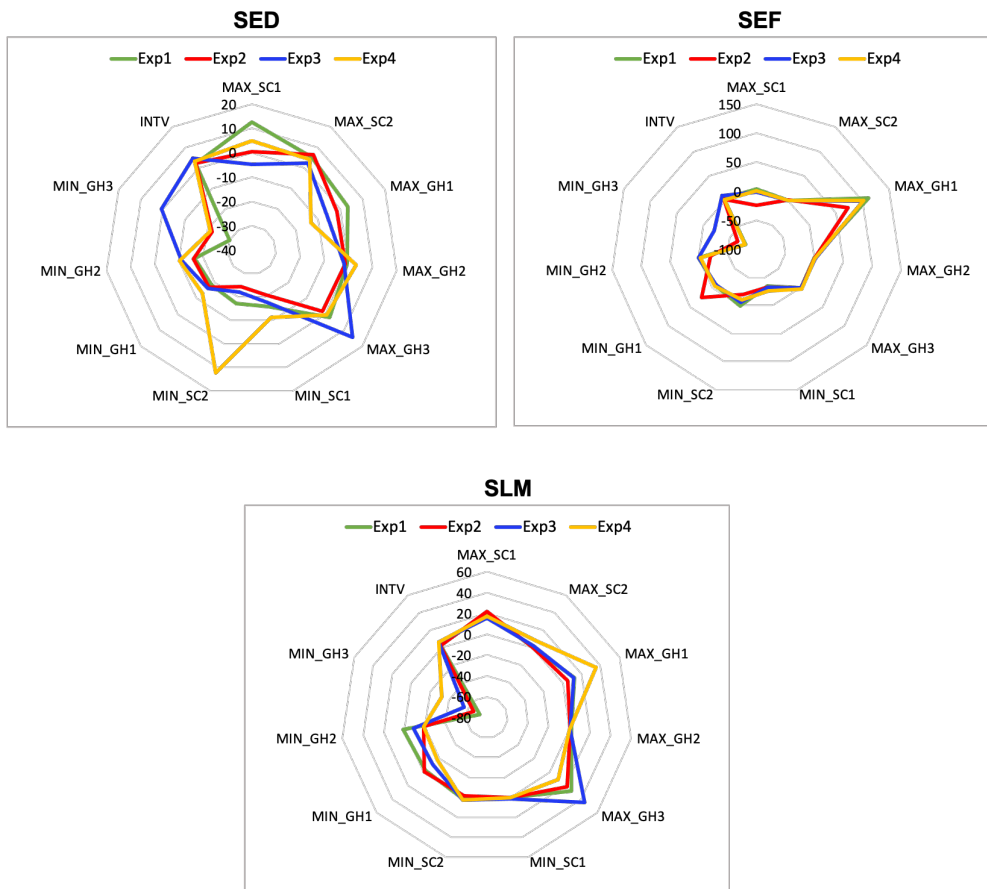
Figure 3.21. Radar charts of the parameters in shoulder elevation and depression (SED), shoulder extension and flexion (SEF), and shoulder lateral- and medial rotation (SLM) exercise from the experts.

Based on these results, the following observation according to **RP 3.2** can be suggested:

- **Observation 3.2)** The findings of this experiment suggest that although experts have several years of experience, they may perform care and treatment differently from each other. Different methods of care and treatment may induce a detrimental effect on the joints and muscles of a patient. Thus, a customized and suitable care-education method for individuals should be provided on the basis of quantitative data analysis.

3.7.7 Questionnaire I: Reviews using the robot

In this evaluation, the results of a survey on the feasibility and the potential possibility of care education using patient robots are interpreted (**RP 3.3**). The first survey was conducted with four experts using the proposed patient robotic system. The survey consisted of the following four questions:

- Q1) Does the patient robot with real-time monitoring program provide a user-friendly interface?

- Q2) Do the robot's movements perform similarly to those of an actual human?

- Q3) How are you satisfied with the patient robot for the training of the trainee?

- Q4) In the future, would you be willing to use the patient robot for care training of ROM exercises?
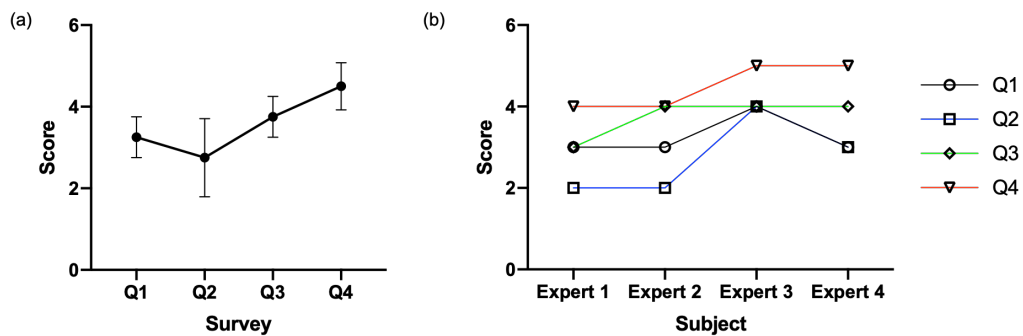
Figure 3.22. The questionnaire result from four experts using the patient robot in care training (a) Graph of the mean and deviation of all experts according to the survey items (b) Scores on individual survey items by experts. The scores range from one to five..

Fig. 3.22 shows the results of the questionnaire from the four experts. The mean scores of Q1, Q2, Q3, and Q4 were 3.25 (±0.50), 2.75 (±0.96), 3.75 (±0.50), and 4.5 (±0.58) out of a maximum of five, respectively. These results are favorable, although the experts indicated that the perceived feel of the robot was slightly different to that of actual human's joint movement.

3.7.8   Questionnaire II: Reviews of the feasibility

The second survey was conducted with thirty reviewers to investigate the feasibility of the patient robot for care training. These reviewers did not directly use the patient robot, but reviewed and voted the robot's usefulness based on detailed descriptions and experimental videos of the patient robot. The survey consisted of the following three questions:

- Q5) Among the various nursing care training methods, do you think which number is the most effective?

- Q6) Do you think which number needs to be improved the most in patient robots for care education?

- Q7) What do you think about the usability and feasibility of the proposed patient robot in the future?

Table 3.7 shows the voting scores obtained from thirty reviewers. In the case of Q5, the patient robot and role-playing scored 19 and 11, respectively, and there were many subjective opinions that the patient robot would be useful in situations or environments where face-to-face education was limited. In Q6, the scores of the both 'Interaction' and 'Feedback' were scored 12 and 15, respectively. For Q7, which is about the potential of future development of patient robots, the answer was very positive.

Table 3.7. The voting result of the questionnaire II from thirty reviewers.

		Voting answer				
Q5	Item	Book	Video	Medical manequine	Patient robot	Role-payling
	Score	0	0	0	19	11
Q6	Item	Interaction	External design	Feedback (care training skills)	Low-cost	
	Score	12	1	15	2	
Q7	Item	Very weak	Weak	Moderate	Strong	Very strong
	Score	0	0	1	3	26

Based on these findings of the survey, an observation can be defined for **RP 3.3** as follows:

Observation 3.3) It can be concluded that the patient robot proposed in this study will be helpful to trainees with a friendly interface and effective care training ability in the future.

3.8 Discussion

This Chapter presented the patient robot for care for quantitative evaluation and efficient training of caregivers. The mechanism of the patient robot was designed based on the actual human physical size and reproduced the musculoskeletal symptoms. To investigate the feasibility of the proposed patient robot, medical experts and novices were invited for the feasibility experiment, and quantitative data such as joint angle, torque, and pressure value using the pressure sensors were obtained during the range of motion (ROM) exercises. There was a statistically significant difference between the expert and student groups in the patient robot's ROM exercises. In particular, the elbow exercise has shown notable results, demonstrating that using the elbow joint-simulated robot with real-time care training and monitoring program results in significant improvements in pre-and post-evaluation. However, a limitation of the study is that it is difficult to generalize the results yet because of insufficient data from the subjects. Nonetheless, though the range of angle of the robot's joint was hypothesized to be the specific range based on the opinions of professional caregivers, the value and feasibility of using the proposed method in improving the care training for caregivers were significant.

Further, this research aimed to experimentally investigate whether there was a difference in the quantitative data results among the experts during the care training. Consequently, our findings suggested that even experts with many years of experience may have different methods, thus, introducing a negative impact on care and treatment. Therefore, the necessity and the feasibility of the care training assistant robot should be utilized to improve accuracy and elaborated care skills in elderly care education.

Chapter 4

Pain inference and expression for patient robot

This Chapter aims to develop a pain inference and expression for a care training assistant robot that can express pain states in joint care education. First, to develop an automated feedback system for patient care training, the study introduces a fuzzy logic-based care training evaluation method that can infer the pain level of a robot. The fuzzy-logic-based pain inference method is developed to calculate the robot's current pain levels by combining four key parameters of the quantitative data obtained from the patient robot. Next, a novel pain facial expression database (RU-PITENS) was introduced for an avatar with pain expression. The RU-PITENS database contains pain images of Japanese people, and an experiment of pain stimulus is conducted based on transcutaneous electrical nerve stimulation, which is low-cost and easy to use in daily life. Based on the pain images in the RU-PITENS database, an avatar with pain expression was propose to achieve the goal of the study. To obtain pain intensity from images, a Siamese network based on a convolutional neural network (ConvNet) with three layers was used and classified the pain intensity into five pain groups by calculating the intensity for each image. The pain facial expression system will be constructed to express five types of pain (no pain at all, very faint, weak, moderate, and strong pain) with avatars according to the intensity of the pain output of robot in care training environments. It is anticipated that an advanced patient robotic system provides efficient feedback on the care and nursing training by utilizing the proposed method of pain inference and expression.

4.1 Motivation

In CNT, the pain level can be defined as a quantitative value that can evaluate how well a student performs care training without burdening the joint of the patient robot during care education. The pain level is directly related to the care ability of the caregiver. The care or nursing skills can be assessed by statistical methods or surveys. Wang *et al*. [23] assessed the survey responses from doctors by using the arm robot developed, Kim *et al*. [63] compared the robot with in-person by using questionnaire results to improve the reliability of clinical assessment. Takanobu *et al*. [29] proposed the dental patient robot with a questionnaire assessment. However, the evaluation based on surveys tends to be biased by an individual's perspective [70]. Thus, more accurate and efficient quantitative assessment methods for care skills are required. Most care training studies use statistical or empirical techniques that can analyze results manually. These methods are proper for analysis of each parameter and easy to use when investigating the effect of parameters on care training. However, it is difficult for trainees to evaluate their treatment quantitatively in a real-time system, and there is a limitation in calculating the final score automatically after finishing care education. Therefore, there is a need to develop a method for automatically inferring the care and nursing skills and the robot's pain level based on data acquired from sensors mounted on the robot. In addition, the caregivers should periodically investigate whether the patient is feeling pain or not and observe painful expressions on the patient's face during care conducting because the patient may experience difficulty in communication with caregivers.

4.2 Objectives and research problems

4.2.1 Specific objectives

The objectives of the method for pain inference and expression of the patient robot introduced in this Chapter to achieve the goals are as follows:

- To provide automated quantitative assessment feedback on care training to the caregiver.

- To develop a method for pain inference for the care training system.

- To build a database to generate a robot's avatar by recruiting subjects of various ages.

- To expresses the current pain state through the robot's avatar.

4.2.2 Research problems

To achieve the goals, several research problems must be solved as follows:

- **RP 4.1)** Are there any significant differences between the initial trial and final trial based on the proposed pain inference method?

- **RP 4.2)** Are there any significant differences between the student and the expert group based on the proposed pain inference method?

- **RP 4.3)** Is it proved that facial images representing pain obtained from a subject via a TENS device are included in the actual pain area?

4.3   Pain inference

Pain is a response that protects the body from damage when the patient is subjected to physical pressure from external factors, and the pain level is a quantitative value that can be used to assess a student's ability to train care's skill without causing any pain to the patient robot's joints during care education. **Fig. 4.1** illustrates the whole framework of the proposed pain expression of patient robot in this Chapter. More detailed description based on this framework is given in the next Section.
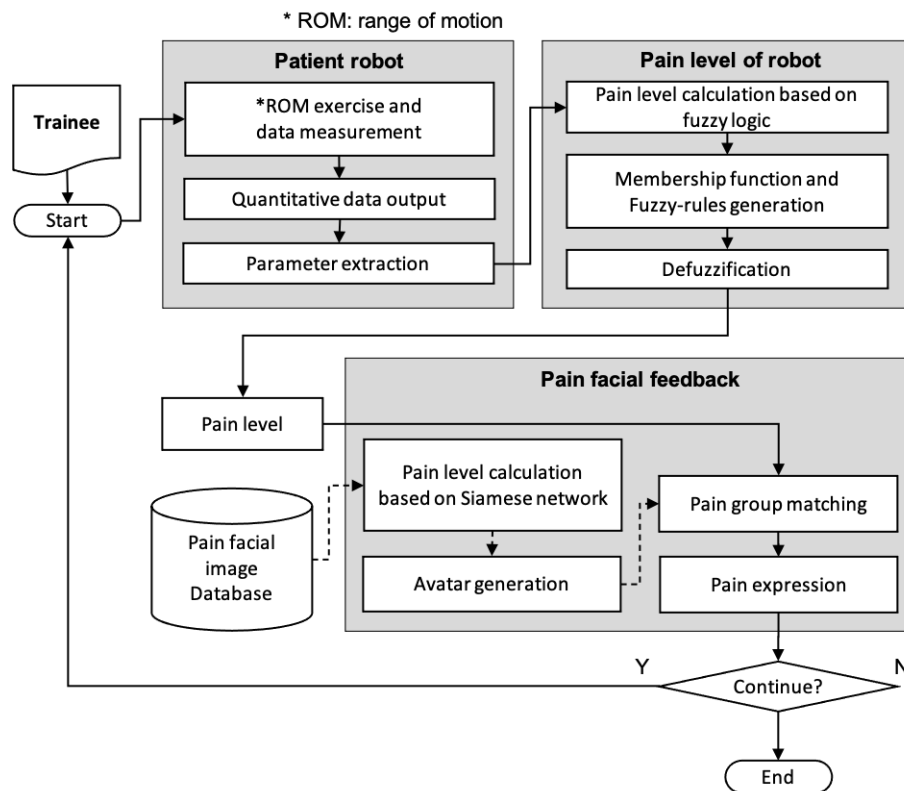
Figure 4.1. The whole framework of the proposed pain expression.

4.3.1 Hypothesis

Before building the model for measuring pain level, the study in this dissertation consolidated several hypothesis:

- The resistance torque increases when the joint of the patient robot is out of specific degrees (refer to Chapter 3). The range of motion of the patient robot's joint was designed based on expert opinion to mimic the joint of a patient with musculoskeletal disease. **Table 4.1** shows the pain inference factors of the patient robot, and it is assumed that the patient robot may felt pain when the joint angle of the patient robot is out of a determined parameter's range.

- The reference data (pain inference factors) for generating membership functions is based on data from five trials involving an expert who has years (two to ten years) of experience in the medical field. In future studies, the reference data may include data from patients with musculoskeletal or neurological diseases.

The reference data given to generate pain inferences is determined by the expert's opinion. Therefore, the final robot's pain value obtained by calculating the robot's sensor data collected during care education is to infer the distance from the reference data. Thus, the pain level of the robot is evaluated based on the reference data (expert's opinion), and the comparative evaluation between groups can be possible using the proposed pain inference method.

Table 4.1. Pain inference factors.

Factor (unit)	Joint	Elbow	Shoulder		
	Exercise	EEF	SEF	SED	SLM
	Reference Joint	Elbow	GH1	SC1	GH3
	Parameter	Value			
Angle (degrees)	Low	100	20	-5	-15
	Moderate	95 to 125	10 to 100	-15 to 15	-20 to 20
	High	120	90	10	15
Torque (Nm)	Low	-10	5	-5	0
	Moderate	-15 to 35	0 to 15	-10 to 10	-5 to 10
	High	30	10	5	5
Angular velocity (degree/s)	Low	-1	-1	-1	-1
	Moderate	-1.5 to 1.5	-1.5 to 1.5	-1.5 to 1.5	-1.5 to 1.5
	High	1	1	1	1
PSMA	Low	40	N/A	N/A	N/A
	Moderate	20 to 80	N/A	N/A	N/A
	High	60	N/A	N/A	N/A

Note: PSMA indicates the pressure signal of magnitude area. N/A means not assigned.

4.3.2 Fuzzy logic-based pain inference

To generate the model for pain inference, this study uses the fuzzy-logic theory, which is a proper method to solve ambiguous problems. The specific purposes for using fuzzy-logic theory for pain inference are as follows:

- This study does not consider classifying the state of pain but requires an output value of pain intensity

- The relationship of various input variables that determine pain level is required to measure the pain level

- The fuzzy logic makes it possible to define such relationships and allowable ranges of movement that the joint of the robot can allow

- This study focuses on the relationship among various factors is more important than the feature extraction of various factors that determine pain level

The fuzzy set theory of Zadeh [71] is frequently used as a suitable method to consider ambiguous problems that are complex or uncertain in real-world contexts. A fuzzy system has the advances that it determines the relationships between input and output variables and it can describes the interpretation of relationships among input variables [72]. The output values of the fuzzy-logic method can be obtained by using the **Eq. 4.1**.

$$f_s(X) = \frac{\sum_{l=1}^{M} \theta_l \prod_{k=1}^{P} \mu_{F_k^l}(x_k)}{\sum_{l=1}^{M} \prod_{k=1}^{P} \mu_{F_k^l}(x_k)} \tag{4.1}$$

where x, k, M, and P indicate the input variable, the kth element of the vector x, the number of membership functions, and features, respectively. $\mu_{F_k^l}(x_k)$ is the membership function and θ_l is the weight.

To generate fuzzy inference for fuzzy-based pain intensity (FLPI), input variables of the angle, angular velocity, torque, and the mean of the pressure signal magnitude area (PSMA) were obtained from the robot's joint. Here, as shown **Fig. 4.2**, the fuzzy model is divided into two approaches based on the ROM exercises of care education: i) fuzzy logic-based pain inference of the ROM exercise of the elbow joint (FLPI-EROM); ii) fuzzy logic-based pain inference of the ROM exercises of the shoulder complex (FLPI-SROM).

- FLPI-EROM: This model is based on input variables such as angle, torque, angular velocity, and PSMA for pain inference in the extension-flexion movement of the elbow complex.

- FLPI-SROM: This model is based on input variables such as angle, torque, and angular velocity for pain inference in the ROM exercises (SEF, SED, and SLM) of the shoulder complex. In particular, since the hardware configuration of the shoulder complex does not include a pressure sensor, there is no pain inference factor for the pressure value.
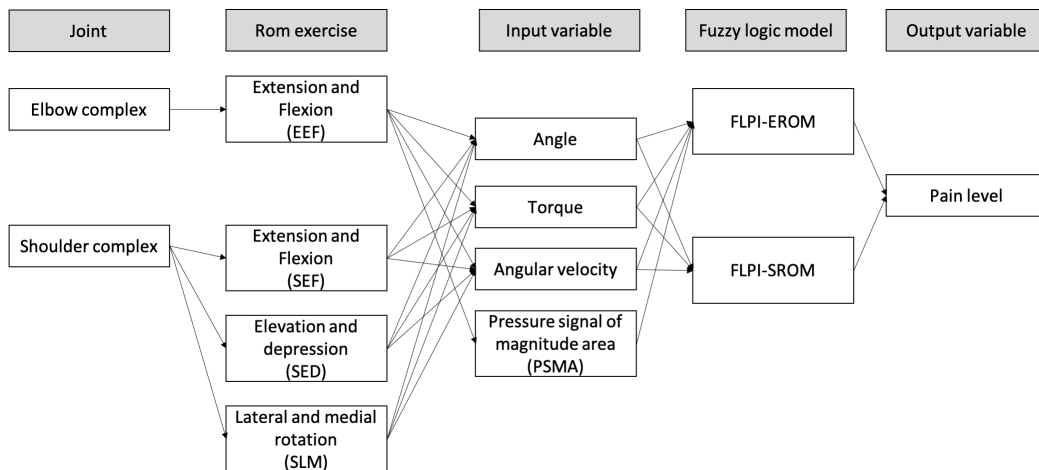
Figure 4.2. Scheme of the models of fuzzy logic-based pain inference.

As the first step in creating the fuzzy logic model, two trapezoidal membership functions (boundary variables) and one triangular membership function (intermediate variables) were used to generate the fuzzy rules as shown in **Fig. 4.3**. In this study, a trapezoidal membership function on the left and right for the angle and torque input parameters was used. The reason for this implementation is that the patient robot has a limited a range of motion in order to reproduce the joint motion of the patient. The range in which the patient robot feels pain is defined based on the pain inference factors in **Table 4.1**. The trapezoidal membership function reflects the fact that the patient robot receives the maximum pain when it is out of the range of joint motion. Therefore, a trapezoidal membership function was applied to set the weight of the membership function as '1' in the range where the patient robot feels pain.
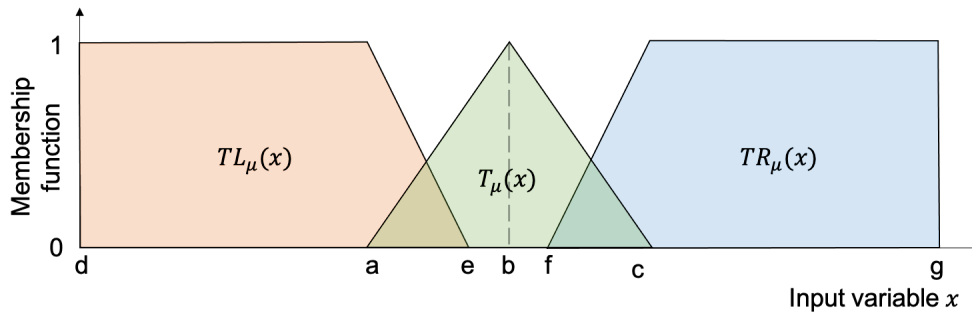
Figure 4.3. Structure of fuzzy membership functions for input variables.

Three types of membership functions can be defined as **Eq. 4.2** to **Eq. 4.4**.

$$T\mu(x) = \begin{cases} 0, & (x \leq a) \ or \ (x \geq c) \\ 1, & x \equiv b \\ (x - a)/(b - a), & a < x < b \\ (c - x)/(c - b), & b < x < c \end{cases} \tag{4.2}$$

75

$$TL\mu(x) = \begin{cases} 1, & d < x \leq a \\ (e-x)/(e-a), & a \leq x < e \\ 0, & x \geq e \end{cases} \qquad (4.3)$$

$$TR\mu(x) = \begin{cases} 0, & x \leq f \\ (c-x)/(c-f), & f < x \leq c \\ 1, & c < x \leq g \end{cases} \qquad (4.4)$$

where x is the input variables. $T\mu(x)$, $TL\mu(x)$, and $TR\mu(x)$ indicate the triangular, left-trapezoidal, and right-trapezoidal membership function, respectively. The parameters a to g are determined as **Table 4.1** and refer to the constants of the input variables that determine the value of the membership function.
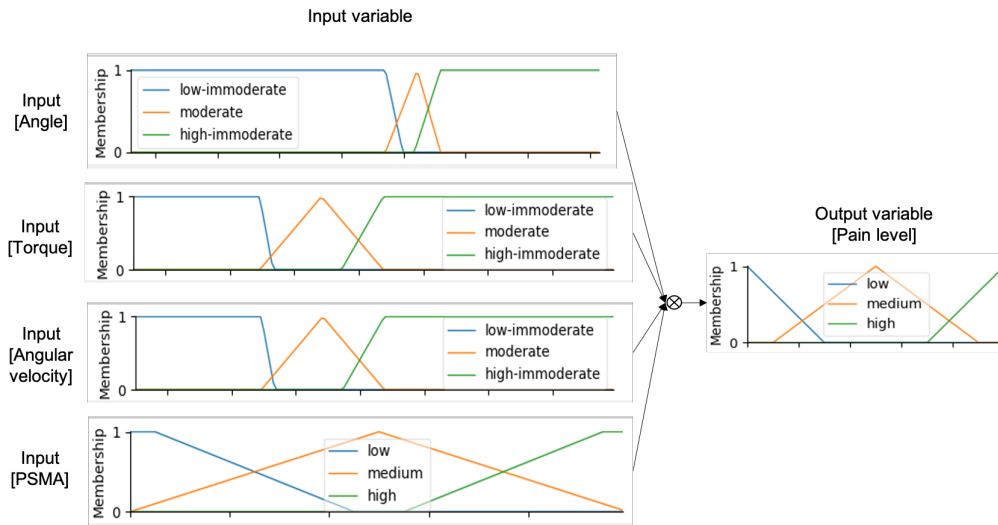
Figure 4.4. The input and out variables for the fuzzy logic-based pain inference.

As shown in **Fig. 4.4**, the input variables of the membership function were divided into three groups as *low-immoderate*, *moderate*, and *high-immoderate*. The input variable *PSMA* of the elbow joint and output variable *pain level* consist of *low*, *medium*, and *high*.

The next step is to generate the fuzzy-rules that define the relationships among the input variables. The fuzzy rules were constructed using an experts' opinion and can be described using **Eq. 4.5**.

$$rule^k : IF \ X_k \ is \ F_1^k \ and...and \ X_p \ is \ F_p^k \ then \ Y^k \qquad (4.5)$$

where F_p^k is the p-th fuzzy set associated with the kth rule. The rule 'IF x_k is F_1^k and $\cdots$ and X_p is F_p^k'corresponds to the antecedent from the kth-rule and 'THEN Y is Y^k'is the consequent of the kth rule.

Finally, a total of N fuzzy-rules were generated, as shown in **Fig. 4.5**. For the FLPI-EROM model, the number of input variables is four (angle, torque, angular velocity, and PSMA), and the membership functions consist of three kinds of antecedent variables (low, medium, and high). The number of fuzzy rules can then be calculated as m^n (m and n indicate the numbers of antecedent and input variables, respectively). Therefore, there were 81 rules ($=3^4$) that each was connected with one of the three antecedent variables for the output (pain level). On the other hand, in the case of the FLPI-SROM model, the number of fuzzy rules is 27 ($=3^3$) because it contains three input variables as angle, torque, and angular velocity and one output variable as pain level.

This study determine the inference engine using the *Mamdani* method to design the fuzzy inference system (FIS). For FIS, there are two main types of methods of mapping inputs to outputs: i) *Mamdani* FIS and ii) *Sugeno* FIS. The *Mamdani*-based FIS has the advantages of being intuitive, well-suited to human inputs, more interpretable fuzzy-rule, and applicable in various fields such as medical diagnostics, industrial manufacturing, hospitals, and banks [73].

Next, the defuzzification refers to the process of converting a fuzzy output value into a crisp value based on an inference engine in order to actually use the measured value from the fuzzy logic. Here, the crisp value indicates the final calculated precise

value by calculating the imprecise fuzzy value; the defuzzifier is an important component of FIS [74]. Since the centroid defuzzification method is the most commonly and frequently used [73] and has a robust performance, it was used as the final diffusion layer in this study. Finally, the pain level output obtained by the input variables ranged from 0 to 10.
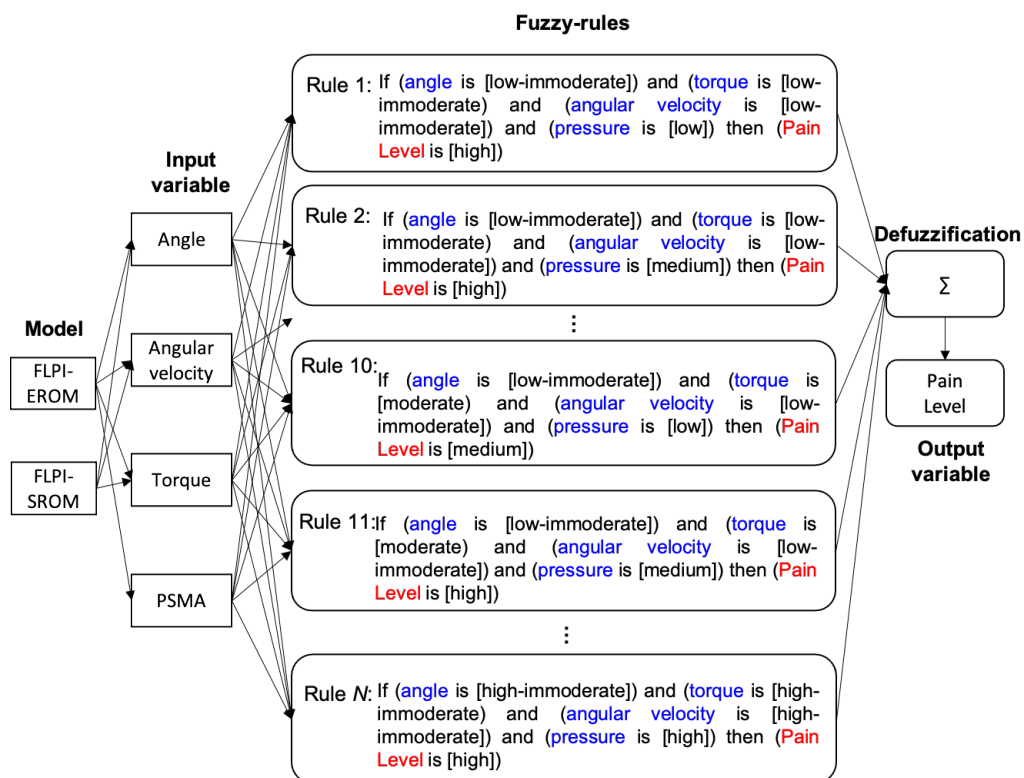
Figure 4.5. Example of the fuzzy rules. FLPI-EROM and FLPI-SROM indicate the fuzzy logic-based pain inference for the ROM exercise of the elbow complex and the shoulder complex, respectively.

4.4 Pain expression

This Section describes the pain database to generate pain expression for the avatar of the proposed system. The novelty of this study is that it proposes a visual feedback method to express the pain intensity of the patient robot to improve caregivers' skills in a training environment. To develop this, a novel pain expression database that contains more than 13,773 facial images from Japanese individuals was first built in this study. Based on this database, the pain avatar of the patient robot was developed by calculating the pain intensity from facial images using a Siamese network.

4.4.1 Databases

To generate the pain facial avatar of the patient robot, an original database was designed, namely pain intensity using transcutaneous electrical nerve stimulation from Ritsumeikan University (RU-PITENS), which contains pain images acquired during transcutaneous electrical nerve stimulation (TENS), and a public database of UNBC-McMaster shoulder pain [75]. The two databases were used for the following purposes:

- The UNBC-McMaster database was used as training data to measure pain intensity obtained from facial images to create a pain avatar.

- The RU-PITENS database was used to test the trained model and finally generate an avatar of patient robot for pain expression.

The purpose of using the two databases and detailed explanations of the images contained in the databases are described in the following Sections.

4.4.2   Original database: Pain intensity using TENS device (RU-PITENS)

Since existing databases contain many images of faces with the face slightly tilted to the side, an additional algorithm was required to align facial images to the front to generate an avatar. Therefore, a new database was built, RU-PITENS, containing frontal images of the faces of subjects, showing images indicating pain intensity caused by the TENS device. This experiment was approved by the Institutional Review Board (IRB) of Ritsumeikan University (BKC-2019-060).

For building RU-PITENS, forty one adults were recruited in the experiment, and the information on the subject's gender and age is described in **Table 4.2**. Participants were classified into ages in their 20s, 40s, 50s, and 60s. The reasons for classifying the age groups in this database and the important factors of the RU-PITENS database in this study are as follows:

- Above all, the study of this dissertation focused on designing avatars to be easily transformable from facial images to enable students to receive education for various patients in the care education system. Therefore, this study aims to generate various avatars independent of age and gender from the RU-PITENS database.

- The patient robot was developed based on the condition of the medical symptoms of specific problematic movement for the elderly in Japan. Therefore, facial images of Japanese people were needed to apply the patient robot to the care and nursing environment in Japan.

- The robot head proposed in this dissertation may be more familiar than the robot's mechanical facial muscle movements because it generates facial images by transforming them into avatars based on the RU-PITENS database. Unfortunately, this means that although much excellent research has been studied to develop the best realistic mechanical robotic heads with articulated faces, these robotic heads may suffer from problems such as *Uncanny Valley* [76, 77] (**Fig. 4.6**), a phenomenon caused by the robot's unnaturalness [78].
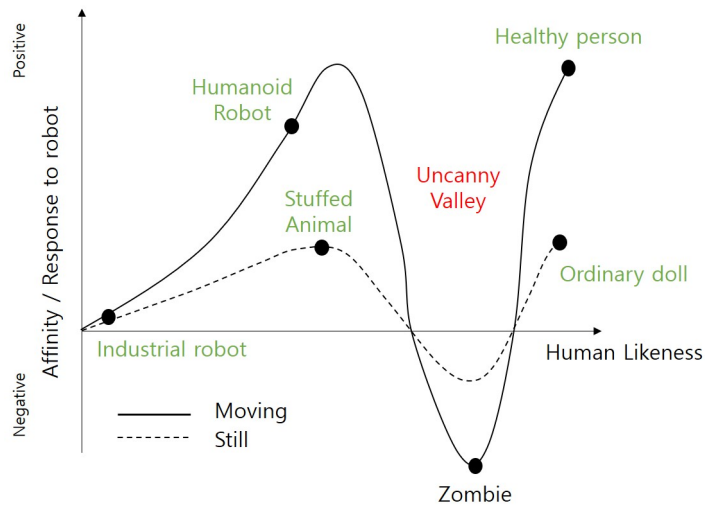
Figure 4.6. The uncanny valley graph. The figure was adapted from [79].

Table 4.2. Demographics of the participant's gender and age in pain intensity using the TENS device (RU-PITENS) database.

Pain intensity using the TENS device (RU-PITENS) database						
		Age range				
Gender	Measure	20 to 29	40 to 49	50 to 59	60 to 69	Total
Male		11	5	5	5	26
Female	N.S	-	5	5	5	15
Total		11	10	10	10	41
Male		23.7	45.0	53.6	64.0	46.6
		(2.1)	(4.6)	(3.0)	(3.9)	(3.4)
	M.A					
Female		-	45.2	56.0	66.2	55.8
			(2.3)	(1.6)	(3.3)	(2.4)
Total		23.7	45.0	53.6	64.0	47.2
		(2.1)	(4.6)	(3.0)	(3.9)	(2.9)

Note: N.S and M.A indicate the number of subjects and the mean age, respectively. Numbers in parentheses are standard deviations.

All subjects had no history of peripheral neuropathy or other pain symptoms, musculoskeletal or facial muscle reaction disorders, trauma, orthopedic hand surgery, or current medication. All of them agreed to participate by signing a consent form, while researchers observed to ensure their safety.

Fig. 4.7 illustrates the experimental environment of the pain simulation and measurement. In this study, a commercial device, HV-F140 (Omron Healthcare Co., Ltd., Kyoto, Japan), was used as the transcutaneous electrical nerve stimulation.
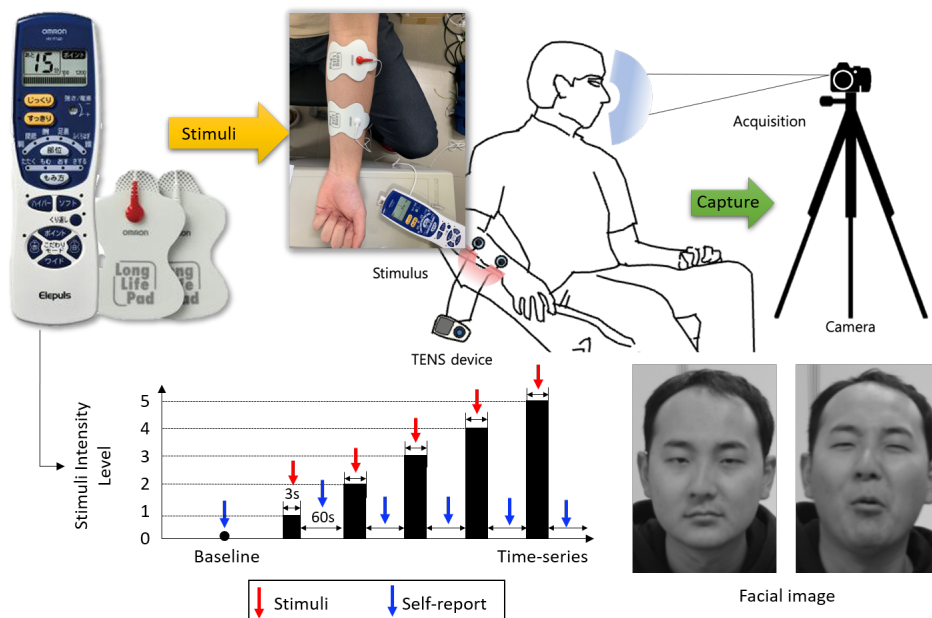
Figure 4.7. The pain stimulus and the acquisition of pain images.

Transcutaneous electrical nerve stimulation (TENS) has the advantages of being inexpensive, non-invasive, and easy to use compared to thermal or pressure stimulators. In addition, the TENS system, which is often used as muscle therapy in daily life, can induce acute pain with high frequencies, and TENS-based pain databases have been collected in [80, 81]. Two durable adhesive pads that can be reused up to 150 times after washing were attached to the skin of the subject's right arm. The experiment was conducted until the participant could no longer tolerate the pain when the intensity of

the TENS was increased or the stimulation level reached the maximum level (the TENS output had five intensity levels and its frequency ranged from 0 to 1,200 Hz). **Fig. 4.8** illustrates an example of the acquired pain facial expression images. A total of 13,773 frames of images were acquired from all subjects.
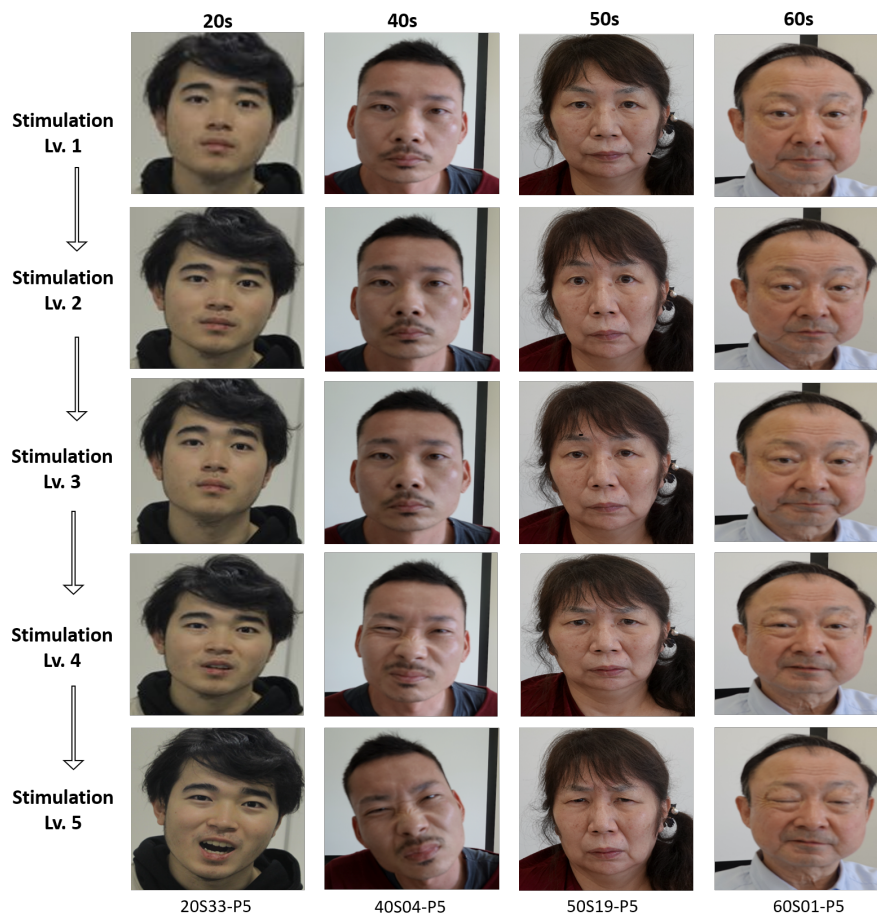
Figure 4.8. Example of pain facial expression in RU-PITENS database.

In the experiment, a survey was conducted for approximately one minute at the end of each level of stimulus, including the baseline and post-experimental tests. The experiment for this database was conducted in the AIS laboratory of Ritsumeikan University and is published as an open database: `https://github.com/ais-lab/RU-PITENS-database`

4.4.3 UNBC-McMaster Database

The purpose of using the UNBC-McMaster database was to train a model to measure pain intensity from facial images in the RU-PITENS database used to generate pain expression avatars. The UNBC-McMaster shoulder pain database [75] contains pain images from 25 patients with shoulder pain through an experiment of shoulder range of motion. The UNBC-McMaster database can be used for model training because it contains the *Prkachin and Solomon Pain Intensity* (PSPI) score, the ground truth of pain level. PSPI (range from 0 to 15) is a score that measures the level of pain in facial expressions, which was first proposed in [82] and and is calculated by several action units (AUs) using a Facial Action Coding System (FACS) [83]. The PSPI score which can be calculated as the sum of several action units (AUs, Action units are the visible indicators of the operation of facial muscles) of AU4 (brow lower), AU6 (cheek raiser), AU7 (eyelid tightener), AU9 (nose wrinkle), AU10 (upper lip raiser), and AU43 (eyes closed) using **Eq. 4.6**. The PSPI value was used as the ground truth to test the model generated to calculate pain intensity from pain images.

$$PSPI = AU4 + max(AU6 \ or \ AU7) + max(AU9 \ or \ AU10) + AU43 \tag{4.6}$$

One notable fact before training the model is that the UNBC-McMaster database is required to balance the number of data entries in each class because the data are unbalanced and skewed. Based on the PSPI score (ranges from 0 to 15), the pain images in the UNBC-McMaster database can be divided into four pain labels: none (PSPI=0), trace (PSPI=1), weak (PSPI=2 and 3), and strong (PSPI>=4). The total number of data entries from UNBC-McMaster is 48,398, as shown in **Table 4.3**. Since pain is subjective and there are no clear criteria for classification, many studies arbitrarily classify the PSPI labels. Therefore, in the study of this dissertation, the PSPI label was determined according to the criteria proposed in the study of [84] by considering the unbalanced data in the UNBC-McMaster database. In the total data, this study decided to include only 1,730 images in each pain group for balanced data based on a minority grade (pain label: strong (PSPI>=4), and the data were randomly

extracted. To use this database for research purposes, an end user license agreement was submitted to the Affect Analysis Group at Pittsburgh [75]. **Fig. 4.9** illustrates the example of pain images in UNBC-McMaster shoulder pain database.

Table 4.3. Definition of pain states based on PSPI for classifying classes in UNBC-McMaster shoulder pain database [75].

Prkachin and Solomon Pain Intensity (PSPI)	Pain state	Number of images
0	None	40,149
1	Trace	3,037
2 and 3	Weak	3,482
from 4 to 15	Strong	1,730

Note: PSPI indicates *Prkachin and Solomon Pain Intensity* score.
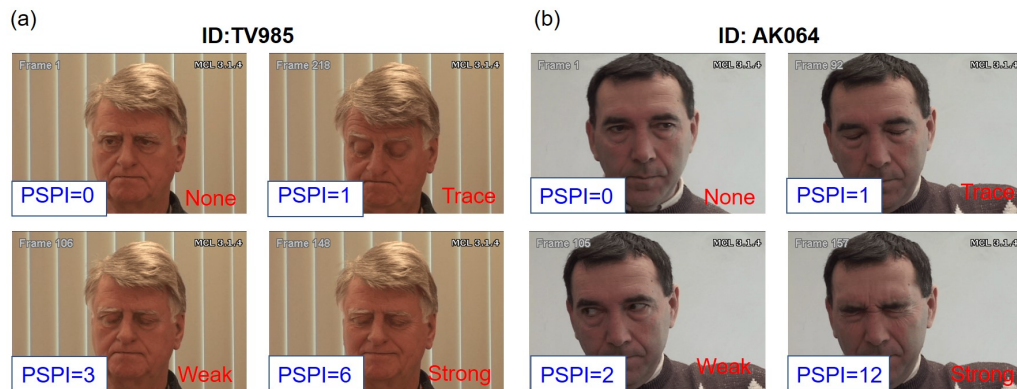
Figure 4.9. Prkachin and Solomon Pain Intensity (PSPI) score of pain images in UNBC-McMaster shoulder pain database [75]. Photograph of (a) subject #TV985 and (b) subject #AK064 have been granted portrait rights from Affect Analysis Group at Pittsburgh, and an explanation of the consent form is provided in Appendix C.

4.4.4 Siamese Network-based pain intensity

The ultimate goal of this Chapter is to create an avatar representing the pain intensity from sequential pain images in RU-PITENS database. Although the proposed method generates an avatar using the face image of the RU-PITENS database, the pain expression images in this database do not have quantitative value (reference) on the expression intensity from the pain's onset to the pain's cessation. Therefore, it is necessary to measure the pain intensity using a verified model. In this study, therefore, a Siamese network was used to measure the intensity of pain from pain images; the reasons for choosing the Siamese network are as follows:

- Since this study develop an avatar expression system based on sequential pain intensity estimation, a model that can measure the change in pain intensity between the current image and the previous image is required.

- It is difficult to distinguish the type of pain and to provide an accurate pain label to the new input data because pain is subjective information that can be measured differently depending on the individual.

According to the considerations of use of the Siamese network described above, the Siamese network-based pain intensity from pain images (SNPI) are measured by using the Siamese network. This network [85] provides one output, which is a value indicating the similarity between two inputs. In many studies [86, 87, 88], it has been utilized as a method for analyzing facial expressions. The Siamese network has two sister networks (sub-networks) with the same shared weight and structure, which consists of a layer for the distance of the feature vectors from the two sister networks.

To optimize the network, the contrastive loss function was utilized to make embeddings of feature vectors more similar if the target classes were similar [89] and to distinguish between input pairs. The contrastive loss function [90] can be defined as in **Eq. 4.7**.

$$Contrastive\ Loss\ (W, Y, \vec{P}_1, \vec{P}_2) = (1 - Y)\tfrac{1}{2}(D_W)^2 + (Y)\tfrac{1}{2}\{max(0, m - D_W)\}^2$$

$$(4.7)$$

where P_1 and P_2 are pairs of samples. Y is a binary label, and the pair samples are similar when $Y = 0$ (negative). In the second term, $m > 0$ denotes the margin for dissimilar pairs. Distance D_w between the outputs of G_W and can be calculated using **Eq. 4.8**.

$$D_W(\vec{P}_1, \vec{P}_2) = \|G_W(\vec{P}_1) - G_W(\vec{P}_2)\|_2 \qquad (4.8)$$

As shown in **Fig. 4.10**, the sister network has a basic ConvNet structure, and the network architecture consists of three ConvNet layers and a fully connected layer with 48 units based on the results of the hyper-parameters that have been empirically changed. To merge the sister networks, a layer that computes the output of the two sister networks was added to the last layer.
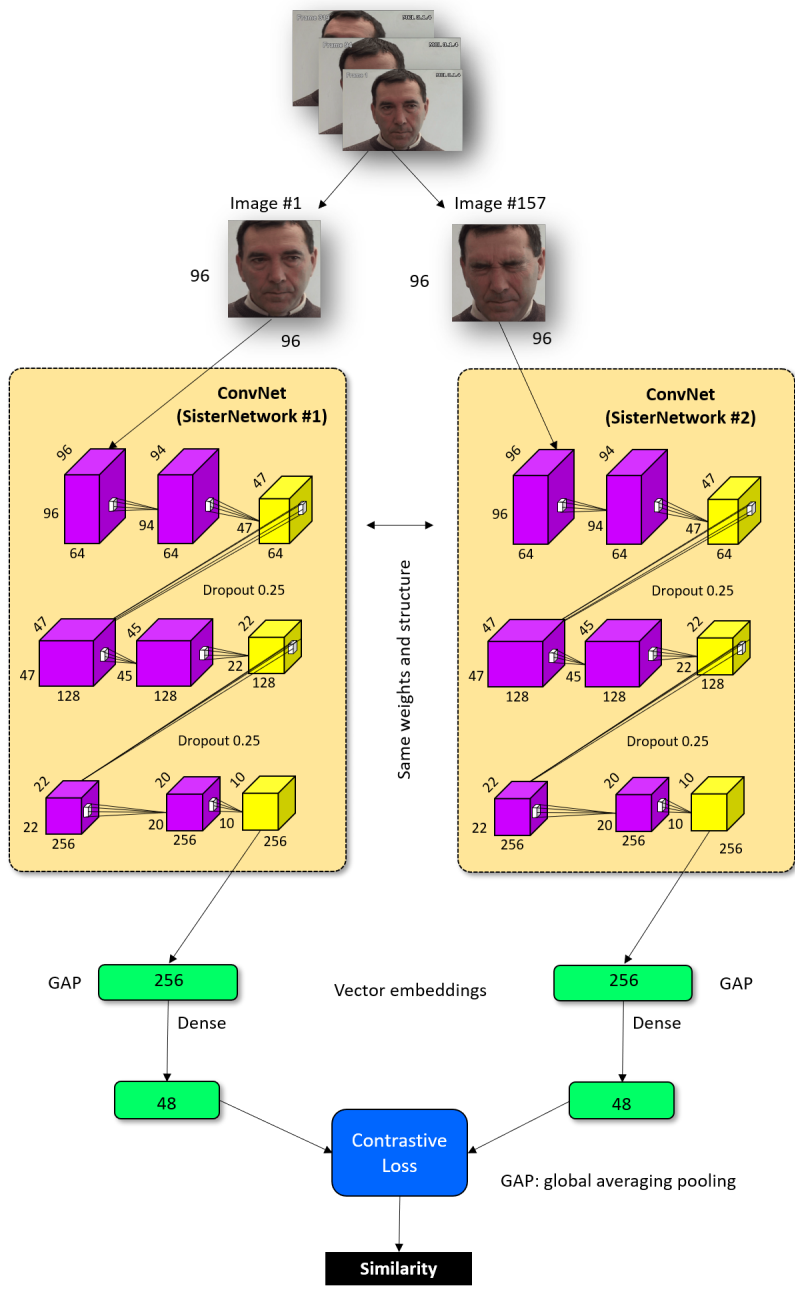
Figure 4.10. The structure of Siamese network for the pain intensity.

4.5   Pain facial avatar

As explained in the purpose of the RU-PITENS database (Section 4.4.2), the most significant advantage of creating an avatar using the facial image is that it can easily transform the robot's avatar. In this study, the avatar is created based on the avatar generation's program by converting the facial image (.jpg) into an object file (.obj) (refer to **Fig. 4.11**) to express the robot's pain. This Section describes how to create an avatar from a subject's facial image and express the pain that the robot avatar felt during education as an avatar (see **Fig. 4.1**).

4.5.1   Avatar generation

To create an avatar object (.obj), a commercial avatar SDK (Itseez3D, Inc., CA, USA) was utilized in this study. The patient robot's avatar, which can express pain, is converted from the original image (.jpg) to an avatar object (.obj) through the avatar SDK added to the Unity program (Unity Technologies, Inc., CA, USA). **Fig. 4.11** illustrates the patient robot's avatar from participant's facial image from RU-PITENS database (the original image is included in **Fig. 4.8**). The avatars generated according to the frames of all original images are classified into five pain groups (PGs): PG_1 (no pain at all), PG_2 (very faint pain), PG_3 (weak), PG_4 (moderate), and PG_5 (strong). In other words, five types of pain avatar can be expressed based on the pain's level of the patient robot that feels pain during passive ROM exercise.

The pain group that determines the patient robot's avatar expression is defined based on the FLPI and SNPI. Here, FLPI indicates the calculated value of the pain intensity felt by the patient robot based on the fuzzy logic method (Section 4.3.2), and SNPI represents the pain intensity calculated from the pain image based on the Siamese network (Section 4.4.4).
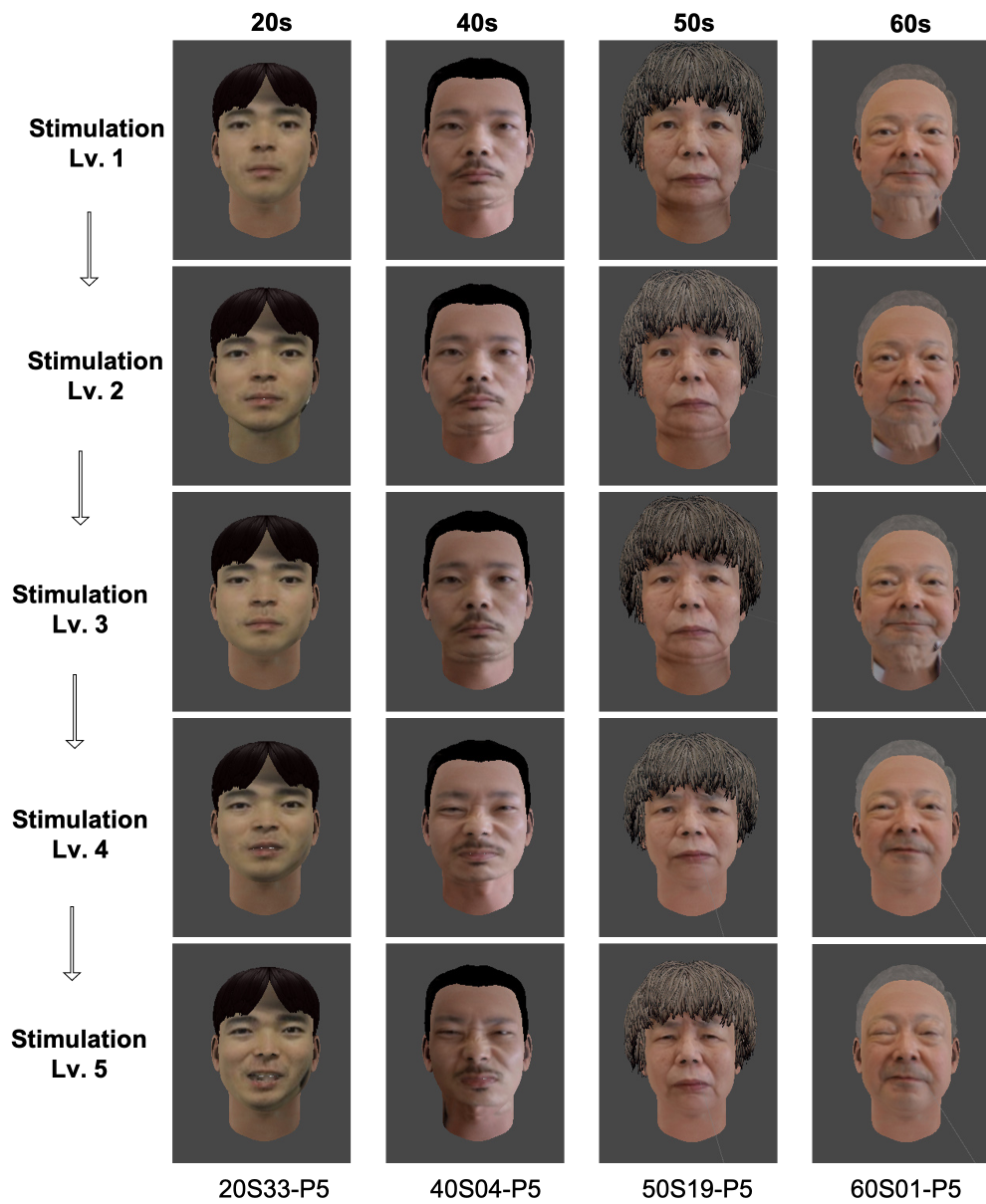
Figure 4.11. Patient robot's avatar from facial image from RU-PITENS database.

4.5.2 Pain group generation

The procedure of the pain group generation can be summarized as follows. The pain intensity from the pain image in the RU-PITENS database in advance (**Fig. 4.12** (a)), and the avatar was generated based on the pain group (**Fig. 4.12** (b)). Then, the users conducted care training using the patient robot, and the intensity of the pain the robot feels was calculated based on the extracted quantitative data of the patient robot (**Fig. 4.12** (c)).
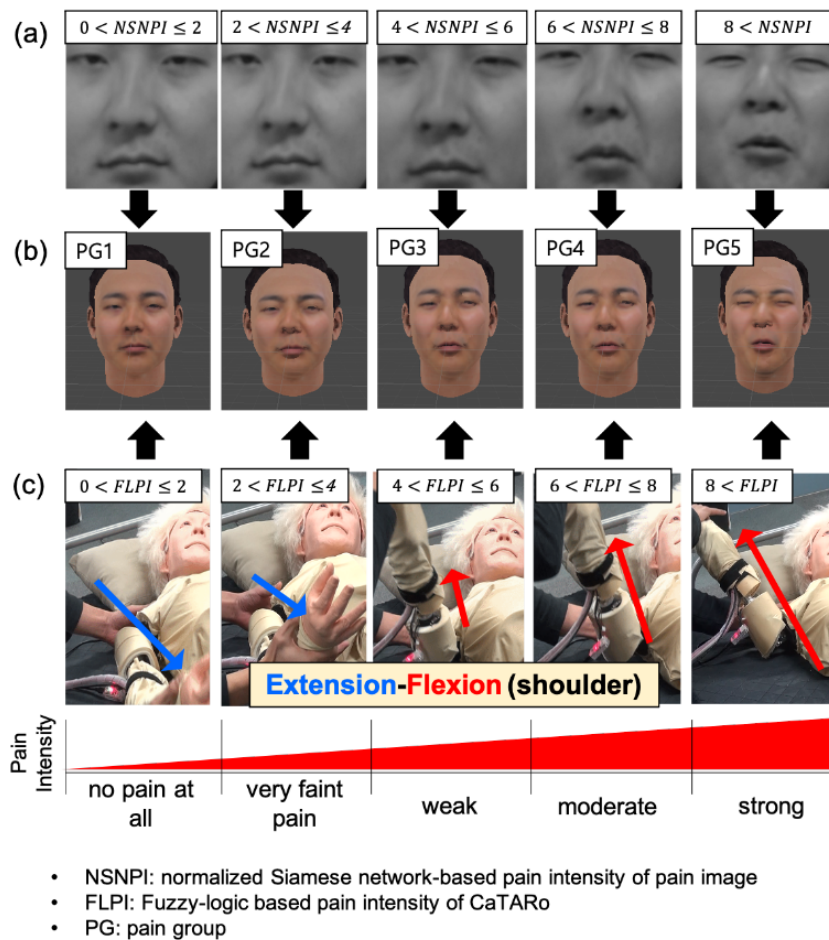
Figure 4.12. The procedure of generating avatars (a) Examples of pain images and calculated SNPI values in the RU-PITENS database (b) Avatars generated according to pain groups (c) ROM exercise using the patient robot.

Finally, the visual feedback system was built by matching the intensity of pain the patient robot felt with an avatar created in advance. The pain group of FLPI and SNPI is determined by **Eq. 4.9**.

$$f[X_i] = \begin{cases} 1, & 0 \leqq X_i < 2 \\ 2, & 2 \leqq X_i < 4 \\ 3, & 4 \leqq X_i < 6 \\ 4, & 6 \leqq X_i < 8 \\ 5, & X_i \geq 8 \end{cases} \tag{4.9}$$

where X_i is the input sample, which can be FLPI$_i$ or SNPI$_i$. The fuzzy logic-based pain intensity of the patient robot (FLPI) was described in Section 4.3.2. FLPI was calculated using the sensor's quantitative data of the patient robot through the fuzzy-logic method and the pain group of FLPI, PG$_i^{FLPI}$ can be determined using the function $f[X_i]$ as **Eq. 4.9**.

On the other hand, in Section 4.4.4, the Siamese network was described, and by calculating the SNPI from the acquired pain images in RU-PITENS database, an avatar can be generated, as shown **Fig. 4.11**. The formula for determining the output SNPI from pain images including five types of pain is as follows:

$$NSNPI_i = (SNPI_i - min(SNPI_i))/(max(SNPI_i) - min(SNPI_i)),$$

$$\tag{4.10}$$

$$PG_i^{SNPI} = f[NSNPI_i].$$

where i and SNPI denote the number of samples and Siamese network-based pain intensity, respectively. To obtain the value of PG$_i^{SNPI}$, SNPI is normalized to NSNPI based on the min-max method. Finally, PG$_i^{SNPI}$ is determined as **Eq. 4.9**.

4.6 Experiment and results

4.6.1 Purpose

The purpose of this experiment is to investigate whether the proposed method automatically infers the pain level of the patient robot and how it differs from the statistical results analyzed manually. In particular, the difference between the expert group and the student group is investigated in the obtained pain interference results, and the method to generate the patient robot's avatar that expresses pain state is tested using the pain inference. The subjects participating and experimental protocol in this Chapter are the same as in the experiment introduced in Chapter 3.

4.6.2 Result of fuzzy-based pain inference

Fig. 4.13 depicts an example of the quantitative data (i.e., elbow joint angle, torque, pressure signal magnitude area (PSMA)) output from the elbow joint of the patient robot and the pain level output by using the fuzzy logic method (FLPI). The top figure of **Fig. 4.13** shows the elbow kinematics of the patient robot; the angle, torque, and PSMA of the robot are simultaneously output when the elbow of the robot moves by extension and flexion. **Fig. 4.13** (a) and **Fig. 4.13** (b) show that when the elbow joint angle of the robot decreases, the torque increases because the subject has performed the movement to extend the elbow of the robot. **Fig. 4.13** (c) shows the PSMA results, where pressure has values alternately between extension and flexion; these pressure sensor values are different for each participant in the experiment because each participant may have applied different degrees of force and used different hold positions on the wrist of the robot. **Fig. 4.13** (d) shows the FLPI value, and the pain groups PG were categorized according to the FLPI (refer to **Fig. 4.12** (b)), and the purple-dot PG1 has a range of FLPI of 0 to 1.99, the black-dot PG2 has a pain level of 2 to 3.99, and the green-dot of PG3 ranges from 4 to 5.99, and the green-dot of PG4 ranges from 6 to 7.99, and the red-dot of PG5 has a FLPI ranging from 8 to 10.
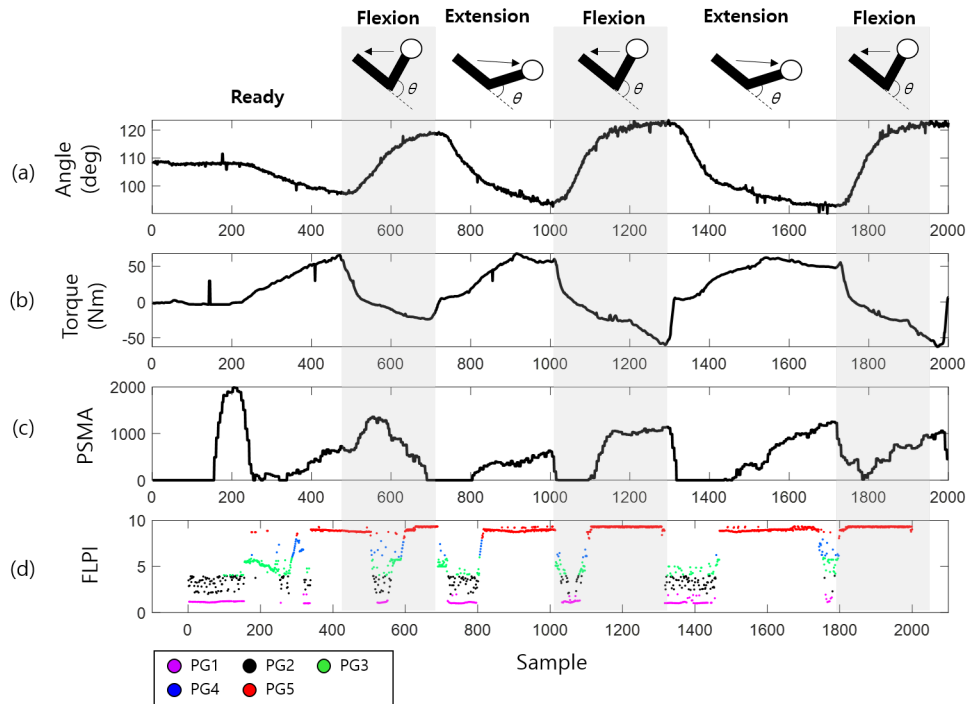
Figure 4.13. Example of quantitative data of the robot and the fuzzy logic-based pain level (FLPI) in elbow extension and flexion (EEF) exercise: (a) Elbow joint angle (c) Torque (d) Pressure signal magnitude area (PSMA) (e) Output of the FLPI. PG indicates the pain group.

4.6.3 Effect of fuzzy-based pain inference in the repetitive ROM exercises

This evaluation investigates the effect of the fuzzy logic-based pain inference (FLPI) in the repetitive tasks on care education using the patient robot (**RP 4.1** and **RP 4.2**). Based on the four types of ROM exercises for joint care education, the FLPI was measured as shown in **Table 4.4** and **Table 4.5**. As a result of investigating normality using the Shapiro-Wilk test, all groups were nonparametric. Therefore, statistical tests were performed using the Kruskal-Wallis test, and the significance level was set at α=0.05.

Table 4.4. The result of the fuzzy logic-based pain intensity (FLPI) in the repetitive ROM exercises in the expert group.

ROM exercise	Initial-trial	Medial-trial	Final-trial	p-value
Shoulder Elevation-depression (SED)	5.18 (2.89)	5.79 ^{a,b} (1.49)	5.14 (1.45)	<.001
Shoulder Lateral-medial rotation (SLM)	4.42 (1.84)	4.13 ^{c,d} (1.24)	4.23 ^{e} (1.94)	<.05
Shoulder Extension-flexion (SEF)	6.54 (2.12)	6.21 ^{f,g} (2.53)	6.58 (1.84)	<.001
Elbow Extension-flexion (EEF)	4.39 (1.96)	4.24 ^{h} (1.93)	4.12 ^{i} (1.91)	<.05

Note: Each trial contains 10 repetitive ROM exercises. The alphabets from a to i above the numbers are the result of statistical analysis using Dunn's multiple comparison test, indicating the groups in which statistically significant differences were shown (p <.05).

a, c, f, h: Initial-trial vs. Medial-trial

b, d, g: Medial-trial vs. Final-trial

e, i: Initial-trial vs. Final-trial

In the case of the expert group, the results in initial, medial, and final trial had statistically significant differences. In the results of the post-hoc test using Dunn's test, statistically significant differences ($p<0.01$) were shown in several comparisons (the alphabetical indicators from a to i in **Table 4.4**. When comparing the results of caring education for SED, SLM, and EEF excluding SEF in the initial and final trials, the FLPI values tended to decrease to approximately 0.04, 0.19, and 0.27, respectively.

Table 4.5. The result of the fuzzy logic-based pain intensity (FLPI) in the repetitive ROM exercises in the student group.

ROM exercise	Initial-trial	Medial-trial	Final-trial	*p*-value
Shoulder Elevation-depression (SED)	6.39 (2.59)	6.12 ^{a,b} (3.16)	5.38 ^{c} (2.57)	<.001
Shoulder Lateral-medial rotation (SLM)	6.28 (3.15)	5.93 ^{d,e} (2.95)	6.01 ^{f} (3.26)	<.001
Shoulder Extension-flexion (SEF)	6.16 (2.95)	6.31 ^{g,h} (2.67)	6.29 ^{i} (2.06)	<.001
Elbow Extension-flexion (EEF)	5.97 (2.25)	5.36 ^{j,k} (2.65)	5.64 ^{l} (1.98)	<.05

Note: Each trial contains 10 repetitive ROM exercises. The alphabets from *a* to *l* above the numbers are the result of statistical analysis using Dunn's multiple comparison test, indicating the groups in which statistically significant differences were shown (p <.01).

a, d, g, j: Initial-trial vs. Medial-trial

b, e, h, k: Medial-trial vs. Final-trial

c, f, i, i: Initial-trial vs. Final-trial

Table 4.5 shows the result of the FLPI in the repetitive ROM exercises in the student group. The results in initial, medial, and final trial showed the statistically significant differences. In the results of the post-hoc test using Dunn's test, statistically significant differences (p<0.01) were shown in all comparisons (the alphabetical indicators from *a* to *l* in **Table 4.5**. As a result, when the initial and the final trial were compared, the FLPI values of the student group for SED, SLM, SEF, and EEF decreased to about 1.01, 0.17, 0.13, and 0.33, respectively. Based on the results in **Table 4.4** and **Table 4.5**, the following observation can be defined for **RP 4.1** of this Chapter as follows:

Observation 4.1) The pain inference technique in this Chapter showed significant differences in the initial, medial, and final trials in repetitive ROM movements. Therefore, it can be concluded that the pain inference method of care training using a patient robot can provide feedback on a caregiver's stable posture and care skills while reducing robot pain in the repetitive task.

Fig. 4.14 illustrates the results of comparing the FLPI between expert and student groups in repetitive tasks. The differences between experts and students in SED, SLM, SEF, and EEF were 0.59, 1.81, -0.19, and 1.41, respectively, and there were statistically significant differences in SED, SLM, and SED exercise ($p<0.05$). The observations of the results in **Fig. 4.14** can be presented for **RP 4.2** as follows:

Observation 4.2) The proposed pain inference method helps to compare intuitively the differences between groups.
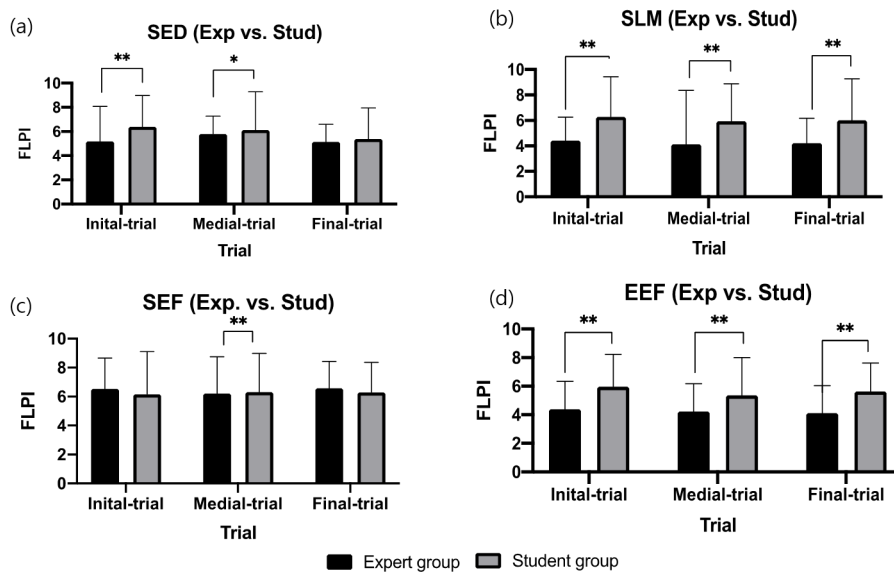
Figure 4.14. Comparison result of the fuzzy logic-based pain intensity (FLPI) of the patient robot in the repetitive ROM exercises between the expert (Exp) and student group (Stud) (a) Shoulder elevation and depression (SED) (b) Shoulder lateral and medial rotation (SLM) (c) Shoulder extension and flexion (SEF) (d) Elbow extension and flexion exercise (EEF). An asterisk (*) indicates statistical significance at $p <0.05$, and double asterisk (**) indicate statistical significance at $p <0.01$.

4.6.4 Pain sensitivity-based FLPI

Even different subjects with the same disease may report vastly different levels of pain depending on the severity of trauma and patients' pathophysiological condition [91]. This study hypothesis that robots have different pain sensitivities like a human, and designed robots with pain sensitivity (PSEN) such as **Table 4.6**.

Table 4.6. The weighing of the robot's pain sensitivity.

	Pain sensitivity (PSEN)					
	Case 1	Case 2	Case 3	Case 4	Case 5	Case 6
Weight	0.1	0.3	0.5	0.7	0.9	None

The higher the weight value of the PSEN indicates that the robot is more sensitive to pain and vice versa. The final FLPI can be obtained by using the pain sensitivity, it can be calculated as **Eq. 4.11**.

$$FLPI_k = FLPI_k + FLPI_k \times PSEN,$$

$$FLPI_k = \begin{cases} 0, & FLPI_k \leq 0 \\ 10, & FLPI_k \geq 10 \\ FLPI_k, & 0 < FLPI_k < 10. \end{cases} \tag{4.11}$$

where k denotes the input samples. The FLPI close to ten indicates that the user's care ability is insufficient, while the value of FLPI close to zero indicates that the care ability is sufficient.

Fig. 4.15 illustrates an example of the result of FLPI according to the robot's personality. **Fig. 4.15** (a) shows the angle and torque of the patient robot in EEF exericse. When performing the flexion exercise, it can be observed that the value of torque increase rapidly. As a result, the value of FLPI is affected due to the abrupt change in torque (**Fig. 4.15** (b)). In **Fig. 4.15** (b), the positive area of FLPI (<5) had less response to the pain sensitivity, while the negative part of FLPI (>5) was defined (refer to **Eq. 4.11**) so that the more pain sensitivity is high, the more FLPI's response is sensitive. The reason is that if the robot has a high sensitivity to pain, it can respond more to the pain caused by the inexperienced care skills of users during care education.
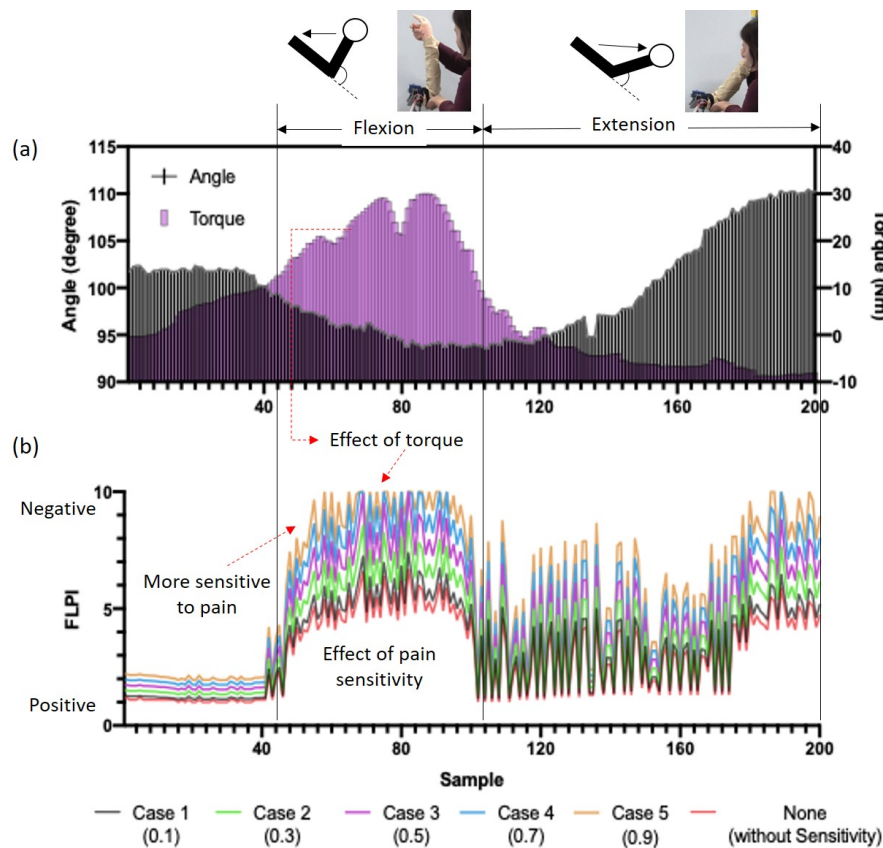
Figure 4.15. Example of the fuzzy logic-based pain intensity (FLPI) of the patient robot calculated according to the pain sensitivity in extension and flexion exercise of the elbow complex (EEF) (a) angle and torque raw data (b) FLPI.

99

4.6.5   Result of questionnaire in RU-PITENS database

The pain is a subjective factor that can be measured differently depending on the situation and the individual. To investigate the effect of the pain intensity in the RU-PITENS database, participants answered the questionnaire immediately after the end of stimulation tests for each level (the procedure of the stimulus test is described in Section 4.4.2). The questionnaire consisted of a visual analogue scale (VAS) and a subjective pain score (SPS). The VAS is easy to work with and frequently used for the assessment of variations in intensity of pain [92]. In this experiment, the SPS survey was designed as a subjective indicator of pain. The value of SPS can be classified as follows: no pain at all=0, very faint pain (just noticeable)=1, weak pain=2, moderate pain=3, strong pain=4, and very strong pain=5.

Fig. 4.16 shows the result of the questionnaire from all subjects. In **Fig. 4.16** (a), the SPS continuously increased according to the stimuli levels, and there were statistically significant differences among stimuli levels (F=164, p <0.01, ANOVA test). For the pleasure score, the score decreased with respect to the stimuli level, indicating that it may suggest that the pain stimulus had a negative effect on the subject's emotion. There was a difference of about 2.0 between the maximum level (Lv.5) and the minimum level (Lv.1) in SPS (Q=9.89, p<0.01, Tukey's post-hoc test). An increase in the arousal score with stimuli level suggests a negative effect on the stimulus, and showed a difference of about 3.81 between the minimum (Lv.1) and maximum (Lv.5) stimulation level (Q=14.42, p<0.01, Tukey's post-hoc test). Additionally, according to the evaluation of all parameters for gender, there was no statistically significant difference in most male and female groups. However, when the survey statistics were analyzed by classification by age group (the 20s, 40s, 50s, and 60s), there were differences in each survey result. In the case of SPS and arousal scores, there was a statistically significant difference in all age groups at from Lv. to Lv.5 (ANOVA test), and there was a significant difference from Lv.2 and Lv.5 (ANOVA test) in the pleasure score. Based on these results, the pain images in Lv.5 (stimuli maximum level) were utilized to generate the robot's facial avatar.
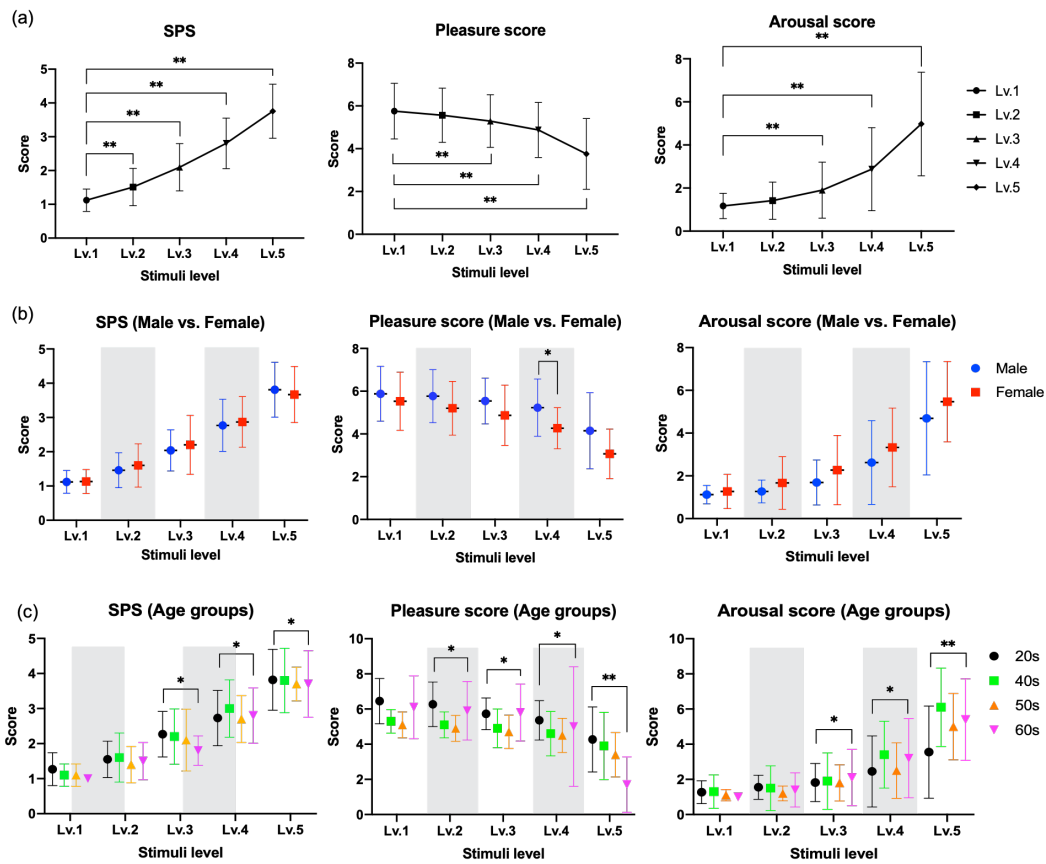
Figure 4.16. Result of the survey in RU-PITENS database (a) All subjects (b) Survey results according to gender group (c) Survey results according to age groups (20s, 40, 50s, and 60s). The test methods were used the analysis of variance (ANOVA) and Tukey's method (post-hoc analysis). The significant level was set at α=0.05. An asterisk (*) indicates statistical significance at p <0.05, and double asterisk (**) indicate statistical significance at p <0.01. SPS and Lv indicate the subjective pain score and the stimuli level.

4.6.6   Result of Siamese network-based pain intensity

To train the Siamese network, the pain images of 96 by 96 resolution were input to the network; A total of 2,856 pair samples were used for training and the remaining 1,226 pair samples for testing in the UNBC-McMaster database. **Fig. 4.17** shows the contrastive loss chart of the Siamese network used in this study. The model was evaluated by changing the number of layers, and L indicates the layer shown in **Fig. 4.17**. As a result of the investigation conducted by increasing the number of layers from L3 to L5, the loss of both training and validation was the least in the ConvNet-L3 model.
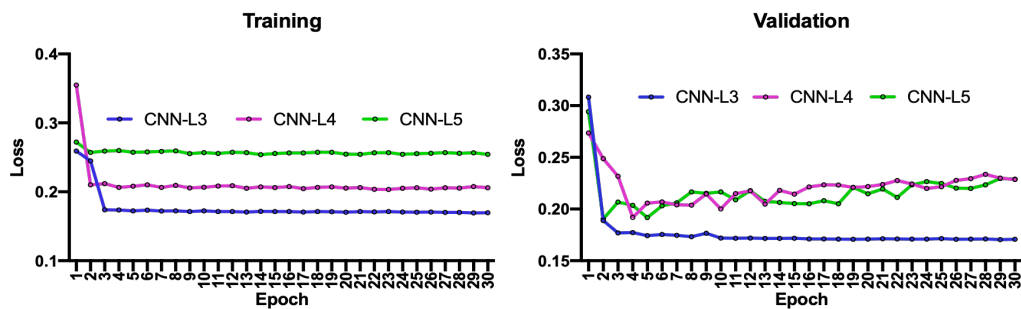
Figure 4.17. The loss of the method of pain intensity using Siamese network.

Fig. 4.18 illustrates an example of feature vectors with corresponding PSPI and SNPI. The ground truth, PSPI, was compared with the SNPI of the proposed method for pain intensity, and also observed changes in pain expressions by extracting facial landmarks from the image. In **Fig. 4.18** (a), a total of 68 facial landmarks were extracted and feature vectors (FV) were calculated as follows: left eyebrow width (FV1), right eyebrow width (FV2), distance between left and right eyebrow (FV3), left eye width (FV4), right eye width (FV5), left eye height (FV6), right eye height (FV7), distance between left eyebrow and left eye (FV8), distance between right eyebrow and right eye (FV9), distance between left eye corner and lip left corner (FV10), distance between right eye corner and lip right corner (FV11), lip width (FV12), inner lip width (FV13), lip height (FV14), distance between nose tip and upper lip (FV15), and nose

height (FV16). From observing frame #354 in **Fig. 4.18** (b), which has the maximum value of the ground truth (PSPI=15), changes in FV8, FV11, FV14, FV12, FV8, and FV9 were observed (**Fig. 4.18** (a)). These feature vectors are related to several action units (AU4: brow lower, AU6: cheek raiser, AU10: upper lip raiser, and AU43: eyes closed) when calculating PSPI. As a result, SNPI also had the highest value at 0.312 in frame #354.
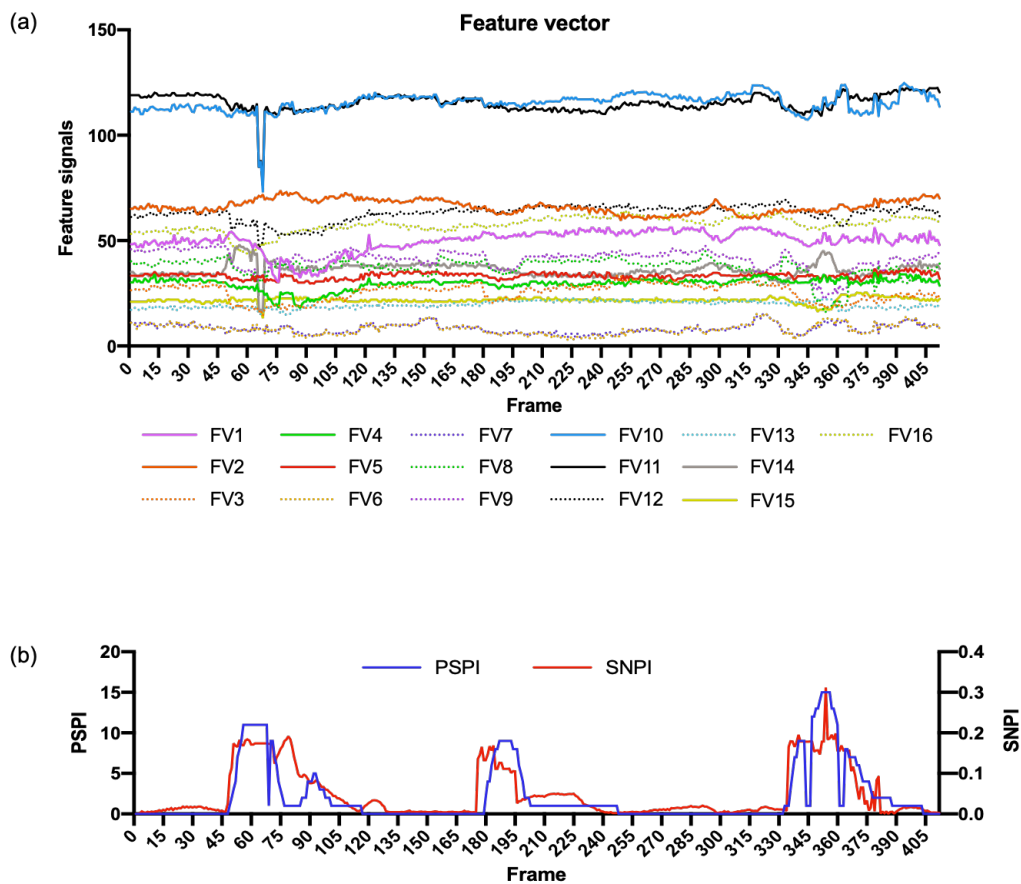
Figure 4.18. Example of the feature signals with corresponding Prkachin and Solomon Pain Intensity Scale (PSPI) and Siamese network-based pain intensity (SNPI) from data '107-hs107-hs107t2aaaff' (UNBC-McMaster Database) (a) Feature vectors (FVs) and (b) Result of the PSPI and SNPI.

To estimate the pain intensity using the Siamese network SNPI compared to the PSPI (ground truth), two measurement methods such as the Pearson correlation coefficient (PCC) and mean absolute error (MAE) were used. The PCC is a statistical test that measures the relationship between two variables. It has a value between -1 and 1, and the closer it is to 1 (positive correlation) or -1 (negative correlation), the higher the correlation was shown **Table 4.7** shows that the ConvNet-L3 model had the best estimations (PCC=0.87 and MAE=3.13).

Table 4.7. The evaluation of the pain intensity of the pain image using Siamese network (SNPI).

	ConvNet-Layer 3	ConvNet-Layer 4	ConvNet-Layer 5
PCC [a]	0.87	0.79	0.55
MAE [b]	3.13	4.89	6.11

[a] Pearson correlation coefficient. [b] Mean absolute error
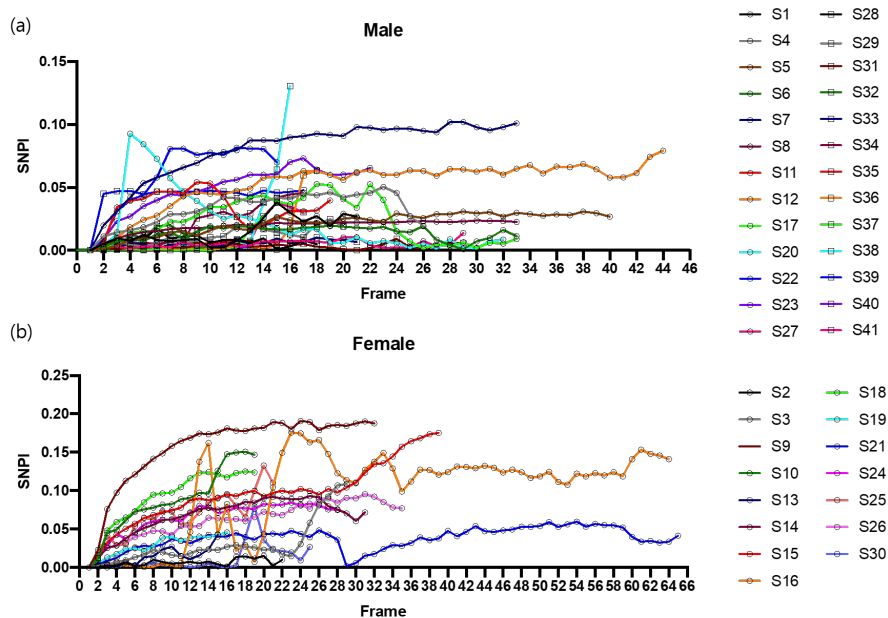
Figure 4.19. The result of pain intensity using Siamese network (SNPI) from all subjects in RU-PITENS database (a) male (b) female.
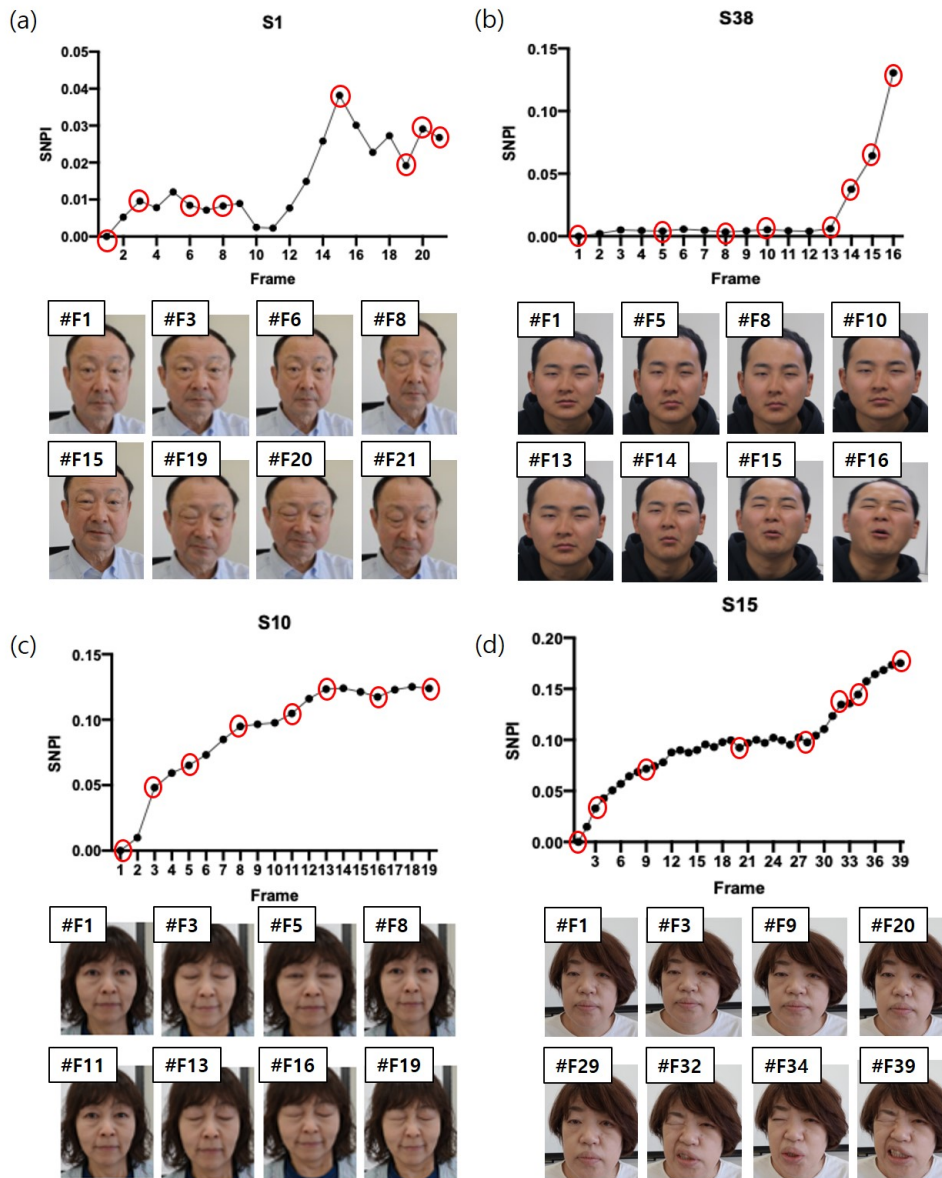
Figure 4.20. The result of pain intensity using Siamese network (SNPI) from subjects in RU-PITENS database (a) S1 (b) S38 (c) S10 (d) S15.

The results of most subjects showed that the intensity of facial pain tended to increase with the intensity of the electrical stimulation, as shown in **Fig. 4.19**. Comparing the pain intensity extracted from the facial image (SNPI) and the questionnaire, as with the result of S1, S10, S15, and S38 (**Fig. 4.20**), four participant's subjective pain (SPS), pleasure, and arousal scales averaged about 4.0 (out of 5 points, the higher

the score, the greater the pain), 3.0 (out of 9 points, the higher the score, the more positive) and 5.75 (out of 9 points, the higher the score, the more arousal) (refer to **Fig. 4.16**). Thus, in general, as the stimulation intensity increased using the TENS device, the intensity of pain obtained from the face and the questionnaire results showed a similar tendency. To address the **RP 4.3**, the following observations can be proposed based on these results.

Observation 4.3) It can be concluded that facial images, including pain intensity, can be acquired through stimulation using the TENS device.
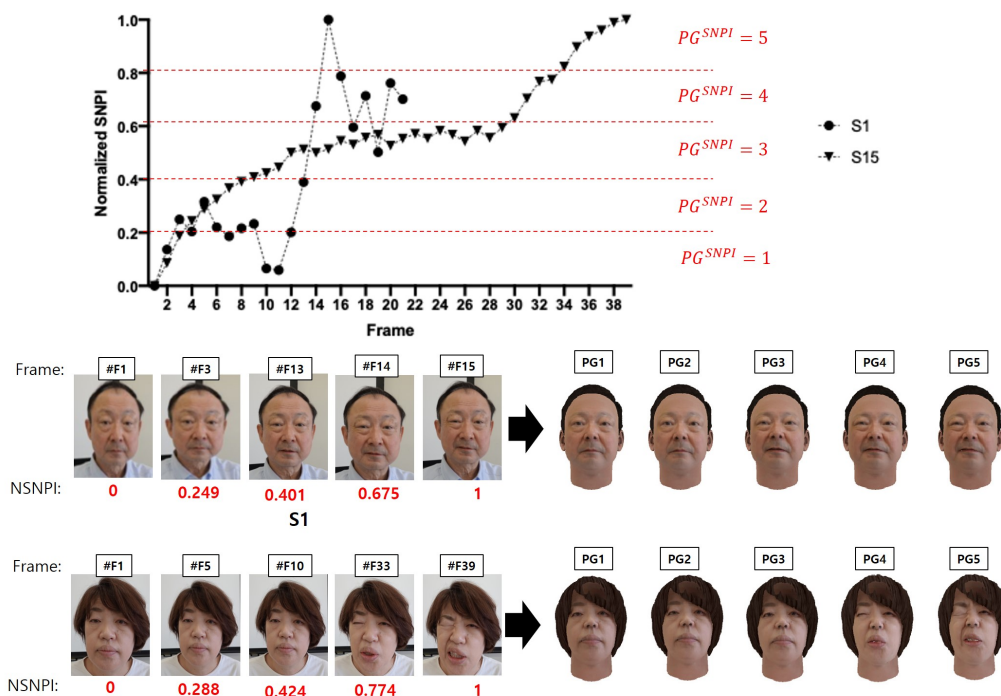
Figure 4.21. Result of pain group (PG) determination and avatar generation according to normalized Siamese network-based pain intensity (NSNPI).

4.6.7 Feasibility testing of robot's pain expression based on pain inference

Fig. 4.22 shows an example of a test of the integrated pain inference and expression technique in ROM exercise of the shoulder extension flexion (SEF). In **Fig. 4.22**, the patient robot can express five types of pain (PG1: no pain at all, PG2: very faint pain, PG3: weak, PG4: moderate, and PG5: strong) based on the method of determining the avatar. In passive SEF exercise, when the user fully flexes the glenohumeral joint of the robot, the angle of the glenohumeral joint ranges from roughly 100 to 110 degrees, and the FLPI value ranges from about 6 to 9. Finally, the avatar expressed a moderate or strong pain intensity as shown in **Fig. 4.22** (c).
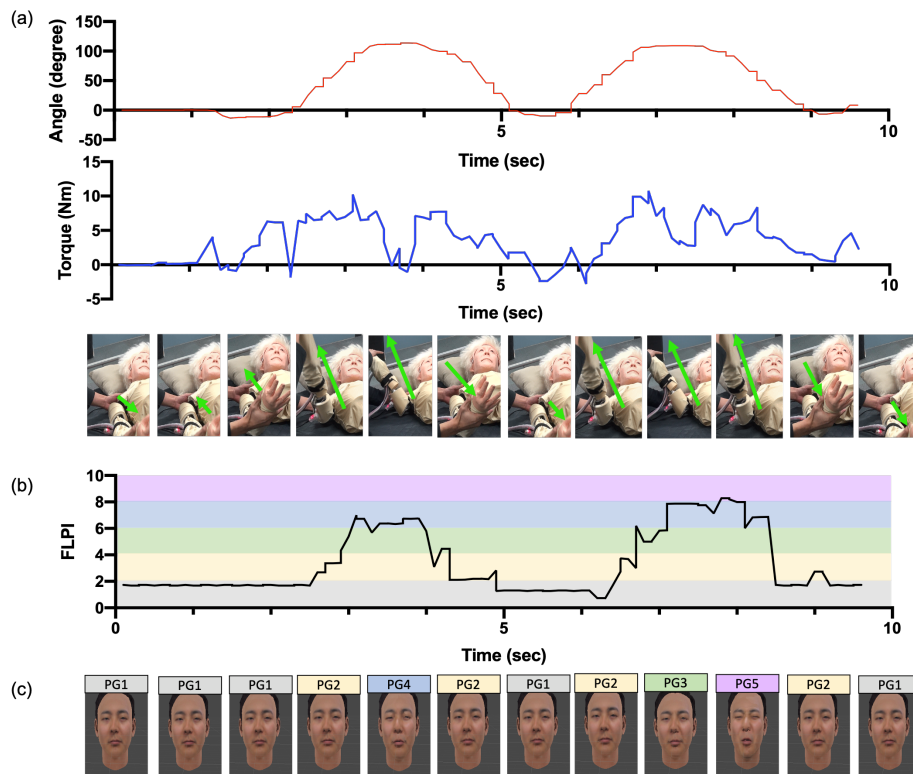
Figure 4.22. Testing of the pain expression of the patient robot in ROM exercise of the shoulder extension-flexion (SEF) (a) The angle and torque value of the glenohumeral joint of the robot (b) Fuzzy logic-based pain intensity of the robot (FLPI) (c) Avatar expression.

4.7 Discussion

The main objective of this Chapter was to propose a pain inference model and a pain expression model for the patient robot that can express pain states in joint care education to improve caregivers' skills in care training. The proposed system makes the following contributions. In Section 4.6.3, the increase in the number of trials of the ROM exercise affected the decrease in the pain intensity felt by the robot. Focusing on the result of the decrease in variance in the final trial rather than the initial trial, it can be concluded that users performed more consistent ROM exercises for care training in the final trial. Thus, it can be concluded that the patient robot has the potential to be an effective method for ROM exercises in joint care education.

In addition, the user relies on the value or graph of the robot's quantitative data output during care training in all ROM exercises. Because the gaze of the user tends to be focused on the robot's joints and joint movements, it is difficult to check how well the user is performing their tasks. However, care education applying the proposed visual feedback method in this work allows the user to receive feedback from facial expressions of pain in the robot in real time and obtain more information through advanced human-robot interaction. Consequently, it anticipated that these visual indicators can play an important role in achieving the ultimate goal of effective care education that allows users to react immediately.

Chapter 5

Robotic emotion expression

This Chapter presents the development of robot emotion detection and mood transition for a patient robot that can express current emotional states in joint care education. The main purposes of the proposed method in this Chapter are (a) to provide feedback that allows the caregiver to react immediately to the emotions felt by the robot during care training and (b) to propose a way for the caregivers and the robot to communicate their emotions, thereby enhancing the caregivers' ancillary qualifications such as stability, optimism, and communication (refer to Section 1.1). First, a method to track the user's emotions in real-time based on the face image is proposed so that the user's emotions are reflected as the robot's emotions, and the robot can express continuous mood transition. To track the user's emotional intensity, a total of 15 feature vectors according to seven types of facial expressions are calculated by extracting facial landmarks. Before starting the user's emotion tracking in real-time, the standard feature vectors for all user facial expressions are obtained through calibration, and when tracking starts, the distance between the input feature vector and the input image is obtained to measure the current emotional intensity. A new facial emotional intensity database from Ritsumeikan University (RU-FEmoI2021) was introduced for the robot's emotional expression for the experiment. The RU-FEmoI2021 database contains facial expression images of 41 Japanese people. This database consists of data obtained by dividing people into age groups in the 20's, 40's, 50's, and 60's. Based on the pain images in the RU-FEmoI2021 database, a robot's avatar is generated based on the user's current facial expression to achieve the interaction between the patient robot and caregivers. It is anticipated that an advanced patient robotic system based on human-robot interaction on the CNT by utilizing the robot's facial expression method.

5.1 Motivation

For the advancement of the patient robot, the scalability of the patient robot to which the robot's emotions are applied is required. The main motivations for the study of robot mood transition for the patient robot are as follows:

- The caregivers must have stability for continuous interaction with the patient because the caregiver's stability can give the patient reassurance [5].

- The caregiver with an optimistic disposition can positively change the patient's low moods and anxious psychology [4]. Even in terms of care education using patient robots, the optimistic disposition of caregivers can influence the robot's current emotions. Since an unskilled learner can give the patient robot an impression of tension during care training, a system that can provide the learner with the robot's current emotion should be introduced.

According to the above motivations, the unskilled caregivers should be trained to improve their ability to consistently create positive expression and a bright atmosphere in patients when the unskilled caregivers are confronted with the patient.

The recent research on the robot's emotion has been developed based on an approach in which the robot's emotion changes according to the current emotion of humans using expressions, texts, and voices [93]. Therefore, the robot's mood state reflects the user's current mood state, and the user can receive feedback from the robot; the first step in the robot's emotional expression is to recognize the human's emotional state. Human emotional states can be expressed through non-verbal and verbal expressions [94]. In [95], in the area of interpreting and capturing human emotional states, the non-verbal facial expressions account for 55% of the total, and verbal expressions (speech with the tone, intonation, and word) account for 45%. Besides, facial expressions are recognized as the most important part of communication [96, 97]. Thus, the study of this Chapter introduces the robot's emotion generation based on the user's current facial emotion.

5.2 Objectives and research problems

5.2.1 Specific objectives

The objectives of the method for robotic emotion transition of the patient robot introduced in this Chapter to achieve the goals are as follows.

- To develop an approach of robotic emotional state transition for generating robot's avatar

- To calculate the user's emotional intensity based on facial's expression using a camera

- To generate the robot's emotional transition that can give feedback by interacting with the user

- To propose a method of the robot's emotional transition according to the robot's personality

5.2.2 Research problems

In order to achieve the goals of the proposed method for robotic emotion transition in this Chapter, several research problems must be solved as follows:

- **RP 5.1)** What kind of method can determine the robot's personality?

- **RP 5.2)** Can the robot recognize and track the user's facial expressions?

- **RP 5.3)** In the continuous change of the user's facial expressions, can the robot's emotional transition continuously change in the pleasure-arousal map?

- **RP 5.4)** Does the robot's personality affect the robot's emotional transition?

5.3 Proposed framework

The framework (**Fig. 5.1**) of the proposed robotic mood transition method consists of (a) calculating the user's facial intensity to provide emotional information to the patient robot and (b) designing an approach to transit robotic emotion for interaction with the user. More detailed technical explanations are given in the next Section.
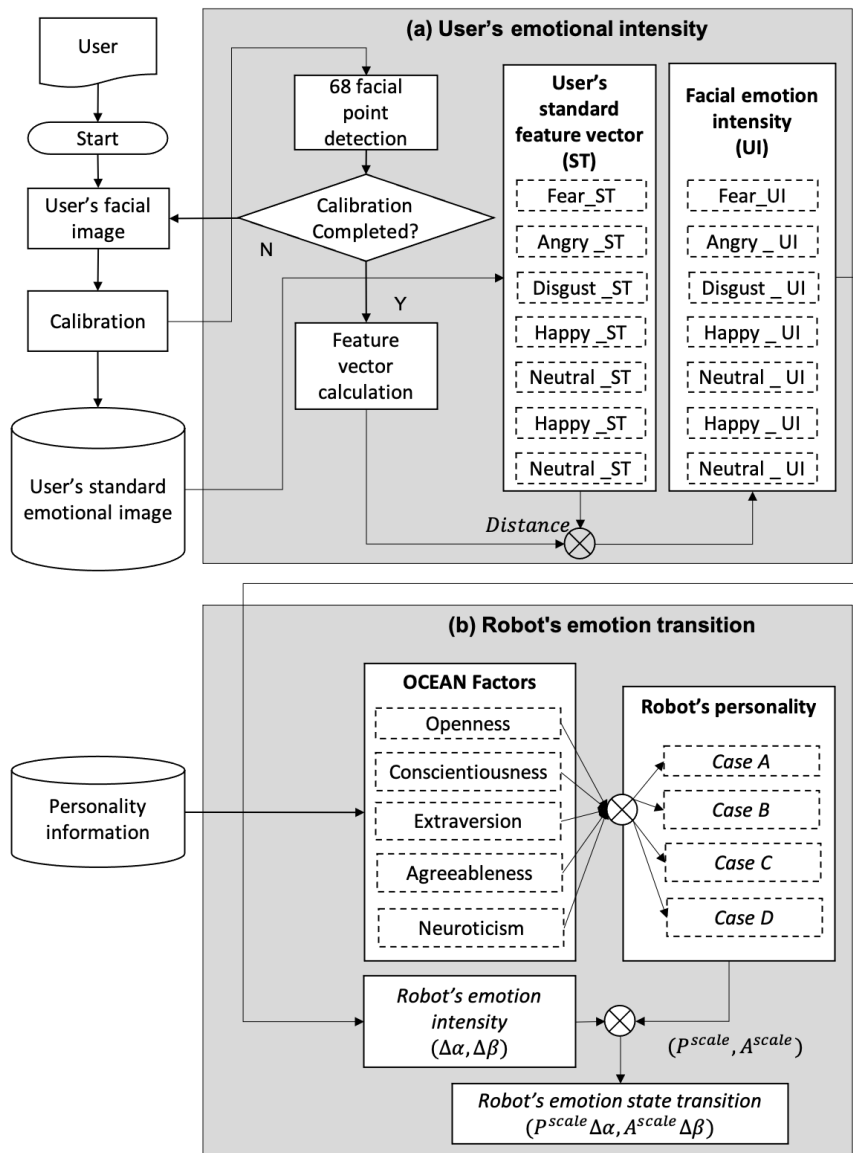
Figure 5.1. The whole framework of the proposed robotic emotional state transition.

5.4   User's emotional intensity

The user's emotional state can influence the psychological state of the robot. For example, if the user feels anxious, the robot may feel anxious, while if the user's emotions are stable, the robot can feel comfortable. In the human-robot interaction environment, the intensity of the n th user's facial expression (UI_n) is required to express the emotional state of the robot (n indicates the number of users). To calculate the user's emotional state UI_n, there are six kinds of steps as follows: i) calibration, ii) finding the facial landmarks, iii) extracting the feature vectors, iv) calculating the dissimilarity between the user and standard facial image, v) obtaining coefficients of user's current emotional intensity, and vi) determining user's current emotion. In this method, all procedures for detecting the user's emotional state are performed by the camera in front of the user.

5.4.1   Facial landmark detection

Facial landmarks are areas that protrude from the face and can be defined as characteristic points that can express facial features such as eyes, eyebrows, nose, mouth, and chin line as shown in **Fig. 5.2** (a). Facial landmark detection is the task of detecting critical landmarks on the facial area and tracking the feature points of the face through a shape prediction method in the range of interest (ROI). In this study, a shape predictor for faces (*shape predictor 68 face landmarks*) provided by the *DLIB* library (C++ toolkit containing machine learning algorithms and tools) [98] was used as a method of finding face points. In order to recognize the position of the facial landmarks, the shape predictor uses an ensemble of regression trees for learning on the given training data, and the accurate position of the facial landmark can be obtained in real-time. **Fig. 5.2** (b) shows the result of 68 facial landmarks detected from an example image in AKDEF datbase [99].
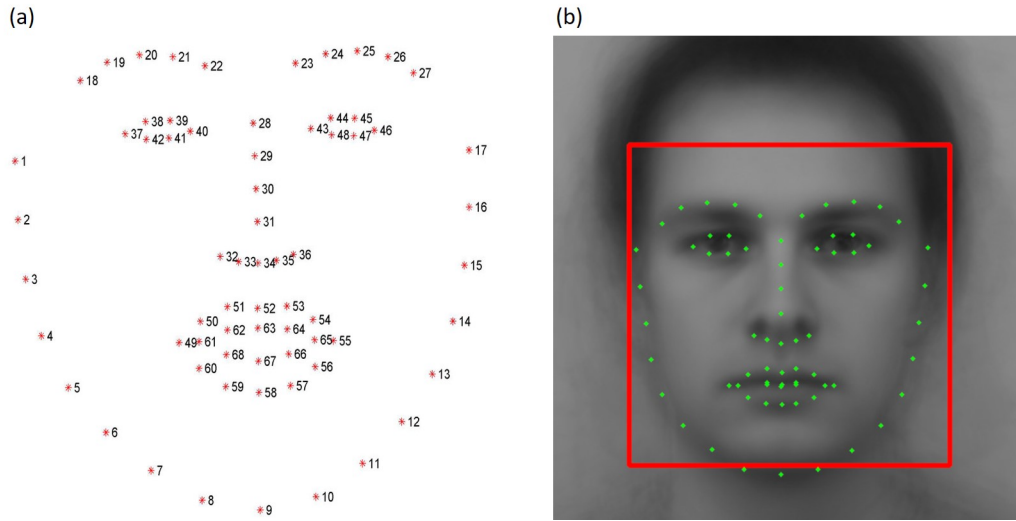
Figure 5.2. Facial landmarks (a) 68 standard coordinates (b) Landmarks with AKDEF datbase (Facial image credit: AKDEF-MNES (the Averaged Karolinska Directed Emotional Faces-Man-Neutral- Straight) [99]).

5.4.2 Calibration

Before starting calculating user's emotional state, the standard feature vectors are required to track the user's facial expression in step (a) (refer to **Fig. 5.1**). Therefore, before starting tracking, a calibration step of capturing the user's face according to each facial expression is performed. **Fig. 5.3** illustrates the procedure of the calibration from seven facial expressions such as fear (F), angry (A), neutral (N), happy (H), disgust (D), sad (S), and surprise (R). When the user expresses each facial emotion as much as possible, standard landmarks ($LM_{std,\ k}$) of each expression is extracted (**Eq. 5.1**) and stored in the buffer until all calibrations are completed.

$$LM_{std,\,k} = \begin{bmatrix} lm^F_{std,\,k} \\ lm^A_{std,\,k} \\ lm^N_{std,\,k} \\ lm^H_{std,\,k} \\ lm^D_{std,\,k} \\ lm^S_{std,\,k} \\ lm^R_{std,\,k} \end{bmatrix} = \begin{bmatrix} k^{th}\ \text{landmark in fear} \\ k^{th}\ \text{landmark in anger} \\ k^{th}\ \text{landmark in neutral} \\ k^{th}\ \text{landmark in happiness} \\ k^{th}\ \text{landmark in disgust} \\ k^{th}\ \text{landmark in sadness} \\ k^{th}\ \text{landmark in surprise} \end{bmatrix} \qquad (5.1)$$
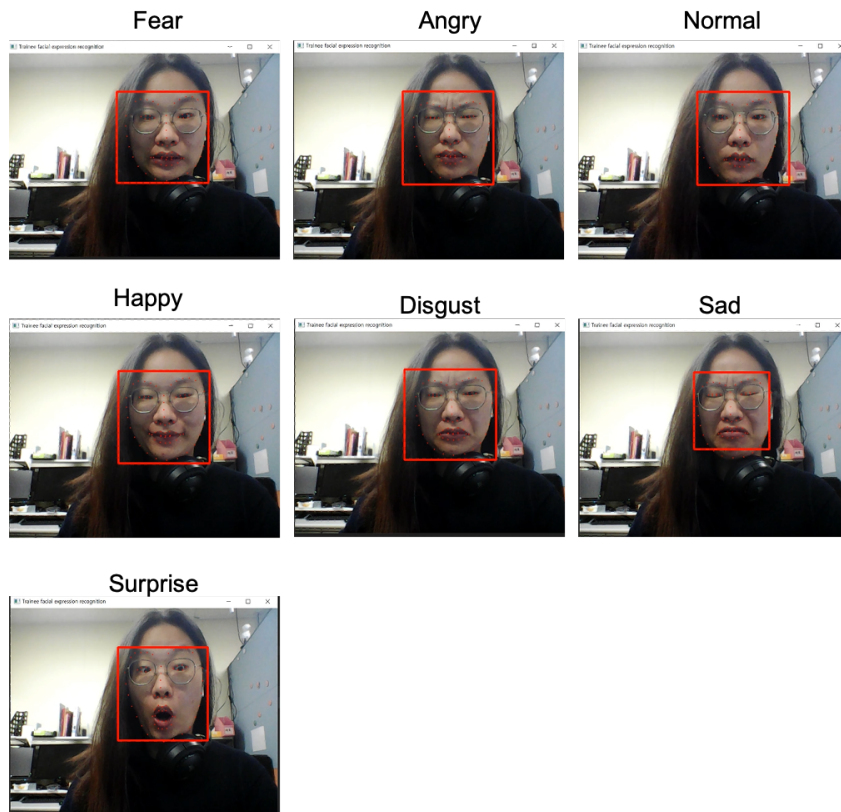
Figure 5.3. The facial landmarks detection from seven facial expressions.

5.4.3 Feature vector extraction

The feature vectors were extracted using a method verified by Sharma *et al.* [100] from 68 facial points based on Euclidean distance measure **Eq. 5.2**.

$$FV(lm^p, lm^q) = \sqrt{(lm_x^p - lm_x^q)^2 + (lm_y^p - lm_y^q)^2} \qquad (5.2)$$

where lm^p and lm^q refer to the landmarks of the feature vector $FV_{(lm^p, lm^q)}$ to be obtained. Based on the coordinates of the two landmarks, the distance was calculated and total 15 feature vectors were extracted as shown in **Fig. 5.4**, and **Table 5.1** represents the description of feature vectors. The criterion for selecting 15 feature vectors is defined by the action unit (AU) defined in the Facial Action Coding System (FACS) [101], and explanations related to each expression are as follows (except for neutral expressions):

- Fear (F): the expression of *Fear* is related to the movement of the facial muscles of inner brow raiser (AU1), outer brow raiser (AU2), brow lowerer (AU4), upper lid raiser (AU5), lid tightener (AU7), lip stretcher (AU20), and jaw drop (AU26); FV3, FV8, FV9, FV15, FV12, and FV14 are extracted to estimate these movement.

- Anger (A): the expression of *Anger* is related to the movement of the facial muscles of brow lowerer (AU4), upper lid raiser (AU5), lid tightener (AU7), and lip tightener (AU23); FV3, FV6, FV7, FV8, FV9, FV12, FV13, and FV14 are extracted to estimate these movement.

- Happiness (H): the expression of *Happiness* is related to the movement of the facial muscles of cheek raiser (AU6) and lip corner puller (AU12); FV10, FV11, and FV12 are extracted to estimate these movement.

- Disgust (D): the expression of *Disgust* is related to the movement of the facial muscles of nose wrinkler (AU9), lip corner depressor (AU15), and lower lip de-

pressor (AU16); FV15, FV12, FV10, FV11, and FV16 are extracted to estimate these movement.

- Sadness (S): the expression of *Sadness* is related to the movement of the facial muscles of inner brow raiser (AU1), brow lowerer (AU4), lip corner, and depressor (AU5); FV3, FV8, FV9, FV10, and FV11 are extracted to estimate these movement.

- Surprise (R): the expression of *Surprise* is related to the movement of the facial muscles of inner brow raiser (AU1), outer brow raiser (AU2), upper lid raiser (AU5), and jaw drop (AU26); FV4, FV5, FV8, FV9, and FV14 are extracted to estimate these movement.
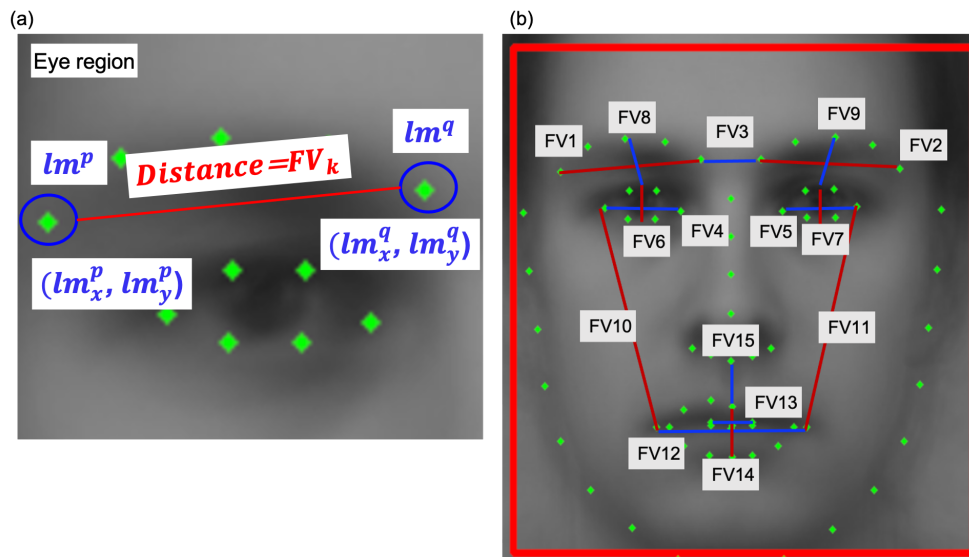
Figure 5.4. Features vectors (a) The method to calculate between two landmarks (b) 15 feature vectors (Facial image credit: AKDEF-MNES (the Averaged Karolinska Directed Emotional Faces-Man-Neutral- Straight) [99])).

Table 5.1. The descriptions of 15 feature vectors from the coordinate map with 68 facial landmarks.

Facial region	Feature vectors	Description
Eyebrows	FV1	Left eyebrow width
	FV2	Right eyebrow width
	FV3	Distance between left and right eyebrow
Eyes	FV4	Left eye width
	FV5	Right eye width
	FV6	Left eye height
	FV7	Right eye height
	FV8	Distance between left eyebrow and left eye
	FV9	Distance between right eyebrow and right eye
	FV10	Distance between left eye corner and lip left corner
	FV11	Distance between right eye corner and lip right corner
Mouth	FV12	Lip width
	FV13	Inner lip width
	FV14	Lip height
Nose	FV15	Distance between nose tip and upper lip

5.4.4 Facial emotional intensity

To obtain the intensity of each facial expression, a current feature vector $\overrightarrow{FV}_k^{cur}$ is calculated by extracting the landmarks when an image is an input from a camera in real-time. The feature vector $\overrightarrow{FV}_k$ refers to the 15 feature vectors described in the Section above. Referring to **Fig. 5.5**, this Section explains how to measure the intensity of the current emotional state $\overrightarrow{FV}_k^{cur}$, that is, the dissimilarity (distance) of the standard emotional state $\overrightarrow{FV}_k^{M=(F,A,N,H,D,S,R)}$ acquired in the *calibration* step. Here, F, A, N, H, D, S, and R indicates the fear, angry, neutral, happy, disgust, sad, and surprise expression, respectively.
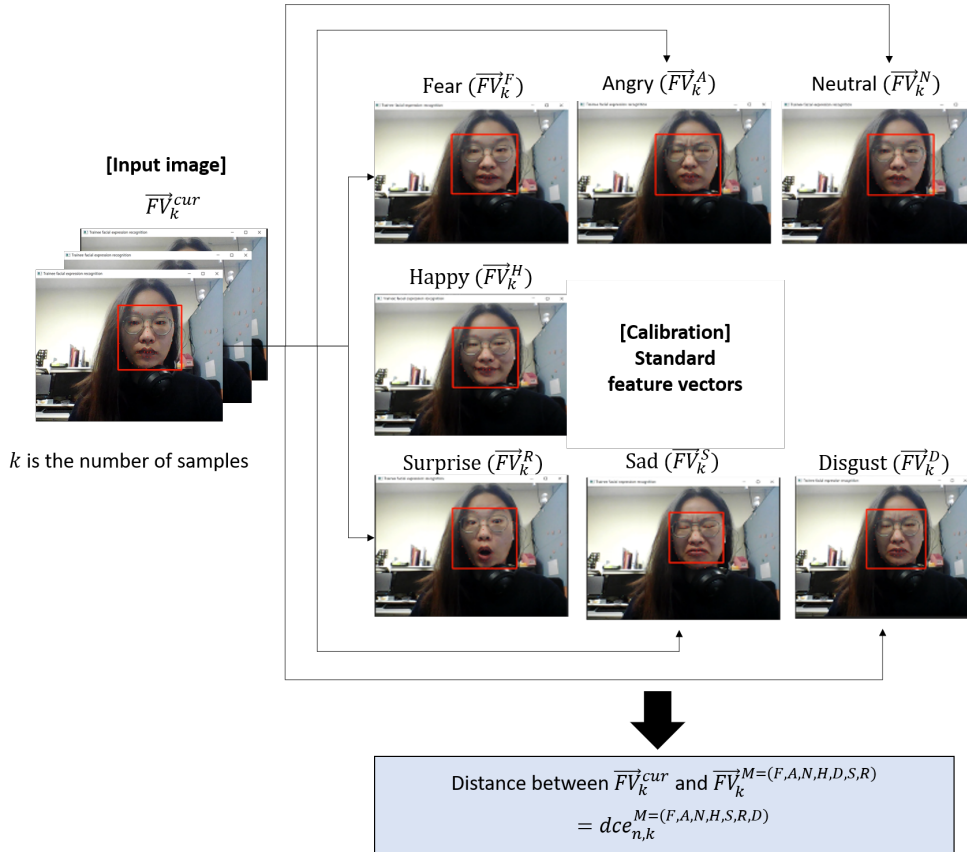
Figure 5.5. The procedure of the method to calculate distance between the standard feature vector FV_k^M and the current feature vector FV_k^{cur} of input image.

First, the dissimilarities ($dce_k^{M=(F,A,N,H,D,S,R)}$) [56] were calculated between the user's current feature vector ($\overrightarrow{FV}_k^{cur}$) from input image and standard feature vectors $\overrightarrow{FV}_k^M, M = (F, A, N, H, D, S, R)$. The dissimilarities ($dce_k^{M=(N,H,A,S)}$) of the four facial expressions in [56] were extended to seven expressions in this research, and the dissimilarities ($dce_k^{M=(F,A,N,H,D,S,R)}$) were defined using **Eq. 5.3**.

$$dce_{n,k}^m = \frac{1}{(\|\overrightarrow{FV}_k^{cur} - \overrightarrow{FV}_k^m\|)} \tag{5.3}$$

where m indicates the index of the expressions such as $F, A, N, H, D, S,$ and R. When the distance between the current emotional feature vector $\overrightarrow{FV}_k^{cur}$ and the standard feature vector $\overrightarrow{FV}_k^M$ is small, the similarity is high. Therefore, the dissimilarity dce_k^M of the two feature vectors can be calculated as the inverse of the distance $\|\overrightarrow{FV}_k^{cur} - \overrightarrow{FV}_k^M\|$.

Finally, the user's current emotional intensity $cei_k^{M=(F,A,N,H,D,S,R)}$ ($cei \in [0,1]$) can be normalized based on the dissimilarity ($dce_k^M = (F, A, N, H, D, S, R)$). **Algorithm 1** is the pseudo code of the current emotional intensity (CEI).

$$cei_k^F = \frac{dce_k^F}{dce_k^A + dce_k^N + dce_k^H + dce_k^D + dce_k^S + dce_k^R} \tag{5.4}$$

$$cei_k^A = \frac{dce_k^A}{dce_k^F + dce_k^N + dce_k^H + dce_k^D + dce_k^S + dce_k^R} \tag{5.5}$$

$$cei_k^N = \frac{dce_k^N}{dce_k^F + dce_k^A + dce_k^H + dce_k^D + dce_k^S + dce_k^R} \tag{5.6}$$

$$cei_k^H = \frac{dce_k^H}{dce_k^F + dce_k^A + dce_k^N + dce_k^D + dce_k^S + dce_k^R} \tag{5.7}$$

$$cei_k^D = \frac{dce_k^D}{dce_k^F + dce_k^A + dce_k^N + dce_k^H + dce_k^S + dce_k^R} \qquad (5.8)$$

$$cei_k^S = \frac{dce_k^S}{dce_k^F + dce_k^A + dce_k^N + dce_k^N + dce_k^H + dce_k^R} \qquad (5.9)$$

$$cei_k^R = \frac{dce_k^R}{dce_k^F + dce_k^A + dce_k^N + dce_k^H + dce_k^D + dce_k^S} \qquad (5.10)$$

Algorithm 1: Current emotional intensity

procedure EMOTIONAL INTENSITY PROCEDURE

    landmarkindex ← list to landmark index [FV1=[17, 21], FV2=[22, 26], FV3=[21, 22], FV4=[36, 39], FV5=[42, 45], FV6=[37, 41], FV7=[43, 47], FV8=[19, 37], FV9=[24, 43], FV10=[36, 48], FV11=[45, 54], FV12=[48, 54], FV13=[67, 65], FV14=[51, 57], FV15=[33, 51]]

    M=(fear, angry, normal, happy, disgust, sad, surprise)

    dce_M: dissimilarity to emotions

    newfv: feature vectors for input landmarks

    $stdfv_M$: feature vector to standard emotions

Function `DistanceFunc(`a, b`)`:

    $distance_M$← sqrt((pow((a[0] - b[0]), 2) + pow((a[1] - b[1]), 2)))

    Return $distance_M$;

while *True* **do**

    landmarklist ← list to facial landmark position

    for $lenth(landmarkindex)$ **do**

        newfv ← DistanceFunc(landmarklist[landmarkindex[i][0]], landmarklist[landmarkindex[i][1]])

    $distance_M$← DistanceFunc(newfv, $stdfv_M$)

    dce_M← inverse to $distance_M$

    diSum ← sum to dce_M

    cei_M← round($dce_M/diSum$, 2)

Result: Current emotional intensity ← cei_M

---

sqrt and *pow* indicates the square root and exponent power, respectively.
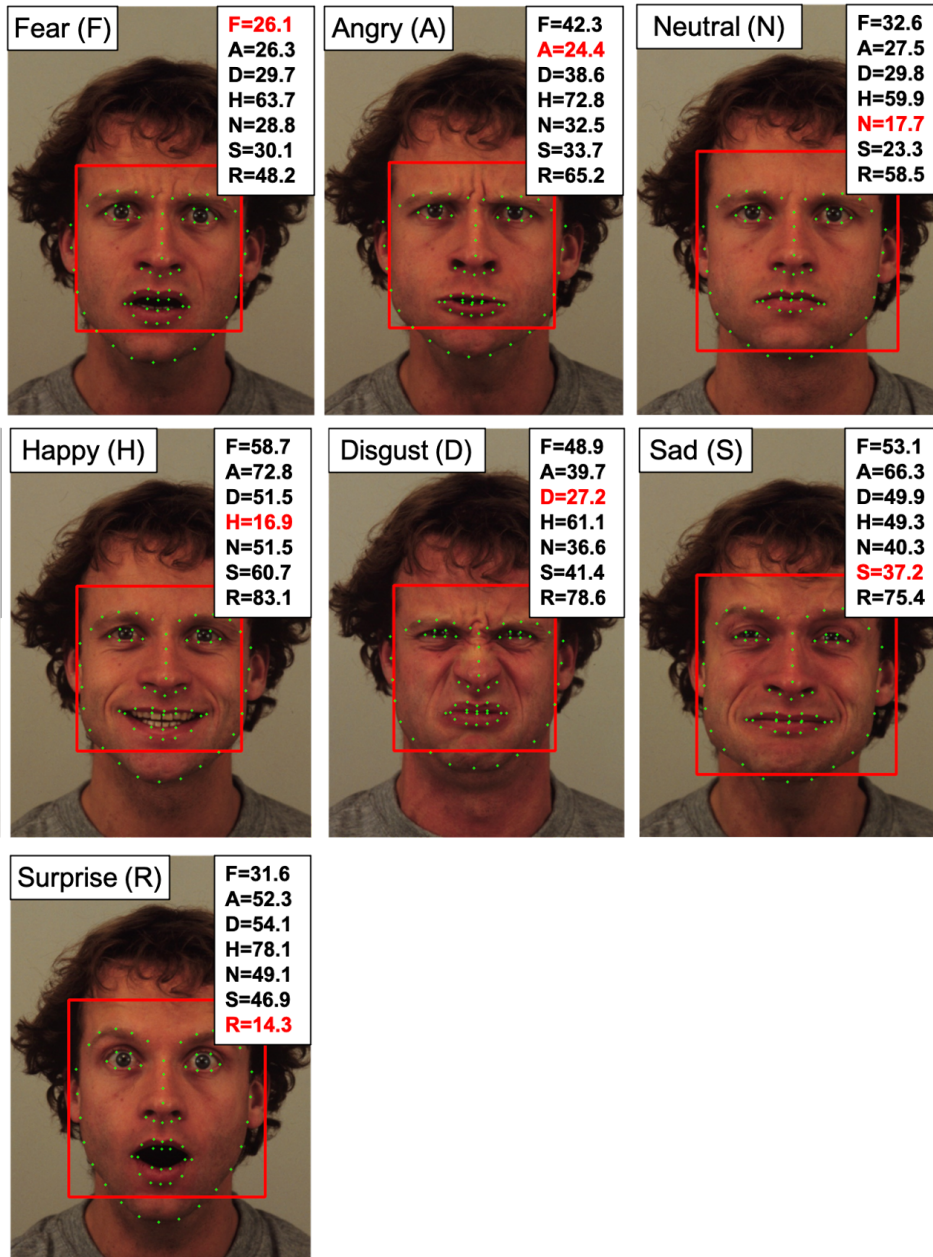
Figure 5.6. Example of dissimilarity dce_k^M of emotional states from '*KDEF-BM34*' in KDEF database [102].

5.5 Robot's emotional transition

As a method for generating robotic expressions, research on producing robots' emotions is conducted after tracking the user's current emotional state. The reported approaches for forming a robot's emotions have been proposed based on the user's emotions. Caregivers must continuously train care skills and qualifications such as stability, optimism, and communication. For example, in a care and nursing environment, the caregiver with an optimistic disposition can cause positive changes in the depression or anxious psychology of the patient. Besides, the caregiver's stability reassures the patient and creates a comfortable environment when communicating with the patient. Therefore, the caregiver needs training to continuously check the patient's mood transition, receive feedback for the patient's current emotion, and have a stable and bright expression. This Section deals with a method of tracking the mood transition of the patient robot according to the caregiver's facial expression for care education using the patient robot.

5.5.1 Robot's emotional state

Han *et al.* [57] proposed the interactive robotic emotional intensity ($\triangle\alpha_i$, $\triangle\beta_i$) based on four kinds of emotions (happiness, neutral, anger, and sadness). The interactive robotic emotional intensity represents the response from user's current emotional intensities on the pleasure-arousal plane. To define the relationship between pleasure and arousal, Russell [52] proposed the emotion's coordinates into the two-dimensional map. **Fig. 5.7** illustrates the mapping of prototype emotions based on the pleasure-arousal plane. The study of this Section measures the emotional intensity of robot (REI), REI_k ($\triangle\alpha_i$, $\triangle\beta_i$) for seven standard emotion factors (fear, angry, neutral, happy, disgust, sad, and surprise expressions).
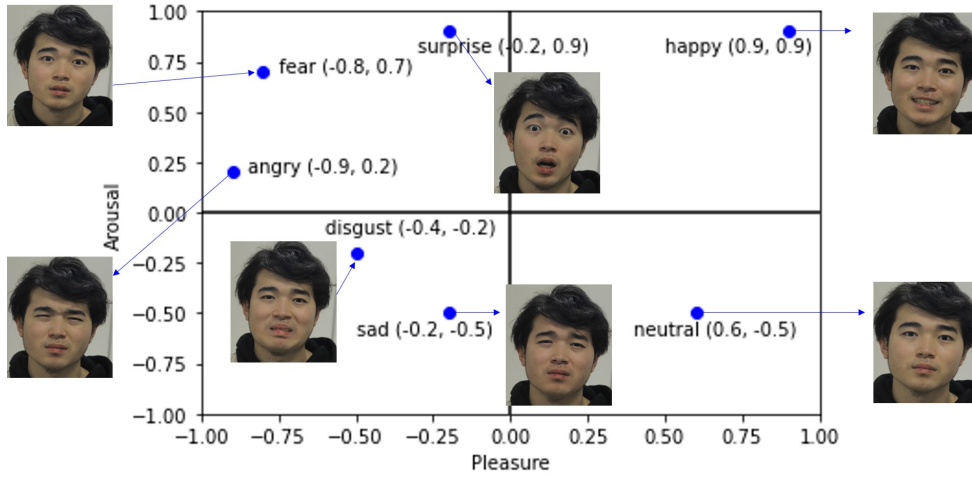
Figure 5.7. The mapping of prototype emotions based on the pleasant-arousal plane.

Table 5.2. Mapping factors.

Axis	Expressions						
	Fear (mf^F)	**Anger** (mf^A)	**Neutral** (mf^N)	**Happiness** (mf^H)	**Disgust** (mf^D)	**Sadness** (mf^S)	**Surprise** (mf^R)
P	-0.8	-0.9	0.6	0.9	-0.4	-0.2	-0.2
A	0.7	0.2	-0.5	0.9	-0.2	-0.5	0.9

Note: P and A indicate the pleasure and arousal axis, respectively.

Table 5.2 shows the mapping factors of seven expressions for projection robot's emotional intensity on the pleasure and arousal axis. Based on the mapping factors, the robotic emotional intensity $REI_k(\Delta\alpha_i, \Delta\beta_i)$ can be calculated using **Eq. 5.11** and **Eq. 5.12**.

$$REI_i{}^{\alpha} \text{ (pleasure axis)} = mf^H_{\alpha,i} \times cei^H_i + mf^S_{\alpha,i} \times cei^S_i + mf^A_{\alpha,i} \times cei^A_i$$
$$+ mp^F_{\alpha,i} \times cei^F_i + mp^D_{\alpha,i} \times cei^D_i + mp^R_{\alpha,i} \times cei^R_i + mp^N_{\alpha,i} \times cei^N_i \tag{5.11}$$

$$REI_i{}^{\beta} \text{ (arousal axis)} = mf^H_{\beta,i} \times cei^H_i + mf^S_{\beta,i} \times cei^S_i + mf^A_{\beta,i} \times cei^A_i$$
$$+ mf^F_{\beta,i} \times cei^F_i + mf^D_{\beta,i} \times cei^D_i + mf^R_{\beta,i} \times cei^R_i + mf^N_{\beta,i} \times cei^N_i \tag{5.12}$$

125

where mf_α and mf_β indicate the mapping factors in pleasure and arousal axis, respectively (**Table 5.2**), and cei_i represents the current emotional intensity and it can be calculated using **Eq. 5.4** to **Eq. 5.10** in Section 5.4.4. **Fig. 5.8** illustrates the example of the result of robotic emotional intensity REI_i. From the i-th input face image, the user's current emotional intensity CEI_i for the seven expressions is calculated, and the robotic emotional intensity REI_i, is calculated based on the mapping factors in **Table 5.2**. For example, in the case of the current image #1 (**Fig. 5.8**), the most potent user's current emotional intensity value among $CEI_i^{M=F,A,N,H,D,S,R}$ obtained is 0.83 at 'Happiness (cei_1^H)'. As a result, REI_1 was calculated and projected as closest to the mapping factor 'Happiness (mf^H=0.9, 0.9)'.

Current emotion #1

$$CEI_1 = \begin{bmatrix} cei_1^H = 0.46 \\ cei_1^S = 0.01 \\ cei_1^A = 0.14 \\ cei_1^F = 0.01 \\ cei_1^D = 0.07 \\ cei_1^R = 0.18 \\ cei_1^N = 0.14 \end{bmatrix} \otimes \text{Mapping factor}$$

REI_1

REI_1
(0.54, 0.94)

Mapping factor
REI_1
REI_2

REI_2
(-0.28, -0.41)

Current emotion #2

$$CEI_2 = \begin{bmatrix} cei_2^H = 0.10 \\ cei_2^S = 0.34 \\ cei_1^A = 0.10 \\ cei_2^F = 0.19 \\ cei_1^D = 0.11 \\ cei_2^R = 0.10 \\ cei_2^N = 0.06 \end{bmatrix} \otimes \text{Mapping factor}$$

REI_2
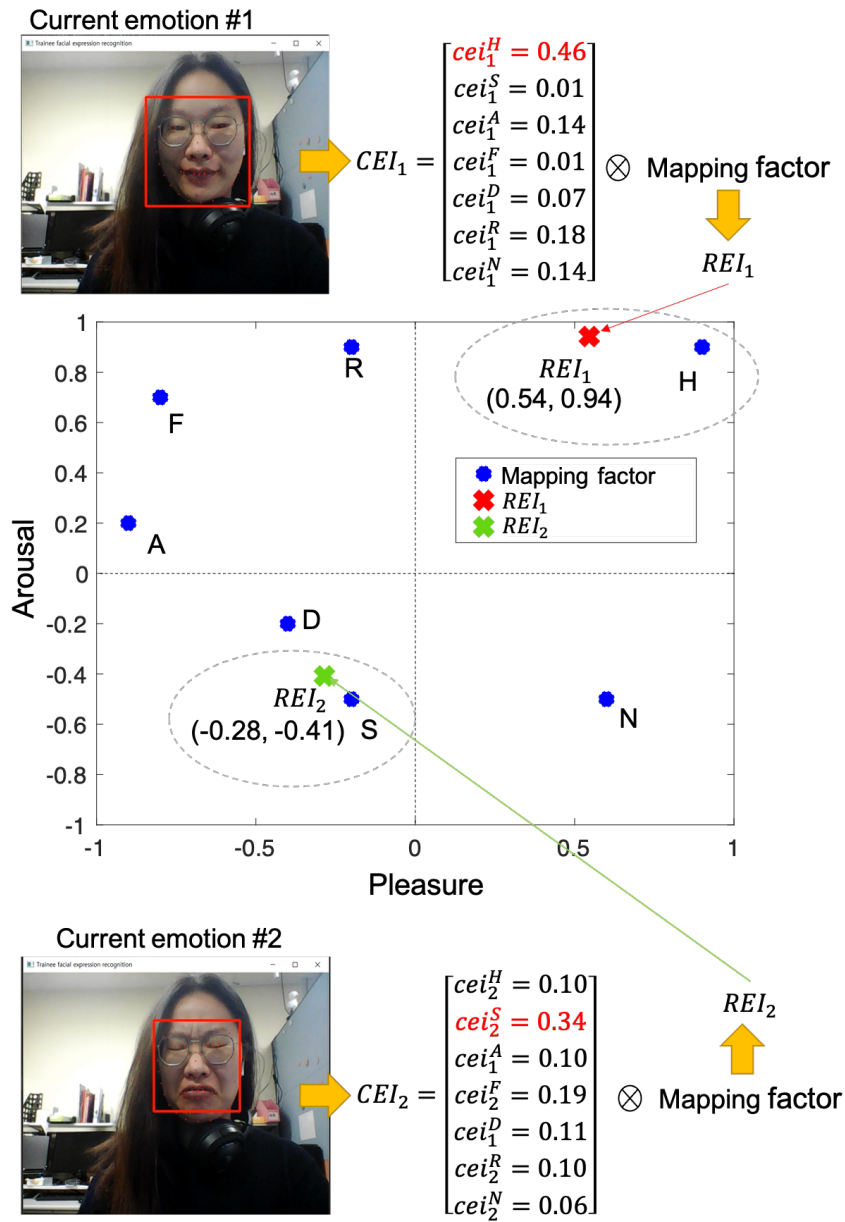
CEI: current user's emotional intensity
REI: robotic emotional intensity

Figure 5.8. Example of the result of robotic emotional intensity (REI).

5.5.2 Robot personality determination

A robot's personality affects the robot's emotional state and transition, and many studies have been investigated the robot's personality [103, 104, 105]. For human-robot interactions that extract robust comprehension, a robot's personality can be determined based on the cognitions and behaviors of a human personality [103]. In most studies, the robot personality was determined by using the *Big five factors (BF)* as openness (BF_O), conscientiousness (BF_C), extraversion (BF_E), agreeableness (BF_A), and neuroticism (BF_N). This *Big five factors* model, *OCEAN*, was derived by Mc-Crae *et al.* [106] to investigate the traits of personal characteristics. The description of *OCEAN* is as follows [107]:

- BF_O: The tendency to appreciate new art, ideas, values, feelings, and behaviors.

- BF_C: The tendency to be careful, on-time for appointments, to follow rules, and to be hardworking.

- BF_E: The tendency to be talkative, sociable, and to enjoy others.

- BF_A: The tendency to agree and go along with others.

- BF_N: The tendency to experience negative emotions such as anger, worry, sadness, and being interpersonally sensitive.

In this study, the robot personality was set to three types as talkative (Case A), shy (Case B), and smiling (Case C). As shown in **Table 5.3**, the weighting of *OCEAN* factors of four types of robot's personality were generated based on the result of the *Spearman* correlation of the five factors with the subject has observed characteristics reported by Gurven *et al.* [108].

Table 5.3. Result of *Spearman* Correlations of the *OCEAN* factors from self-report sample. Table adapted from *Gurven et al*. [108].

Factor	Personality		
	Case A (Talkative)	Case B (Shy)	Case C (Smiling)
Openness (BF_O)	0.070*	-0.508***	0.364***
Conscientiousness (BF_C)	0.133***	-0.428***	0.270***
Extraversion (BF_E)	0.178***	-0.584***	0.444***
Agreeableness (BF_A)	0.069*	-0.496***	0.292***
Neuroticism (BF_N)	-0.016***	0.315***	-0.236***

Note: The asterisk (*) indicates statistical significance at $p < 0.05$ and asterisks (***) indicates statistical significance at $p < 0.001$.

In **Table 5.3**, Case A (Talkative) showed very little correlation with all *OCEAN* factors and self-report results. On the other hand, in Case B (Shy), there was a negative correlation in openness (-0.508) and extraversion (-0.584), and this result means that Case B's personality opposes the extroversion character. In Case C (smiling), there was a positive correlation with extraversion (0.444) but a slight negative correlation with neuroticism (-0.236).

Based on the statistical results, the relationship according to the correlation value was interpreted to provide weights to determine the robot's personality, as shown in **Table 5.4**. Finally, the weight of the *OCEAN* factor concerning the three types of robot characteristics is defined as shown in **Table 5.5**. The observation for the research problem **RP. 5.1** in this Chapter are as follows:

Observation 5.1) Since the robot's personality is motivated by the actual human's personality extracted in [108], it can be more human-friendly than the robot's character set as an arbitrary value. In addition, reliability can be ensured based on statistical results in determining the robot's character.

Table 5.4. Interpretation of relationship between *Spearman* correlation and robot's personality's weighting.

Value of *Spearman* correlation (ρ)	Relationship Interpretation	Robot's personality weighting
-0.9≤	Very high negative	-1
-0.9≤ρ<-0.7	High negative	-0.7
-0.7≤ρ<-0.4	Moderate negative	-0.5
-0.4≤ρ<-0.2	Weak negative	-0.3
-0.2≤ρ<0	None	-0.1
0≤ρ<0.2	None	0.1
0.2≤ρ<0.4	Weak positive	0.3
0.4≤ρ<0.7	Moderate positive	0.5
0.7≤ρ<0.9	High postivie	0.7
≥ 0.9	Very high postivie	1

Table 5.5. The *OCEAN* factor's weighting in three cases for robot's personality.

Factor	Robot's personality weighting		
	Case A (Talkative)	Case B (Shy)	Case C (Smiling)
Openness (BF_O)	0.1	0.5	0.3
Conscientiousness (BF_C)	0.1	-0.5	0.3
Extraversion (BF_E)	0.1	-0.5	0.5
Agreeableness (BF_A)	0.1	-0.5	0.3
Neuroticism (BF_N)	0.1	0.3	-0.3

5.5.3 Robotic mood transition

Using the *OCEAN* factors, Mehrabian [109] presented the pleasure-arousal temperament model and derived the **Eq. 5.13** in order to calculate the pleasure-arousal scale (P^{scale} and A^{scale}, respectively) by analyzing the correlation among five factors.

$$P^{scale} = 0.21 BF_E + 0.59 BF_A + 0.19 BF_N,$$
$$A^{scale} = 0.15 BF_O + 0.3 BF_A - 0.57 BF_N. \tag{5.13}$$

Robot's personality-based robotic emotional intensity (REIP), $REIP_i^{(\alpha, \beta)}$, is calculated by using **Eq. 5.14** and **Eq. 5.15**.

$$REIP_i^{\alpha} = \begin{cases} -(P^{scale} \cdot REI_i^{\alpha}), & if\ (P^{scale} < 0\ and\ REI_i^{\alpha} < 0) \\ P^{scale} \cdot REI_i^{\alpha}, & others \end{cases} \tag{5.14}$$

$$REIP_i^{\beta} = \begin{cases} -(A^{scale} \cdot REI_i^{\beta}), & if\ (A^{scale} < 0\ and\ REI_i^{\beta} < 0) \\ A^{scale} \cdot REI_i^{\beta}, & others \end{cases} \tag{5.15}$$

Finally, the robot's mood transition (RMT), $RMT_i^{(\alpha, \beta)}$ is constantly affected by the previous state $RMT_{i-1}^{(\alpha, \beta)}$ [56] and it can be calculated by using **Eq. 5.16**.

$$RMT_i^{\alpha, \beta} = RMT_{i-1}^{\alpha, \beta} + REIP_i^{\alpha, \beta} \tag{5.16}$$

where i denotes the number of samples. In the initial state when the image is first input ($i=1$), $RMT_{i=1}$ is equal to the robot's emotional intensity $REI_{i=1}$ because $RMT_{i=1}$ is not affected by changes according to the robot's personality in the initial state. On the other hand, in the case of the robot's mood transition occurs continuously ($i>1$), the robot's mood transition $RMT_{i, (i>1)}$ is projected by reflecting the $REIP_i$ from the previous RMT_{i-1}.

Fig. 5.9 illustrates the example of calculating the robot's emotional intensity REI from the input images of the three emotions (happiness (Emotion #1), anger (Emotion #2), and sadness (Emotion #3)), and calculating the REIP according to the three types of robot's characteristics defined in **Table 5.5**. For case A (talkative), there was little change in REIP values because the values of the P^{scale} (0.099) and A^{scale} (-0.012) obtained from *OCEAN* were insignificant. In case B (shy), the P^{scale} (-0.343) and A^{scale} (-0.246) were negative due to its *OCEAN* effect, and it can be observed that the REIP value shifted to the negative plane. On the other hand, in case C (smiling), since the case C was greatly influenced by extroversion and openness factors, the REIP was shifted significantly toward the positive plane.
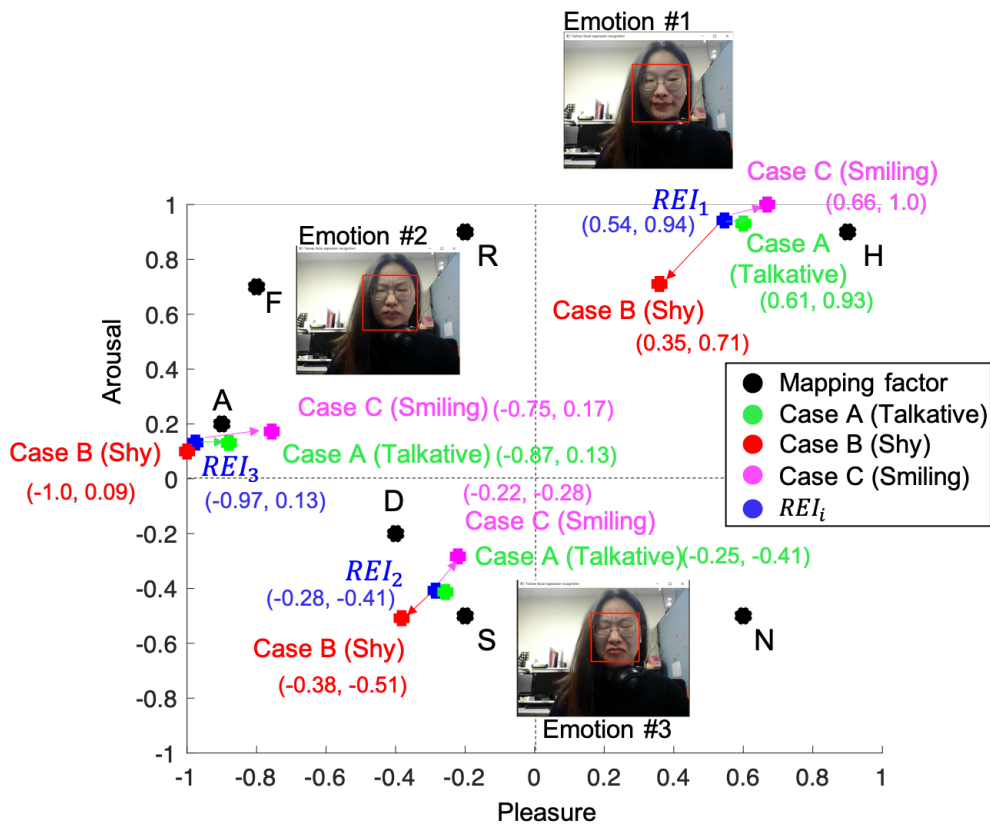

Figure 5.9. Example of robot's emotional intensity (REI) with robot's personality.

Fig. 5.10 illustrates the example of the robot's mood transition in the case of talkative (case A), shy (case B), and smiling (case C). By calculating the final robot's mood transition RMT using **Eq. 5.16**, it is observed that there is a significant difference in the robot's mood transition depending on the robot's personality. More detailed results and interpretation are discussed in the following Section.
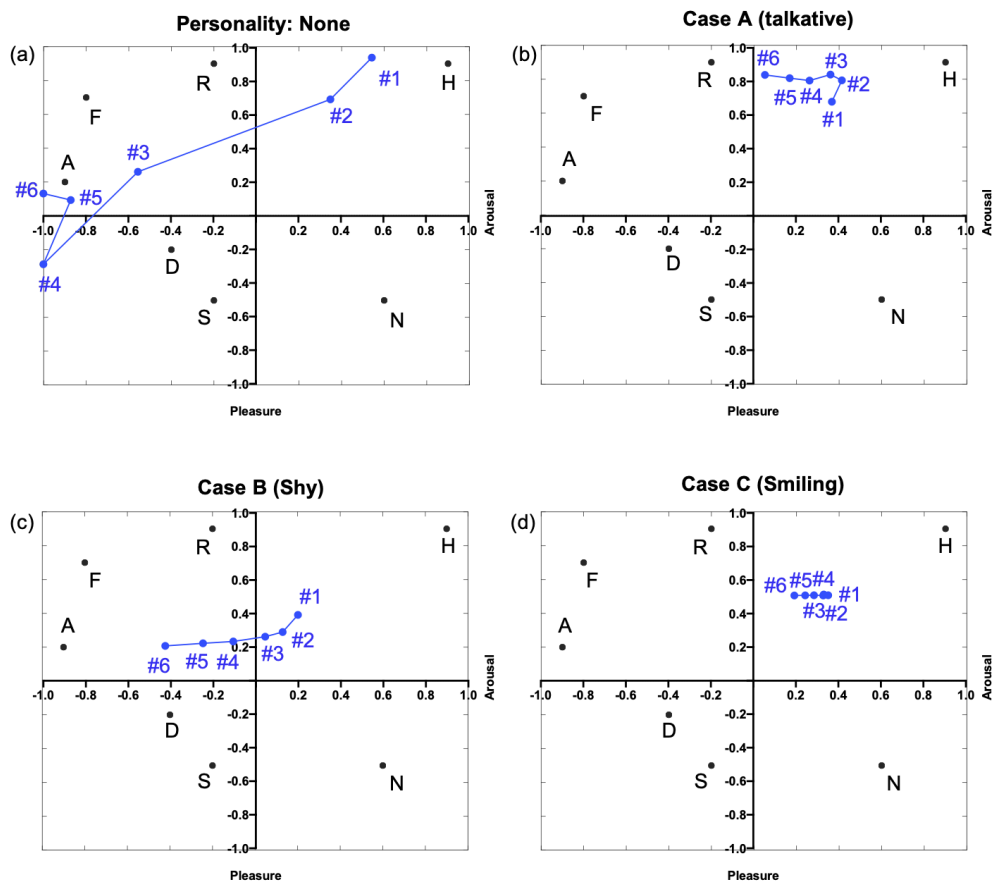

Figure 5.10. Example of robot's mood transition (a) none personality (b) case A (talkative) (c) case B (shy) (d) case C (smiling).

5.6 Experiment and results

5.6.1 New database: Facial emotion intensity (RU-FEmoI2021)

To measure the user's facial emotion intensity and generate the robot's emotional transition, a new facial emotion intensity (RU-FEmoI2021) database was built in this experiment. In particular, this RU-FEmoI2021 database was constructed by distinguishing four age groups in the 20s, 40s, 50s, and 60s, collecting facial images harmoniously according to age groups, and the purposes are as follows:

- Since the ultimate goal of this doctoral thesis (refer to Section 1.3), which is to measure the user's emotional intensity and generate the robot's emotional transition, is to generate an avatar of the patient robot. Therefore, the face images and meaningful findings in this RU-FEmoI2021 database are finally utilized to determine the patient robot's avatar in Chapter 6.

- The avatar-based robot head has the advantage of being easy to transform, so the face images of the subjects are used to divide the gender and age group to express the robot avatar in various ways.

As shown in **Table 5.6**, total forty one healthy subjects (Japanese people) were recruited to the study by advertisements posted on the participant's recruitment for experiment of the company. Facial images from 41 subjects, 26 males (mean age 46.6±3.4) and 15 females (mean age 55.8±2.4), were used for facial feature analysis and emotional intensity.

The subjects had no history of facial musculoskeletal disorders and paralysis, neurological pathology, and orthopedic surgery. This study briefed each subject on the study's purpose, and the subjects provided written informed consent prior to participation in the experimental procedures. The study was approved by the Ritsumeikan University Institutional Review Board (approval: BKC-2019-060). The experiment for this database was conducted in the AIS laboratory of Ritsumeikan

University and is published as an open database: `https://github.com/ais-lab/`
`RU-PITENS-database`

Table 5.6. Demographics of the participant's gender and age in facial emotion intensity (RU-FEmoI2021) database.

Facial emotion intensity (RU-FEmoI2021) database						
		Age range				
Gender	Measure	20 to 29	40 to 49	50 to 59	60 to 69	Total
Male		11	5	5	5	26
Female	N.S	-	5	5	5	15
Total		11	10	10	10	41
Male		23.7 (2.1)	45.0 (4.6)	53.6 (3.0)	64.0 (3.9)	46.6 (3.4)
Female	M.A	-	45.2 (2.3)	56.0 (1.6)	66.2 (3.3)	55.8 (2.4)
Total		23.7 (2.1)	45.0 (4.6)	53.6 (3.0)	64.0 (3.9)	47.2 (2.9)

Note: N.S and M.A indicate the number of subjects and the mean age, respectively. Numbers in parentheses are standard deviations.

5.6.2   Experimental environment and protocol

The experiment was conducted in a laboratory room, and the apparatuses including a main camera *Sony RX100VII* (Sony Group Corporation, Tokyo, Japan), video camera *Sony HDR-PJ790 HD Handycam* (Sony Group Corporation, Tokyo, Japan), and laptop camera *Samsung Odyssey NT800G5W* (Samsung Electronics, Seoul, South Korea) were used to acquire the facial images and record the video as shown in **Fig. 5.11**.
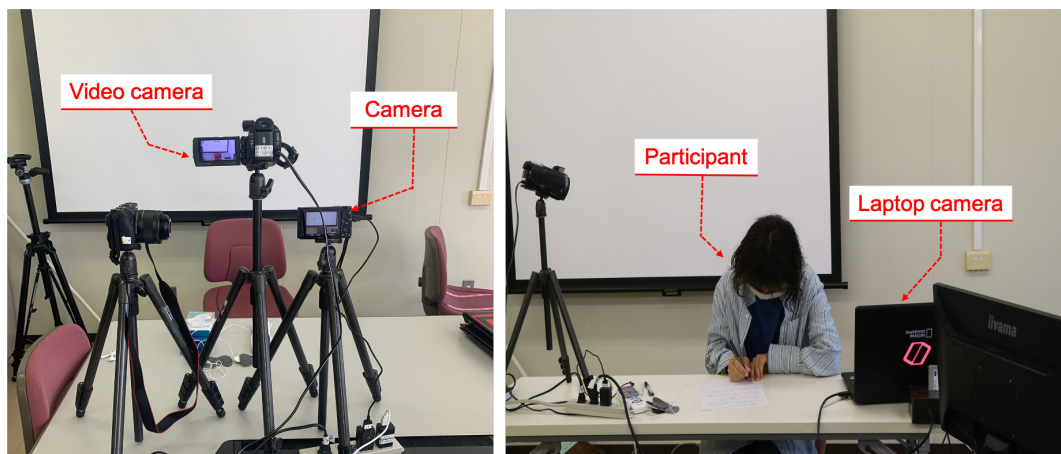
Figure 5.11. Experimental environment for RU-FEmoI2021 database.

Fig. 5.12 (a) shows the protocol of facial expression for the experiment. The subject's facial images were taken sequentially by placing the main camera in front of the subject and requesting seven facial expressions such as fear (F), angry (A), neutral (N), happiness (H), disgust (D), sadness (S), and surprise (R). In addition, the protocol for robotic emotion transition in real-time was designed as shown in **Fig. 5.12** (b).
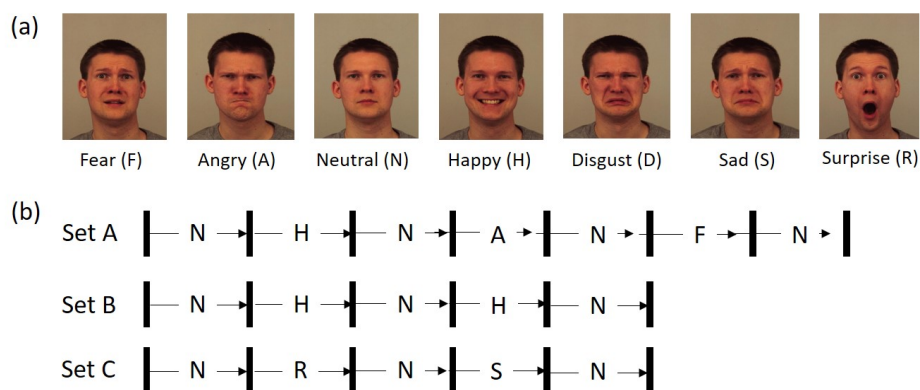

Figure 5.12. Protocol of facial expressions for RU-FEmoI2021 database (a) Example of facial expressions in KDEF database [102] (b) Protocol of facial emotional transition.

Fig. 5.13 illustrate the example of seven facial expression in RU-FEmoI2021 database. The English-numbered mark shown below the subject's face image is the subject's identifier (ID). The first three letters of the identifier are the age group, and the last three letters are the index of the subject. For example, In the ID of '60AS07', '60A' is an age group in the 60s, and 'S07' is an index of the subject, and English letters that follow with a hyphen mean identification of facial expressions.
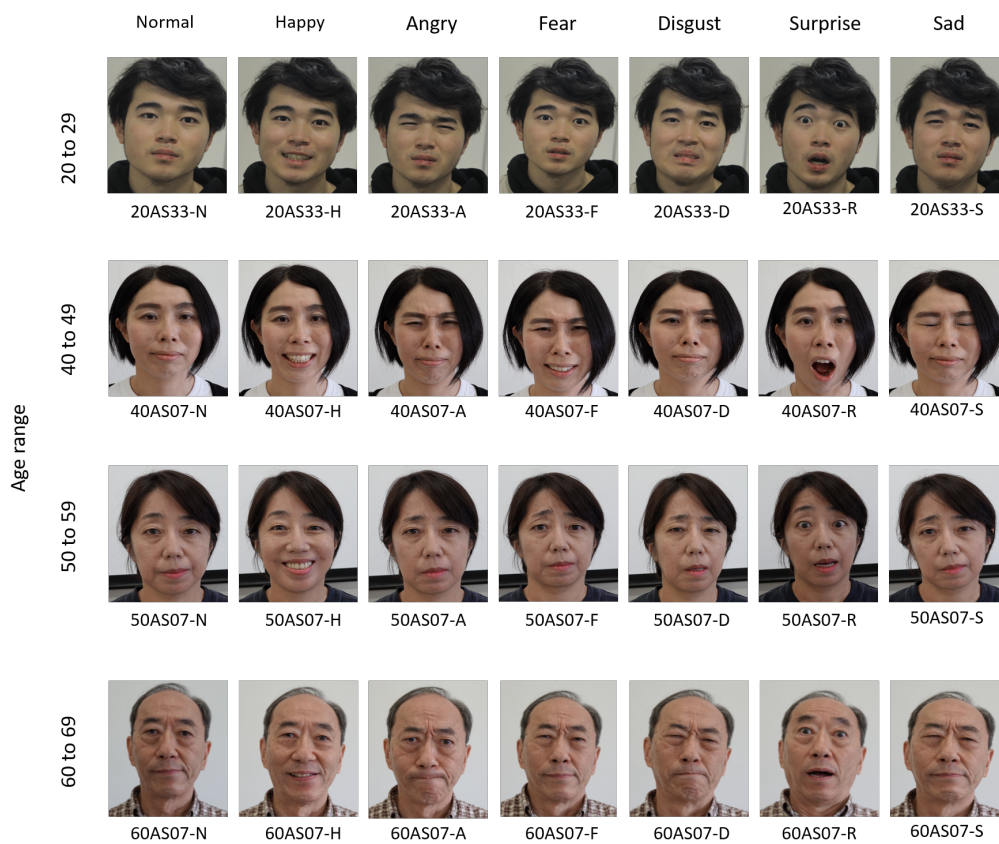

Figure 5.13. Example of facial expressions in RU-FEmoI2021 database.

5.6.3 Result of user's facial emotion state

This evaluation measures the intensity of the user's facial expression obtained from the camera in real-time. The protocol of this experiment is based on **Fig. 5.12** (a). All subjects who participated in the experiment repeated each expression ten times in a sequence (from the neutral expression to the next expression).

Figure 5.14. Testing of the user's emotional intensity (ID: 60AS28) in real-time. Blue text indicates the highest intensity. AFF, ANG, DIS, HAP, NEA, SAD, and SUS indicate the fear (afraid), angry, disgust, happy, neutral, sad, and surprise expression.

Fig. 5.14 is the screenshot of an experiment in which the facial expression's intensity was measured when subject #28 (S8, ID: 60AS28) conducted seven expressions in a real-time environment. The blue text indicates the intensity of the highest expression among the seven expressions in **Fig. 5.14**. **Fig. 5.15** illustrates the results of continuous facial emotional transition of S8. In the expressions of happiness (H), angry (A), and fear (afraid), the appropriately corresponding intensities of happiness, anger, and fear (afraid) showed relatively more remarkable results than the intensities of other emotions. In addition, it was remarkably confirmed that the cycle of changing from a neutral expression to a next expression was performed ten times. On the other hand, in disgust, surprise, and sadness expressions, negative expressions were complicatedly entangled and it was showing rather ambiguous results.
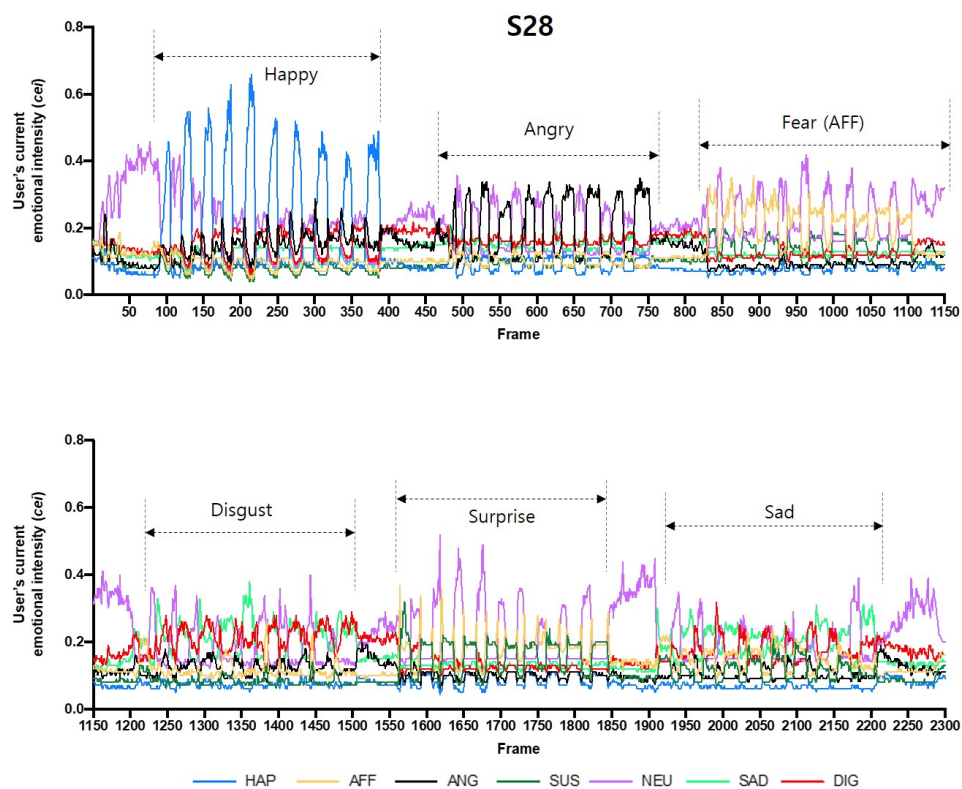

Figure 5.15. Result of the user's emotional intensity (ID: 60AS28) in real-time.

Figure 5.16. Testing of the user's emotional intensity (ID: 40AS06) in real-time. Blue text indicates the highest intensity. AFF, ANG, DIS, HAP, NEA, SAD, and SUS means the fear (afraid), angry, disgust, happy, neutral, sad, and surprise expression.

To take another example, **Fig. 5.16** shows the result of expression intensity according to the facial expressions of subject #06 (S6, ID: 40AS06). As a result of

continuous facial expression changes (**Fig. 5.17**), in the case of angry, sadness, fear (afraid), which were included in the ambiguous area, it could be confirmed that it clearly intersect with the neutral expression. Although the intensity of happiness expression was conspicuous, but there was still an ambiguous boundary between sadness and disgust expression.
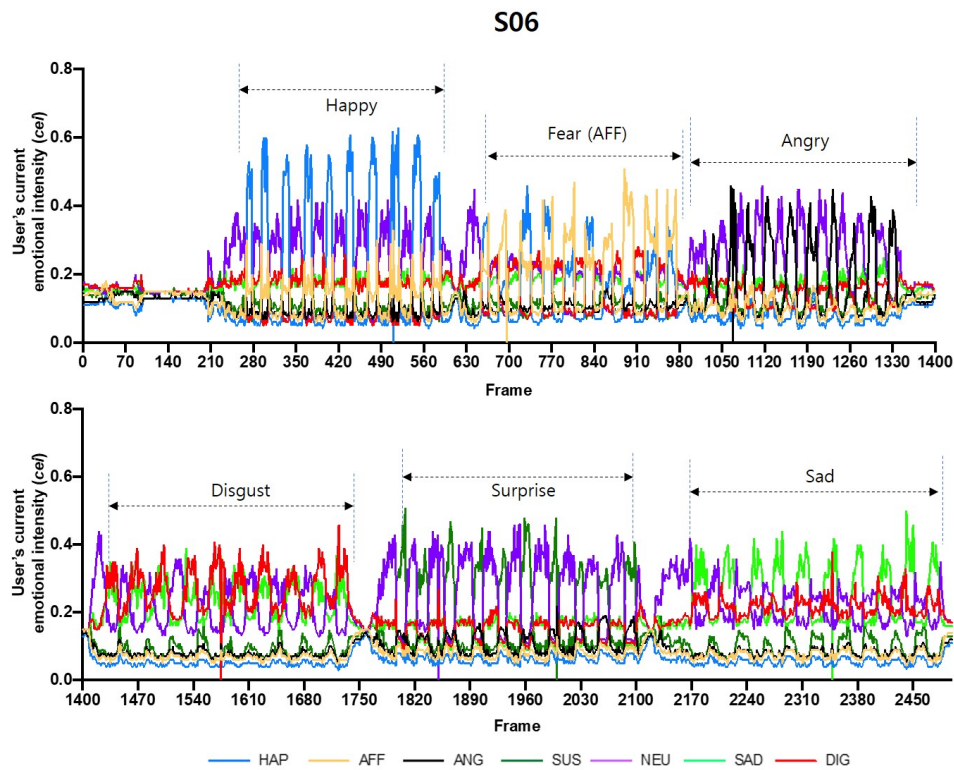

Figure 5.17. Result of the user's emotional intensity (ID: 40AS06) in real-time..

Table 5.7 shows the confusion matrix for the user's facial expression using the proposed method, and the overall accuracy is 91.92%. As shown in the confusion table, it was observed that fear (Precision (PR)=86.18% and Recall (RC)=91.22%) and disgust (PR=80% and RC=88.78%) were frequently confused, and happiness (PR=92.87% and RC=98.54%) was detected very slightly incorrectly in surprise (97.71% and RC=93.66%) expression.

141

Table 5.7. Confusion matrix for the user's facial expression in RU-FEmoI2021 database.

		Predicted Label							Total	RC
		F	A	N	H	D	S	R		
	F	374	10	0	3	20	3	0	410	91.22
	A	12	359	0	2	29	0	8	410	87.56
	N	0	0	392	0	14	4	0	410	95.61
Ground	**H**	4	1	0	404	0	0	1	410	98.54
Truth	**D**	24	17	0	0	364	5	0	410	88.78
	S	20	1	0	0	28	361	0	410	88.05
	R	0	0	0	26	0	0	384	410	93.66
	Total	434	388	392	435	455	373	393	2870	
	PR	86.18	92.53	100	92.87	80	96.78	97.71		

Note: F, A, N, H, D, S, and R mean the fear, angry, neutral, happiness, disgust, sad, and surprise expression. PR and RC indicate the precision and recall, respectively.

The observation of the research problem about the possibility of recognizing the user's facial expression and measuring the intensity by the method proposed in this Chapter is as follows.

Observation 5.2) As a result of measuring the user's facial expression and intensity in real-time, the proposed method showed an accuracy of 91.92%; it can be concluded that it will apply to exchanging emotions in a situation where the patient robot and the user interact.

5.6.4 Result of robotic mood transition

This evaluation investigates the feasibility of the proposed method to track the continuous robotic emotional state according to the robot's personality. As described in Section 5.5.2, the robot's personality is set as Case A (talkative), Case B (shy), and Case C (smiling) as shown in **Table 5.8**, and the effect of the robot's mood transition according to personality is examined.

Table 5.8. The Robot's personality P^{scale} and A^{scale}.

	P^{scale}	A^{scale}
Case A (talkative)	0.099	-0.012
Case B (shy)	-0.343	-0.246
Case C (smiling)	0.225	0.306

Fig. 5.18, **Fig. 5.19**, and **Fig. 5.20** illustrate the example of the robotic mood transition from S1 and S3 in the protocols such as Set 1, Set 2, and Set 3, respectively (protocols was explained in Section 5.6.2). In Set A (**Fig. 5.18**), although the result was significantly different depending on the robot's personality, the Case A (talkative) variance was relatively small because its weight projected on the pleasure and arousal axes was small (P^{scale}=0.099 and A^{scale}=-0.012). On the other hand, in Case B, it can be observed that the robot's mood is rapidly changed from the arousal axis to the negative direction according to the emotional change of S3. Since the Case B (shy) personality has a negative weight on the arousal axis (A^{scale}=-0.246), the robot's mood is more strongly affected when the user's emotional state is negative. In the Case C, it can be observed that when the user's emotion in S3 was detected as happiness (H), the robot's mood increases sharply on the pleasure axis (Sequence #3 in **Fig. 5.18**) and then changes to negative on the arousal axis when it changes to angry (A) (Sequence #4 in **Fig. 5.18**)). The personality as Case C (smiling) has a positive weight (P^{scale}=0.225 and A^{scale}=0.306), it can be observed that it stays in the happiness (H) region even in the neutral (N) state.

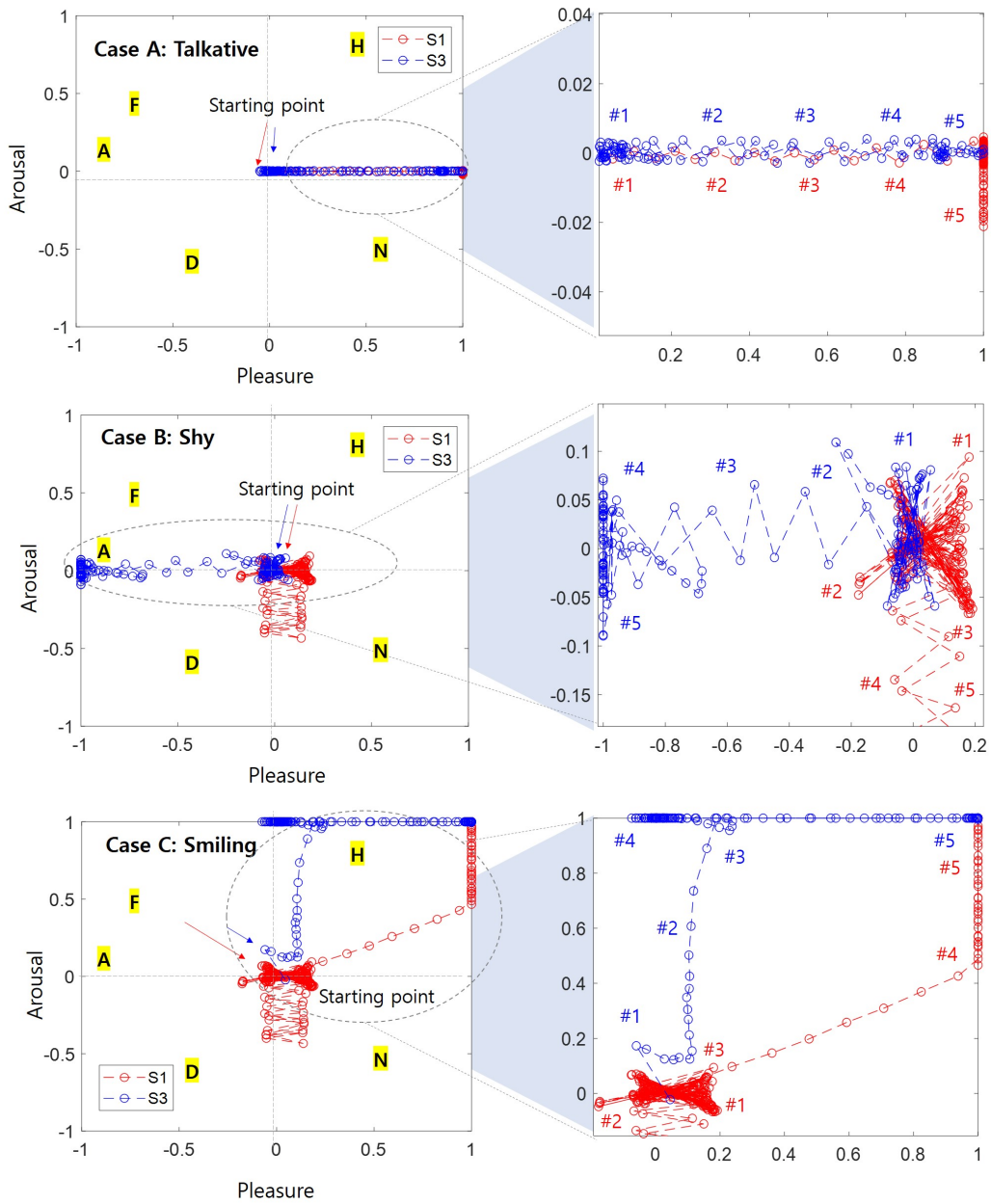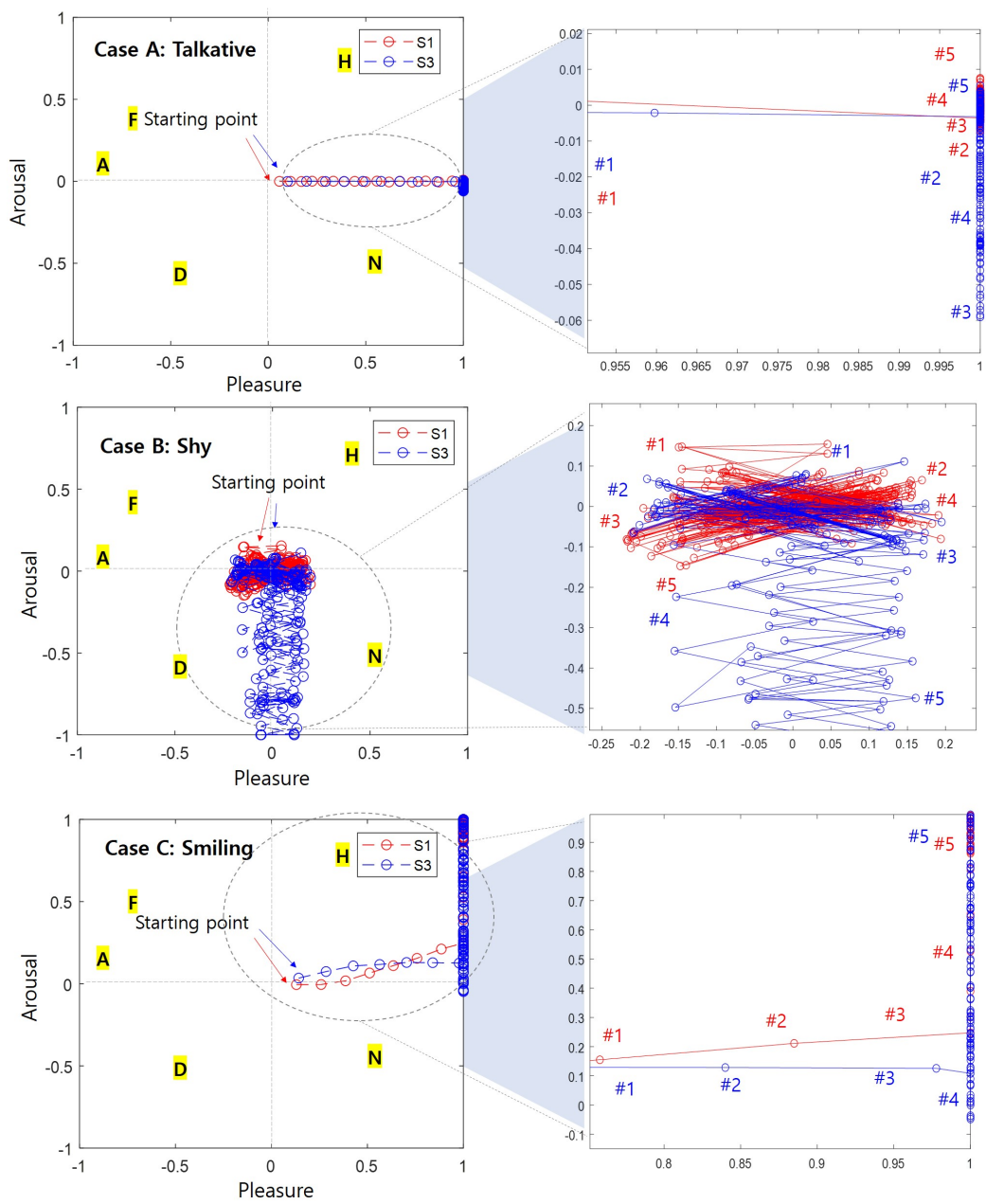**Figure 5.18.** Trajectory of the robotic mood transition with different robot's personality from S1 and S3 in Set A (N-H-N-A-N-F-N).

Figure 5.19. Trajectory of the robotic mood transition with different robot's personality from S1 and S3 in Set B (N-H-N-H-N).
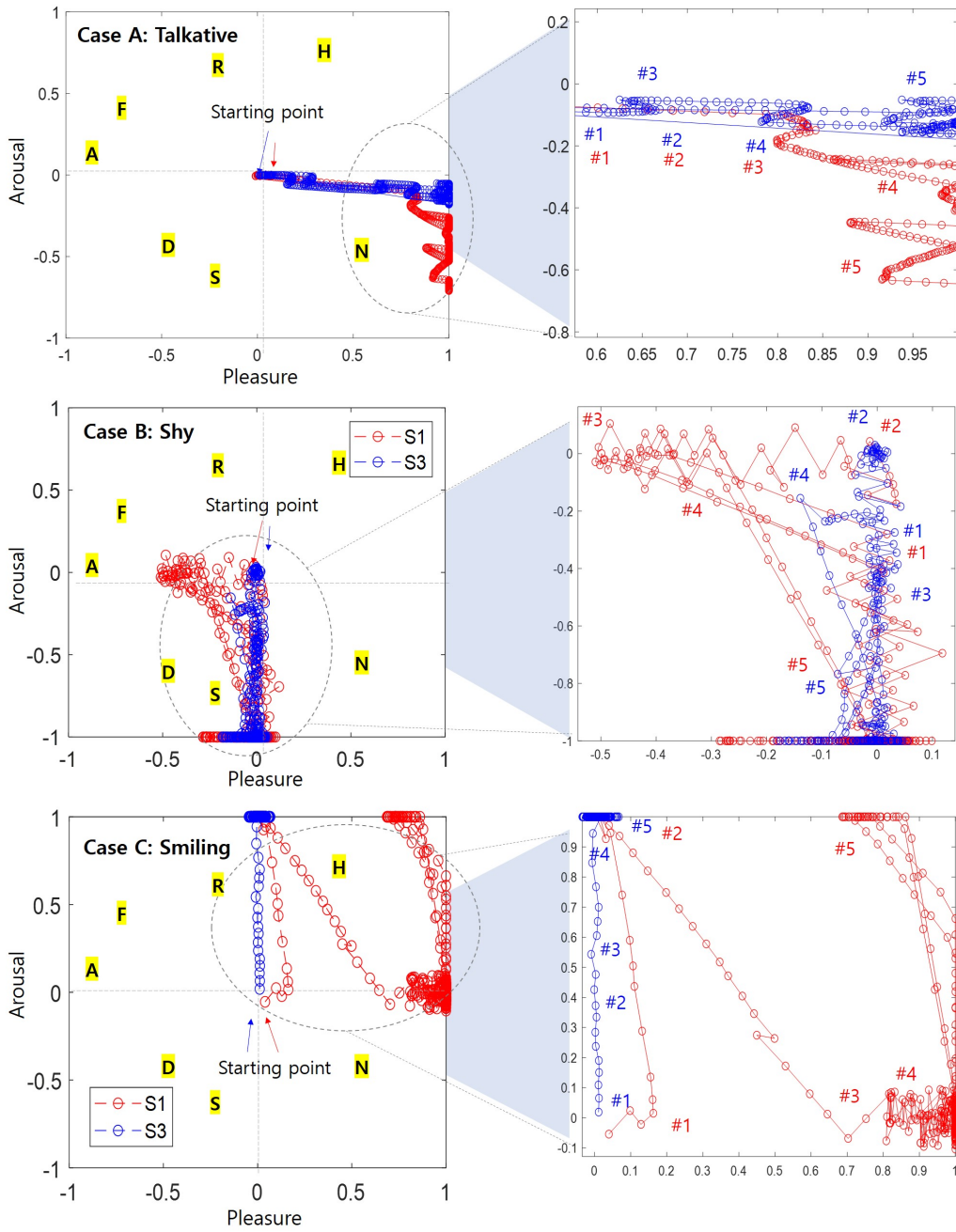
Figure 5.20. Trajectory of the robotic mood transition with different robot's personality from S1 and S3 in Set C (N-R-N-S-N).

Fig. 5.19 shows the trajectory of the robotic mood transition with different personality in Set B. There was no significant change on the arousal axis in Case A (talkative) when expressing a happy expression continuously from a neutral expression. On the other hand, the robot's mood transition in Case B (shy) was found in the midpoint of the pleasure and arousal plane, and the personality as Case C (smiling) showed more heightened results in a positive direction in the mood of H (happy) than other cases such as Case A (talkative) and Case B (talkative).

According to the robot's mood transition result according to the user's emotion's change based on the arousal axis, the robot's mood continuously changes along the arousal axis as in Case A (talkative). In case A of **Fig. 5.20**), it can be observed that the robot's mood changes (Sequence #4 and Sequence #5 in **Fig. 5.20**) based on the pleasure axis as the user's emotions change in the order of neutral, sadness, and neutral expression. In addition, the personality of Case A (talkative) has a negative effect (A^{scale}=-0.012) on the arousal axis, so it can be seen that when the user's emotion is neutral, it continuously decreases in the vertical direction based on the arousal axis. Based on these results, the observation can be suggested to solve the **RP 5.3** and **RP 5.4**.

Observation 5.3) It was observed that the robot's mood continuously changed according to the continuous user's current emotion, and the current robotic mood was accumulated and changed under the influence of the previous robotic mood.

Observation 5.4) In the interaction situation, the degree of reaction or expression may vary depending on the personality of the individuals. Therefore, this study applied the different personalities to the robot's mood transition and it was intended to examine how it affects the robot's mood. Consequently, the evaluation was found that the robotic mood according to the robot's personality had a significant effect on the mood transition in the situation where the change in the user's emotional state was the same.

5.7 Summary

The facial expression and the attitude of the caregivers can be included as a part of care ability, and it supports the patient's emotional state to be stably maintained when the caregiver's expression is comfortable and calm. To apply these conceptual problems to the patient robot system, therefore, the following objectives of this study were achieved. The objectives of this Chapter were (a) to generate the robotic mood for the patient robot's avatar to provide the assessment of the user's care ability in the care education and (b) to investigate the possibility of the robot's mood transition based on the robot's personality. To summarize the proposed method's description, the method to track the robot's mood transition was proposed for expressing the patient robot's emotion in the care training environment. The proposed method was designed for users using the patient robot to react immediately to the robot's emotions and performed based on the user's facial expression intensity in real-time. In addition, to observe the tracking of the change of the robot's mood according to the robot's personality, the robot's personality was defined by statistical results of the actual human personality. The method for determining the robot's personality was successfully applied to help users to improve their interaction skills to respond to various personalities, sensitivities, and situations in the care and nursing environment. Although studies to determine the robot's personality have been conducted in many studies [56, 58], the factors of *OCEAN* were arbitrarily determined or set in a dichotomous way as an extrovert (active trait) or introvert (passive pessimist) personality. To investigate more diverse personality types, however, this paper proposed human-friendly robot emotions by setting three personality types through statistical results of personality by a survey participated in from humans. As a result, the method of this Chapter has been proven to be applicable to the patient robot's facial expression system, which is the primary purpose, and will be expressed as an avatar in the integrated system of the patient robot to be introduced in Chapter 6. In addition, the proposed method is foreseen to be applied to successfully communicate emotions in various fields where humans and robots interact.

Chapter 6

Care training assistant robot based on the pain and emotional expression

This Chapter presents an approach for integrating a care training system based on the patient robot's pain and emotional expression. The main objective of this Chapter is to demonstrate the feasibility and the possibility of the proposed integrated care training system using the patient robot that can provide information on psychological and emotional factors. In Chapter 3, the patient robot for care training was successfully designed to reproduce the patient with the musculoskeletal symptom, and it can be concluded that the feasibility of the patient robot was proved. In Chapters 4 and 5, the study of the robot's pain inference and the mood transition was well-established in order to express the robot's pain and emotional expression in care education. Based on the methods proposed in the previous Chapters, a projector-based robotic head is proposed to express the robot's pain and emotional state in care education. The use of the robotic head can relieve the robot's pain and improve the user's care skills by reacting immediately to the pain expression when the robot feels pain according to the care action in a real-time environment, and the user can make it possible to interact emotions with the patient robot. In addition, the main advantage of using a projector-based robot head are its relatively reasonable cost and the ease of transforming the robot's avatar into the appearance of a specific patient over various methods involving physical sensors. This study is anticipated to achieve a new pathway for developing an advanced care training system by using patient robots that can express the current emotional and painful state.

6.1　Motivation

The robotic head provides realistic facial expressions that can be used to support interaction between a robot and a person. Berns *et al.* [110] proposed the method to control robotic facial expression using the robot head *ROMAN*. Kitagawa *et al.* [22] proposed the human-like patient robot for improving the ability of nursing student's skills of injecting the patient's arm into a vein, and the robot was designed with the aim of being manipulated to express various emotions such as neutral, smile, pain, and anger. Although the robot's expression can be communicated in various ways, the method of using a projector, in particular, has the main advantage of low cost and easy to use. One of the most significant advantages is that the facial features (age, gender, specific person, etc.) can be easily and conveniently transformed. The visual-based feedback that may be obtained by using the projector is able to represent various realistic facial expressions. Maejima *et al.* [111] proposed a retro-projected 3D face system for a human-robot interface. Kuratate *et al.* [78, 112] developed a life-size talking head system (Mask-bot) using a portable projector. Pierce *et al.* [113] improved the preliminary *Mask-bot* [78, 112] by developing a robotic head with a 3-DOF neck to research human-robot interactions. The study of [113] argued the opinion that the significant advantage of the projector-based robot head is that it may not depend on complex mechanical structures including motors. Therefore, many motors do not need to be controlled to modify the facial expression, and it is easy to change the avatar or shape of the robotic head. In the study of this dissertation, therefore, the projector-based robotic head that expresses the pain state and emotions for care training is proposed.

6.2 Objectives

The specific objectives of the integration system for care training introduced in this Chapter are (a) to present a novel feedback approach using the patient robot that can express pain and emotional states by integrating the methods proposed in Chapters 3, 4, and 5, (b) to demonstrate the advantages of projector-based robotic head, and (c) to investigate the feasibility of the patient robot's feedback method for expressing emotions and pain in care education.

6.3 Integrated system

The overall system for the proposed care training system as shown in **Fig. 6.1**. The basic methods for developing this system have been proposed in previous Chapter 3, Chapter 4, and Chapter 5. In Chapter 3, the patient robot was developed to reproduce the specific-joint movement with musculoskeletal symptoms. The pain intensity felt by the robot is expressed as the avatar by applying the pain inference method proposed in Chapter 4 to the patient robot. The method for tracking the robot's emotional expression proposed in Chapter 5 is applied to the avatar to express the current robotic emotion state.

The importance and necessity of applying the methods proposed in previous Chapters to this integrated system are summarized as follows:

- Patient robot (Chapter 3): The patient robot reproduces the movements of patients with musculoskeletal symptoms, and trainees use the robot to conduct care training to improve their care skills.

- Pain inference of the patient robot (Chapter 4): The caregivers should periodically check whether the patient feels pain or not and observe painful expressions on the patient's face during care conducting. For this reason, the necessity of developing a method to automatically infer the pain intensity felt by the robot

based on the sensor data collected from the robot was emphasized in Chapter 4. Therefore, the pain inference method in Chapter 4 provides more information (patient robot's pain state) to trainees and is applied to the integrated system to improve the efficiency and quality of the care training feedback method proposed in this dissertation.

- Robot's mood tracking (Chapter 5): The method for tracking the robotic mood based on the trainee's facial emotion expression was introduced to improve the ancillary qualifications (stability, optimism, and communication) of caregivers in Chapter 5. By studying and investigating the effects of caregiver's emotions on robot's mood, this approach is applied to more advanced care education systems.
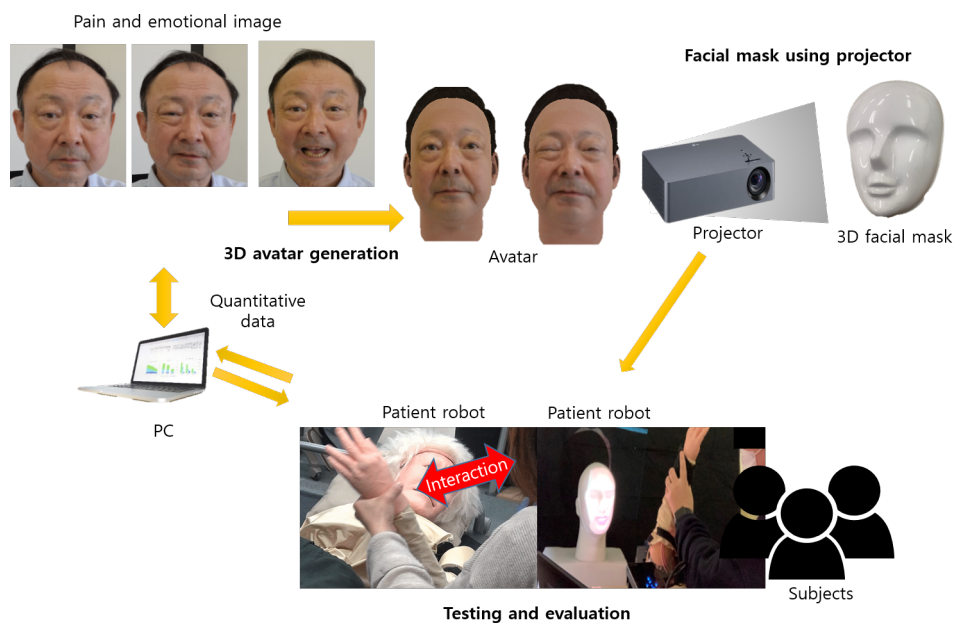
Figure 6.1. Framework of the system for care training assistant robot based on the pain emotional expression.

The original facial images are generated as 3D avatars using the Avatar SDK (It-seez3D, Inc., CA, USA). As shown in **Fig. 6.2** (a), the 3D avatars are converted from original images (.jpg) to avatar objects (.obj) using the Unity program-based SDK. The Avatar SDK acts as the conversion SDK, and object files are acquired from the original image. The 3D avatar (.jpg) image can be converted when the object file is downloaded. After loading the generated 3D avatar object file (.obj) are handled in the Unity program, and facial avatars with pain and emotion expressions for each of the five groups are finally created as shown in **Fig. 6.2** (b).
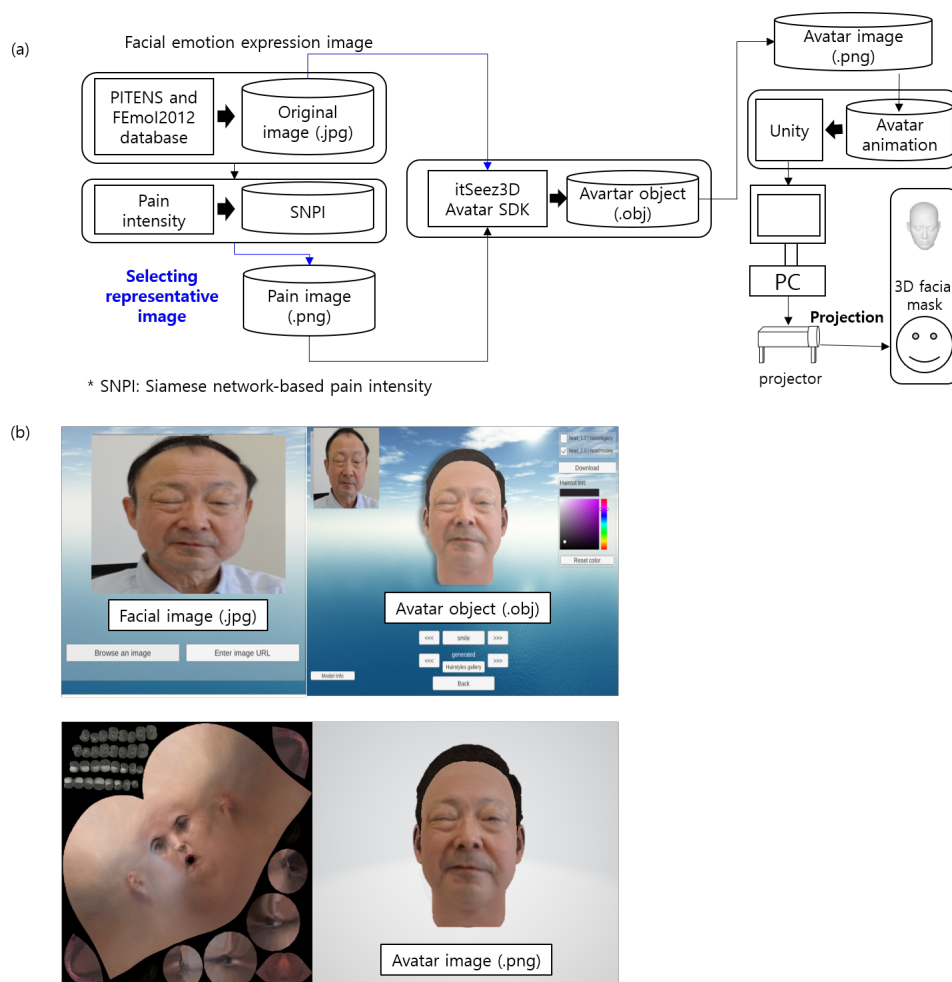
Figure 6.2. Example of the method to generate the avatar (a) Framework (b) Generated facial avatar object (.obj) and imamge (.png).

153

Fig. 6.3 illustrates the example of the avatar for pain and emotional expression. This study tried to create an avatar of a patient robot considering various age groups and genders without depending on a specific target's facial shape and appearance. Several images for avatars are based on the RU-PITENS database designed in Chapter 4 and the RU-FEmoI2021 database proposed in Chapter 5. It has been proven that the pain image in the RU-PITENS database is an image expressed when the subject felt pain and is divided into five pain groups according to the intensity of pain obtained from the image.
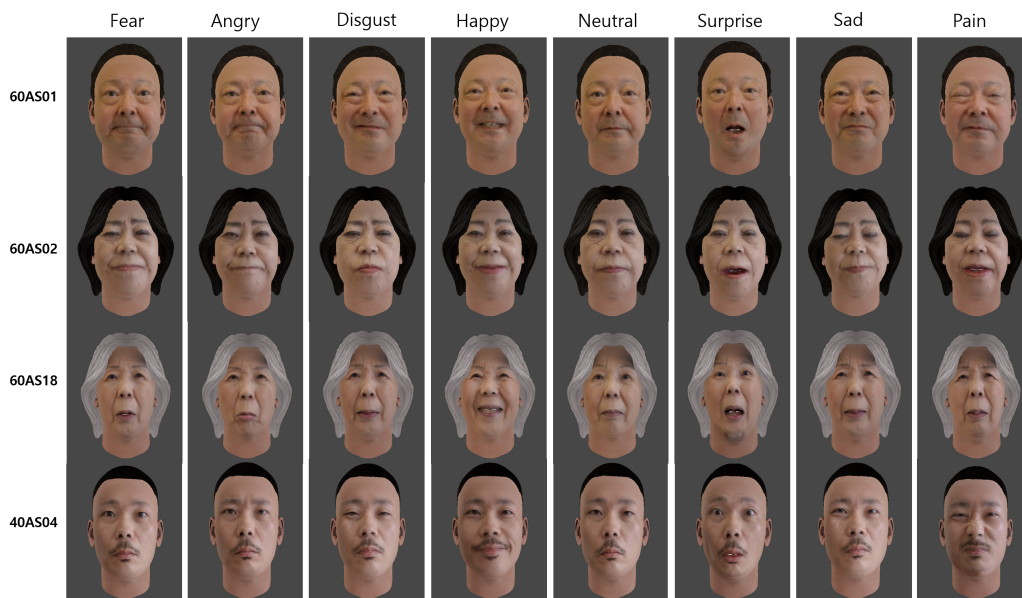
Figure 6.3. Example of avatar generation using the facial images in RU-PITENS and RU-FEmoI2021 database.

To generate the animation, the unity's animator was adopted to animate the avatar's facial expressions. Each group maintained an interval of about 0.5 seconds, and animation according to the facial expressions of the avatars was completed as shown in **Fig. 6.4** (a). **Fig. 6.4** (b) depicts the expression transition of the avatar changes from neutral to a specific expression and then returns to the neutral process.
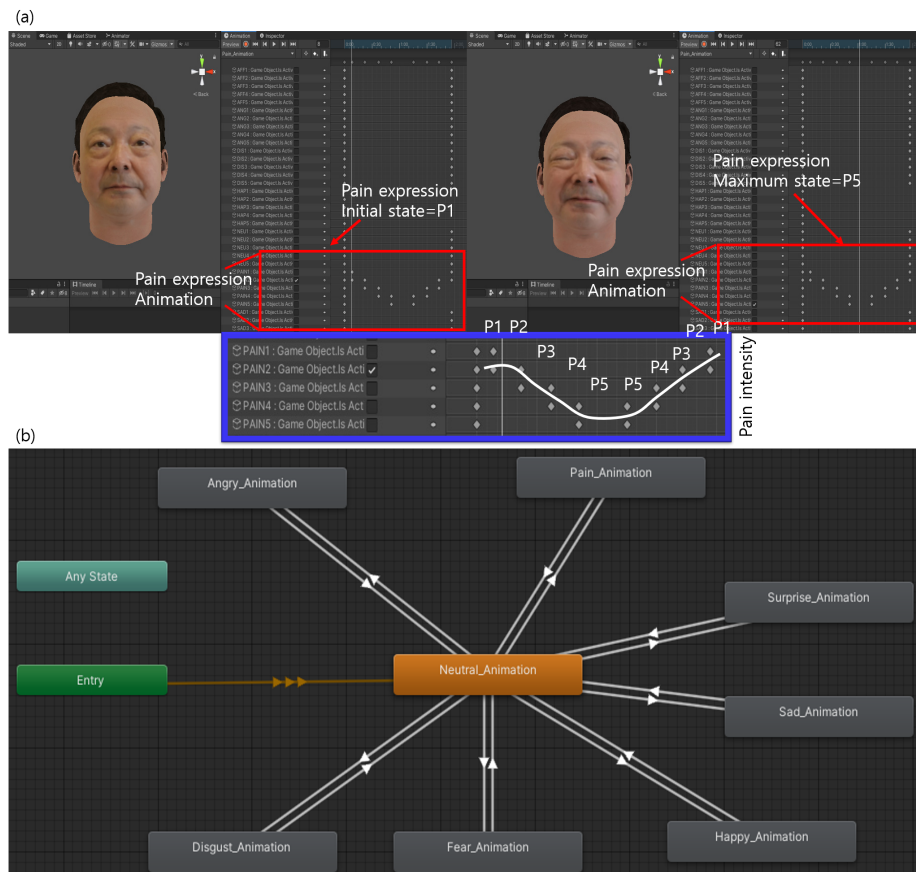
Figure 6.4. The method to animate the avatar's facial expressions (a) Animator (b) Expression transition.

6.4 Experiment

Fig. 6.5 shows the experimental environment of the robot's avatar expression using a projector. A facial mask and a camera that can recognize the user's facial expressions are located on the desk, and a projector is located in front of the desk. The projector is positioned in front of the mask to project the avatar onto the mask, and the user performs the care task using the elbow joint of the patient robot fixed to the desk.
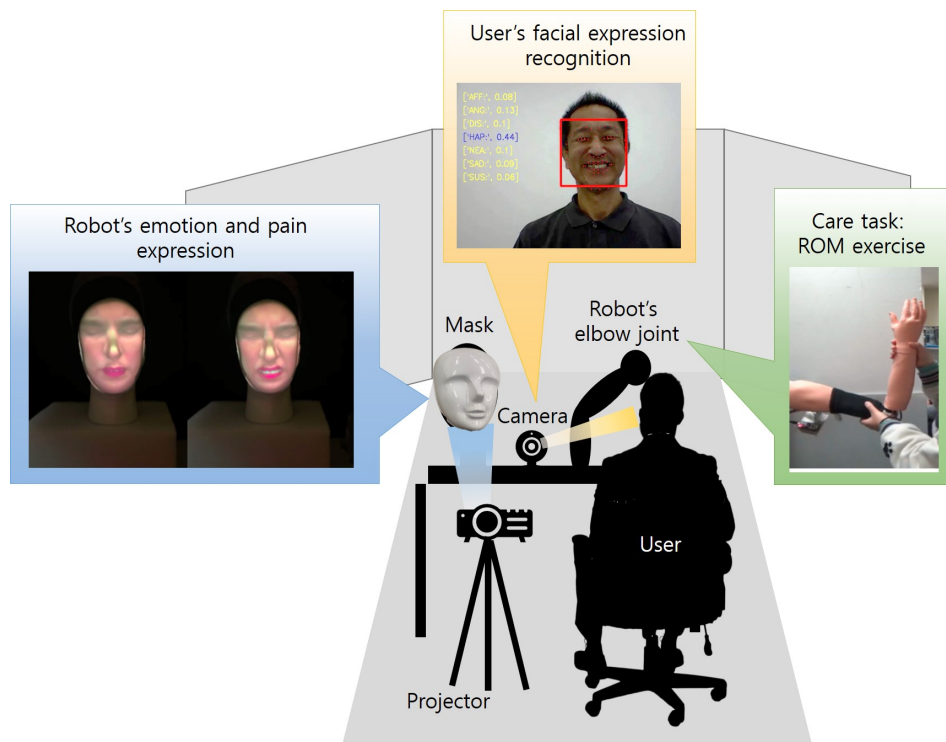
Figure 6.5. Experimental environment for robot's emotion and pain expression of the patient robot.

To express robotic facial expressions, a projector was used for the experiment. **Fig. 6.6** depicts the testing of the projector-based robotic head for the emotion and pain expression.The projector is placed in front of the translucent facial mask, and the avatar's expression is determined based on the information obtained from the patient robot or the user, and the command is transmitted to the Unity program on the computer.
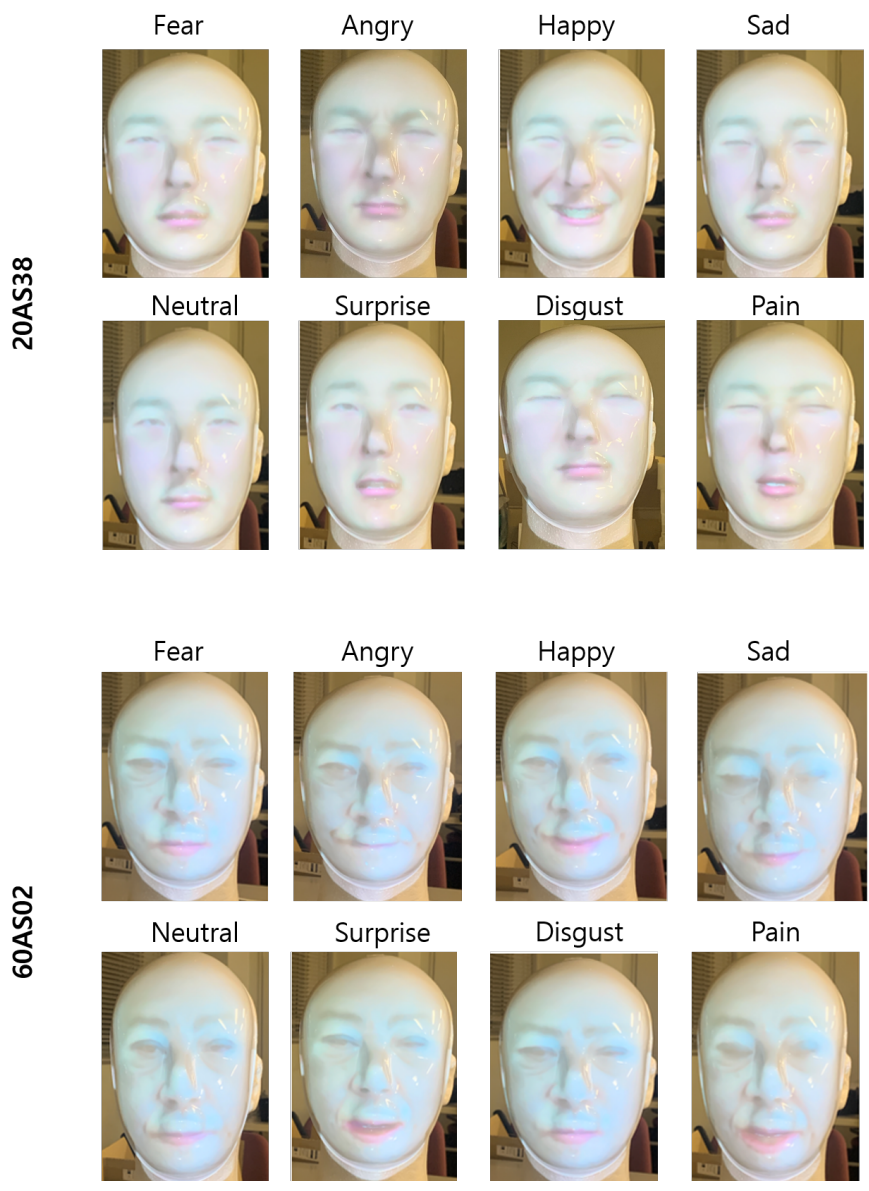
Figure 6.6. Projector-based robot's emotion and pain expression.

Fig. 6.7 shows the testing results of performing elbow exercises (EEF) using the integrated system. In the *Ready* state, the robot head communicates emotions with the user. As the example of the *Ready* state in **Fig. 6.7** (a), the user tried to express *happiness*, and then the robot head expressed the emotion of *happiness*. Fuzzy logic-based pain intensity (FLPI) is calculated based on sensor data of angle, torque, and pressure of the robot's elbow joint, and FLPI is determined as shown in **Fig. 6.7** (b). When the pain group is 1 (=no pain, FLPI ranges from 0 to 1.99), the avatar expresses a neutral expression, but the avatar expresses the maximum pain expression when pain intensity is high (pain group=5, FLPI ranges over 8). **Fig. 6.7** (c) illustrates an example of the testing result in which the robot's avatar and the user communicate their emotions, and the robot's avatar can express emotions according to the user's facial expression.
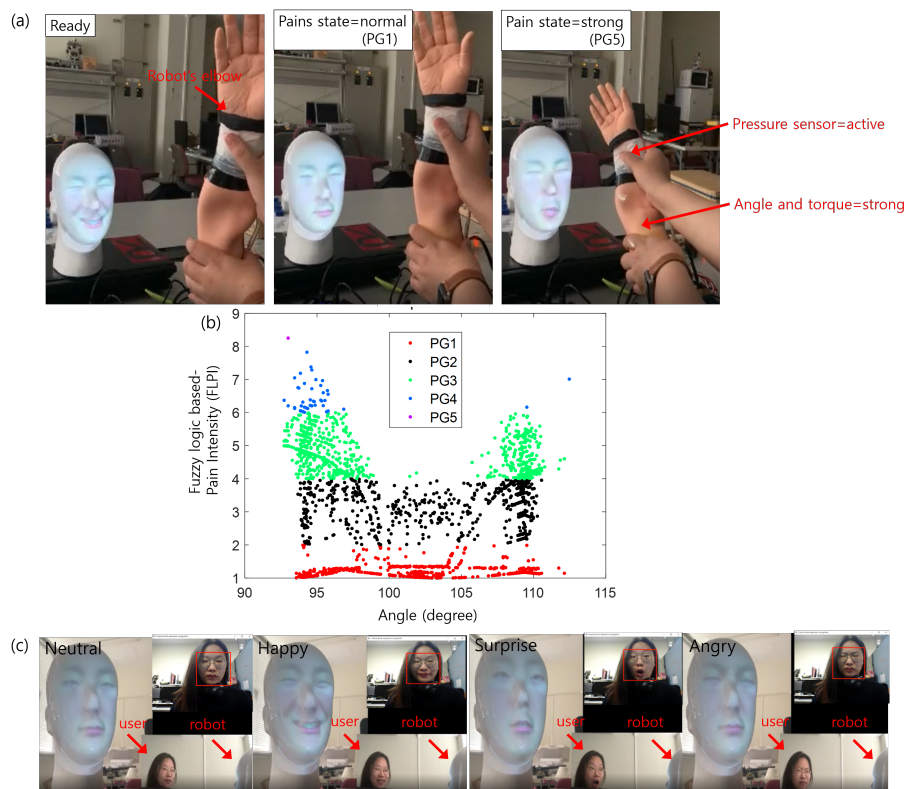
Figure 6.7. Testing of the projector-based patient robot (a) Pain expression (b) Result of the fuzzy logic based-pain intensity (FLPI) of the patient robot (c) Emotional expression.

6.5 Discussion

The integration system for practical care training based on visual feedback was proposed to improve the care skills of caregivers. The most crucial advantage of a projector-based robot head is that it is easier and more convenient to change the avatar than mechanical or physical methods. As shown in **Fig. 6.6**, the avatar with various age groups and genders can be expressed. Therefore, the integrated system in this Chapter provides an environment for learners to train how the patient's mood changes and respond to the patient's pain according to the patient's personality and pain sensitivity by applying the patient's face picture and personality to the patient robot in advance.

Chapter 7

Concluding remarks

The main goals of the work presented in this dissertation were

- to provide the effects of enhancing care skills using patient robots by deeper interpretation of the users' care skills based on quantitative data obtained from the robot for providing an effective patient robot-based care education system

- to infer the pain felt by the patient robot and to intuitively provide the trainee with the patient's pain state

- to provide a novel approach of the patient robot's facial expression-based visual feedback method for care training.

This Chapter describes the paper's goals described in Section 1.3 and summarizes the contributions based on the observations addressed to the research problems in each Chapter. Finally, future works will be discussed to expand existing work.

7.1 Contributions

This Chapter describes the contributions based on new observations made from the results of each Chapter.

Chapter 2 highlighted the importance of the research on the patient robots and feedback in care and nursing education.

Chapter 3 established several contributions by developing a patient robot that reproduces the musculoskeletal symptoms. The statistically significant results were

obtained between the expert group and the student group in ROM exercise using the patient robot, which resulted in notable results demonstrating the effectiveness of care training using the patient robot. In addition, the experiment's findings have demonstrated that, although experts have many years of experience, they performed the care tasks in different methods and behaviors. Therefore, Chapter 3 has demonstrated the feasibility of the proposed patient robot that it is necessary to provide appropriate care and treatment for the patient through analysis of the quantitative data obtained from the patient robot.

In Chapter 4, the robot's pain was inferred using the proposed fuzzy logic method by combining the robot's sensor data collected during the care training. Using the proposed method, this study contributed to intuitively comparing learners' care abilities and consequently demonstrated significant differences in initial, medial, and final trials of ROM movements using the pain inference method. In addition, the database of the facial images with pain expressions from 41 Japanese people was built to generate a robot's pain avatar and the database will be disclosed as an open database to expand the scalability of the research related to the pain expression in various fields.

Chapter 5 proposed to calculate the intensity of the user's facial expression and to track the robot's mood transition to express the emotional state that can interact with users in care education. In terms of care and nursing training, the robot's mood transition approach contributes to facilitating research related to interaction in care training by proposing a more advanced patient robot that allows the user to receive feedback through the patient's facial emotional expression and respond immediately.

Chapter 6 demonstrated the proposed a projector-based robot head which has the advantages of low cost and ease of use. In addition, this work introduced the benefits of a robotic avatar created based on facial images of participants from different age groups and genders.

7.2　Future work

For the scalability of care and nursing training using the approach in this dissertation, it is necessary to consider several well-defined studies in the future.

7.2.1　Various musculoskeletal diseases

The most important future research required for this research is that more care and nursing tasks should be considered. Although the experiment in this dissertation focused only on ROM exercise among various care and nursing tasks, it is necessary to investigate various medical symptoms (ie, stiffness, contracture, muscle weakness) of people in need of nursing and to expand the application. Further, the additional experiment may be extended to perform various ROM exercises and care activities involving different postures (e.g. sitting, standing, etc.) because the ROM exercises were conducted for a single case (lying in bed) in the experiment of this dissertation.

7.2.2　Additional data measurements and protocols

In terms of the experiment, perhaps the part that requires additional validation in this dissertation is to acquire sufficient experimental data to generalize the effect of care education on patient robots. Although this study demonstrated the validity of the patient robot by supporting sufficient investigations and results on the robot's internal modules, the effectiveness of care education using the patient robot has yet to be generalized based on various groups and experimental protocols. Therefore, additional test subjects are required to perform more experiments. Future studies should focus on generalizing the results based on sufficient data on the effectiveness of improved care and rehabilitation skills using the proposed patient robot. Comparisons should also be made between the results obtained from actual patients and the proposed robot patient.

7.3 Summary

This Chapter discussed the objectives and research problems defined in the intro-
duction and showed that several contributions with observations were achieved. The
upper extremity of a patient robot that reproduces patients with musculoskeletal dis-
orders has been developed, and a method for the robot's pain inference and a method
of emotional expression were proposed. The methods proposed in this dissertation
were investigated numerically through various experiments and validated statistically.
This dissertation has the following contributions and scalability for future works:

- Development of a patient robot that can express various diseases and pain

- Care and nursing education system that can respond to various diseases and pain

- Development of a care and nursing training system including an interaction tech-
  nique that can improve the additional qualities of caregivers such as reliability,
  stability, optimism, and communication

- Development of efficient and effective feedback methods for caregivers and
  students in care and nursing training

- Creation of database by acquiring facial images for expressions of pain and
  emotion

References

[1] OECD (2021). Elderly population (indicator). `https://data.oecd.org/pop/elderly-population.htm`, Accessed on 05 April 2021 (doi: 10.1787/8d805ea1-en).

[2] Kyoko Sudo, Jun Kobayashi, Shinichiro Noda, Yoshiharu Fukuda, and Kenzo Takahashi. Japan's healthcare policy for the elderly through the concepts of self-help (ji-jo), mutual aid (go-jo), social solidarity care (kyo-jo), and governmental care (ko-jo). *Bioscience trends*, 12(1):7–11, 2018.

[3] Irma PM Kruijver, Ada Kerkstra, Anneke L Francke, Jozien M Bensing, and Harry BM van de Wiel. Evaluation of communication training programs in nursing care: a review of the literature. *Patient education and counseling*, 39(1):129–145, 2000.

[4] 24 Hour Home Care. What skill set is needed to be an efficient caregiver? `https://www.24hrcares.com/blog/what-skill-set-is-needed/`, 2018.

[5] Partners for Home Care. Top qualities to look for in a good caregiver. `https://partnersforhomecare.ca/top-qualities-to-look-for-in-a-good-caregiver/`, 2020.

[6] Caring Senior Service. 11 unique skills you need to become a caregiver. `https://www.caringseniorservice.com/blog/unique-skills-to-become-a-caregiver`, 2021.

[7] Yasuko Kitajima, Mitsuhiro Nakamura, Jukai Maeda, Masako Kanai-Pak, Kyoko Aida, Zhifeng Huang, Ayanori Nagata, Taiki Ogata, Noriaki Kuwahara, and Jun Ota. Robotics as a tool in fundamental nursing education. In *International Conference on Digital Human Modeling and Applications in Health, Safety, Ergonomics and Risk Management*, pages 392–402. Springer, 2014.

[8] Zhifeng Huang, Takahiro Katayama, Masako Kanai-Pak, Jukai Maeda, Yasuko Kitajima, Mitsuhiro Nakamura, Kyoko Aida, Noriaki Kuwahara, Taiki Ogata, and Jun Ota. Design and evaluation of robot patient for nursing skill training in patient transfer. *Advanced Robotics*, 29(19):1269–1285, 2015.

[9] Leigh Ann Peteani. Enhancing clinical practice and education with high-fidelity human patient simulators. *Nurse educator*, 29(1):25–30, 2004.

[10] M Wilson, I Shepherd, C Kelly, and J Pitzner. Assessment of a low-fidelity human patient simulator for the acquisition of nursing skills. *Nurse Education Today*, 25(1):56–67, 2005.

[11] Latha Venkatesan and Poonam Joshi. *Textbook of Nursing Education*. 1st Edition. Elsevier India, 2015.

[12] Dorling Kindersley Publishing Staff Carers Australia (Organization). *Carer's Handbook*. A Practical Australian Guide to Caring for People Who are Sick, Elderly, or Have a Disability. Penguin Books Australia, 2007.

[13] Alexander Street. Nursing education in video: Third edition. `https://alexanderstreet.com/products/nursing-education-video-third-edition`, 2021.

[14] Illinois State University. Best actors: Nursing students play the role of patients. `https://news.illinoisstate.edu/2019/11/best-actors-nursing-students-play-the-role-of-patients/`, 2021.

[15] Santiago González Izard, Juan A Juanes, Francisco J García Peñalvo, Jesús Mª Gonçalvez Estella, Mª José Sánchez Ledesma, and Pablo Ruisoto. Virtual reality as an educational and training tool for medicine. *Journal of medical systems*, 42(3):1–5, 2018.

[16] Healthy Simulation. Manikin. `https://www.healthysimulation.com/manikin/`, 2021.

[17] Gaumard. Pediatric hal s2225. `https://www.gaumard.com/s2225`, 2021.

[18] Tomohiro Fujisawa, Motoki Takagi, Yoshiyuki Takahashi, Kaoru Inoue, Takafumi Terada, Yukio Kawakami, and Takashi Komeda. Basic research on the upper limb patient simulator. In *2007 IEEE 10th international conference on rehabilitation robotics*, pages 48–51. IEEE, 2007.

[19] Tetsuya Mouri, Haruhisa Kawasaki, Yutaka Nishimoto, Takaaki Aoki, and Yasuhiko Ishigure. Development of robot hand for therapist education/training on rehabilitation. In *2007 IEEE/RSJ International Conference on Intelligent Robots and Systems*, pages 2295–2300. IEEE, 2007.

[20] Chunbao Wang, Yohan Noh, Mitsuhiro Tokumoto, Chihara Terunaga, Matsuoka Yusuke, Hiroyuki Ishii, Salvatore Sessa, Massimiliano Zecca, Atsuo Takanishi, Kazuyuki Hatake, et al. Development of a human-like neurologic model to simulate the influences of diseases for neurologic examination training. In *2013 IEEE international conference on robotics and automation*, pages 4826–4831. IEEE, 2013.

[21] Zhifeng Huang, Ayanori Nagata, Masako Kanai-Pak, Jukai Maeda, Yasuko Kitajima, Mitsuhiro Nakamura, Kyoko Aida, Noriaki Kuwahara, Taiki Ogata, and Jun Ota. Robot patient for nursing self-training in transferring patient from bed to wheel chair. In *International Conference on Digital Human Modeling and Applications in Health, Safety, Ergonomics and Risk Management*, pages 361–368. Springer, 2014.

[22] Yoshiro Kitagawa, Tomohito Ishikura, Wei Song, Yasushi Mae, Mamoru Minami, and Kanji Tanaka. Human-like patient robot with chaotic emotion for injection training. In *2009 ICCAS-SICE*, pages 4635–4640. IEEE, 2009.

[23] Chunbao Wang, Yohan Noh, Kazuki Ebihara, Chihara Terunaga, Mitsuhiro Tokumoto, Isamu Okuyama, Matsuoka Yusuke, Hiroyuki Ishii, Atsuo Takanishi, Kazuyuki Hatake, et al. Development of an arm robot for neurologic

examination training. In *2012 IEEE/RSJ International Conference on Intelligent Robots and Systems*, pages 1090–1095. IEEE, 2012.

[24] Kathleen M Horan. Using the human patient simulator to fostercritical thinking in critical situations. *Nursing Education Perspectives*, 30(1):28–30, 2009.

[25] Stephen Abrahamson, Judson S Denson, and Richard M Wolf. Effectiveness of a simulator in training anesthesiology residents. *Academic Medicine*, 44(6):515–9, 1969.

[26] James S Denson and Stephen Abrahamson. A computer-controlled patient simulator. *Jama*, 208(3):504–508, 1969.

[27] Ashley E Darcy Mahoney, Lauren E Hancock, Angela Iorianni-Cimbak, and Martha AQ Curley. Using high-fidelity simulation to bridge clinical and classroom learning in undergraduate pediatric nursing. *Nurse education today*, 33(6):648–654, 2013.

[28] Elizabeth Diener and Nelda Hobbs. Simulating care: Technology-mediated learning in twenty-first century nursing education. In *Nursing forum*, volume 47, pages 34–38. Wiley Online Library, 2012.

[29] Hideaki Takanobu, Akito Omata, Fumihiko Takahashi, Keishi Yokota, Kenji Suzuki, Hirofumi Miura, Mutsumi Madokoro, Yoshikazu Miyazaki, and Koutarou Maki. Dental patient robot as a mechanical human simulator. In *2007 IEEE international conference on mechatronics*, pages 1–6. IEEE, 2007.

[30] Yohan Noh, Masanao Segawa, Akihiro Shimomura, Hiroyuki Ishii, Jorge Solis, Kazuyuki Hatake, and Atsuo Takanishi. Wka-1r robot assisted quantitative assessment of airway management. *International Journal of Computer Assisted Radiology and Surgery*, 3(6):543–550, 2008.

[31] Xinyao Sun, Simon Byrns, Irene Cheng, Bin Zheng, and Anup Basu. Smart sensor-based motion detection system for hand movement training in open surgery. *Journal of medical systems*, 41(2):1–13, 2017.

[32] Shang Lu, Yerly Paola Sanchez Perdomo, Xianta Jiang, and Bin Zheng. Integrating eye-tracking to augmented reality system for surgical training. *Journal of Medical Systems*, 44(11):1–7, 2020.

[33] Zhifeng Huang, Chingszu Lin, Masako Kanai-Pak, Jukai Maeda, Yasuko Kitajima, Mitsuhiro Nakamura, Noriaki Kuwahara, Taiki Ogata, and Jun Ota. Robot patient design to simulate various patients for transfer training. *IEEE/ASME Transactions on Mechatronics*, 22(5):2079–2090, 2017.

[34] Zhifeng Huang, Chingszu Lin, Masako Kanai-Pak, Jukai Maeda, Yasuko Kitajima, Mitsuhiro Nakamura, Noriaki Kuwahara, Taiki Ogata, and Jun Ota. Impact of using a robot patient for nursing skill training in patient transfer. *IEEE Transactions on Learning Technologies*, 10(3):355–366, 2016.

[35] Chingszu Lin, Taiki Ogata, Zhihang Zhong, Masako Kanai-Pak, Jukai Maeda, Yasuko Kitajima, Mitsuhiro Nakamura, Noriaki Kuwahara, and Jun Ota. Development of robot patient lower limbs to reproduce the sit-to-stand movement with correct and incorrect applications of transfer skills by nurses. *Applied Sciences*, 11(6):2872, 2021.

[36] Sherry Baron, Thomas Hales, and Joseph Hurrell. Evaluation of symptom surveys for occupational musculoskeletal disorders. *American journal of industrial medicine*, 29(6):609–617, 1996.

[37] United Nations. World population prospects the 2012 revision. `https://esa.un.org/unpd/wpp/publications/Files/WPP2012_HIGHLIGHTS.pdf`, 2013.

[38] MMF Oliveira, MSC Gurgel, MS Miranda, MA Okubo, 12 LFA Feijó, and GA Souza. Efficacy of shoulder exercises on locoregional complications in women undergoing radiotherapy for breast cancer: clinical trial. *Brazilian Journal of Physical Therapy*, 13(2):136–143, 2009.

[39] EJ Yang, HJ Kim, HS Ahn, and EH Lee. The effect of early upper extremities passive exercise on the hand edema and upper spasticity of the hemiplegia

patient after stroke. *Journal of Korean Clinical Nursing Research*, 12(1):147–157, 2006.

[40] Hyun Ju Kim, Yaelim Lee, and Kyeong-Yae Sohng. Effects of bilateral passive range of motion exercise on the function of upper extremities and activities of daily living in patients with acute stroke. *Journal of physical therapy science*, 26(1):149–156, 2014.

[41] Takeya Ono, Masahiro Miyoshi, Sadaaki Oki, Michele Eisemann Shimizu, Namiko Umei, Kayoko Shiraiwa, Hidenori Takemoto, Koji Shimatani, Masaki Hasegawa, and Akira Otsuka. The effect of rom exercise on rats with denervation and joint contracture. *Journal of Physical Therapy Science*, 21(2):173–176, 2009.

[42] Nobutoshi Yamazaki and Takayuki Tanaka. Development of a human joint imitated dummy. *Biomechanisms*, 18:175–185, 2006.

[43] Gadi Gilam, James J Gross, Tor D Wager, Francis J Keefe, and Sean C Mackey. What is the relationship between pain and emotion? bridging constructs and communities. *Neuron*, 107(1):17–21, 2020.

[44] Corrado Corradi-Dell'Acqua, Anita Tusche, Patrik Vuilleumier, and Tania Singer. Cross-modal representations of first-hand and vicarious pain, disgust and fairness in insular and cingulate cortex. *Nature communications*, 7(1):1–12, 2016.

[45] Anjali Krishnan, Choong-Wan Woo, Luke J Chang, Luka Ruzic, Xiaosi Gu, Marina López-Solà, Philip L Jackson, Jesús Pujol, Jin Fan, and Tor D Wager. Somatic and vicarious pain are represented by dissociable multivariate brain patterns. *Elife*, 5:e15166, 2016.

[46] Lisa Feldman Barrett. The theory of constructed emotion: an active inference account of interoception and categorization. *Social cognitive and affective neuroscience*, 12(1):1–23, 2017.

[47] Hisashi Ishihara, Yuichiro Yoshikawa, and Minoru Asada. Realistic child robot "affetto" for understanding the caregiver-child attachment relationship that guides the child development. In *2011 IEEE International Conference on Development and Learning (ICDL)*, volume 2, pages 1–5. IEEE, 2011.

[48] Yuki Yamashita, Hisashi Ishihara, Takashi Ikeda, and Minoru Asada. Investigation of causal relationship between touch sensations of robots and personality impressions by path analysis. *International Journal of Social Robotics*, 11(1):141–150, 2019.

[49] Luis-Felipe Rodríguez and Félix Ramos. Development of computational models of emotions for autonomous agents: a review. *Cognitive Computation*, 6(3):351–375, 2014.

[50] Nikolaos Mavridis. A review of verbal and non-verbal human–robot interactive communication. *Robotics and Autonomous Systems*, 63:22–35, 2015.

[51] Albert Mehrabian and James A Russell. *An approach to environmental psychology.* the MIT Press, 1974.

[52] James A Russell and Merry Bullock. Multidimensional scaling of emotional facial expressions: similarity from preschoolers to adults. *Journal of personality and social psychology*, 48(5):1290, 1985.

[53] Iris Bakker, Theo Van Der Voordt, Peter Vink, and Jan De Boon. Pleasure, arousal, dominance: Mehrabian and russell revisited. *Current Psychology*, 33(3):405–421, 2014.

[54] Yoshiro Kitagawa, Wei Song1 Mamoru Minami, and Yasushi Mae. Human-like patient robot for injection training by chaotic behavior. In *2nd International Symposium on Test Automation and Instrumentation, ISTAI 2008*, 2008.

[55] E Jerry Phares. *Introduction to personality.* Scott, Foresman & Co, 1988.

[56] Meng-Ju Han, Chia-How Lin, and Kai-Tai Song. Robotic emotional expression generation based on mood transition and personality model. *IEEE transactions on cybernetics*, 43(4):1290–1303, 2012.

[57] Naoki Masuyama and Chu Kiong Loo. Robotic emotional model with personality factors based on pleasant-arousal scaling model. In *2015 24th IEEE International Symposium on Robot and Human Interactive Communication (RO-MAN)*, pages 19–24. IEEE, 2015.

[58] Naoki Masuyama, Chu Kiong Loo, and Manjeevan Seera. Personality affected robotic emotional model with associative memory for human-robot interaction. *Neurocomputing*, 272:213–225, 2018.

[59] Tin Aung, Dominic Montagu, Karen Schlein, Thin Myat Khine, and Willi McFarland. Validation of a new method for testing provider clinical quality in rural settings in low-and middle-income countries: the observed simulated patient. *PLoS One*, 7(1):e30196, 2012.

[60] A Garg, BD Owen, and B Carlson. An ergonomic evaluation of nursing assistants' job in a nursing home. *Ergonomics*, 35(9):979–995, 1992.

[61] Caroline Bunker Rosdahl and Mary T Kowalski. *Textbook of basic nursing*. Lippincott Williams & Wilkins, 2008.

[62] Patricia A Potter and Anne Griffine Perry. *Basic nursing: Essentials for practice*. Mosby, 2003.

[63] Jonghyun Kim, Hyung-Soon Park, and Diane L Damiano. Accuracy and reliability of haptic spasticity assessment using hess (haptic elbow spasticity simulator). In *2011 annual international conference of the IEEE engineering in medicine and biology society*, pages 8527–8530. IEEE, 2011.

[64] Brian C Werner, Chris M Kuenze, Justin W Griffin, Matthew L Lyons, Joseph M Hart, and Stephen F Brockmeier. Shoulder range of motion: validation of an innovative measurement method using a smartphone. *Orthopaedic Journal of Sports Medicine*, 1(4_suppl):2325967113S00106, 2013.

171

[65] 3D4Medical. Complette anatomy. `https://3d4medical.com/`, 2021.

[66] NITE. Human characteristics database. `https://www.nite.go.jp/en/jiko/s_standard/human_db/index.html`, 2013.

[67] Inyong Ha, Yusuke Tamura, Hajime Asama, Jeakweon Han, and Dennis W Hong. Development of open humanoid platform darwin-op. In *SICE Annual Conference 2011*, pages 2178–2181. IEEE, 2011.

[68] BS Medicine. Shoulder range of motion exercises. `https://www.bostonsportsmedicine.com/rehabilitation-protocols/shoulder-stretching-exercises/`, 2021.

[69] St. Jude Children's Research Hospital. Passive shoulder range of motion. `https://www.stjude.org/treatment/patient-resources/caregiver-resources/patient-family-education-sheets/rehabilitation/passive-shoulder-range-of-motion.html`, 2021.

[70] Miran Lee, Kodai Murata, Ko Ameyama, Hirotake Yamazoe, and Joo-Ho Lee. Development and quantitative assessment of an elbow joint robot for elderly care training. *Intelligent Service Robotics*, 12(4):277–287, 2019.

[71] Lotfi A Zadeh. Outline of a new approach to the analysis of complex systems and decision processes. *IEEE Transactions on systems, Man, and Cybernetics*, (1):28–44, 1973.

[72] Mohit Kumar, Matthias Weippert, Reinhard Vilbrandt, Steffi Kreuzfeld, and Regina Stoll. Fuzzy evaluation of heart rate signals for mental stress assessment. *IEEE Transactions on fuzzy systems*, 15(5):791–808, 2007.

[73] BM Gayathri and CP Sumathi. Mamdani fuzzy inference system for breast cancer risk detection. In *2015 IEEE International Conference on Computational Intelligence and Computing Research (ICCIC)*, pages 1–6. IEEE, 2015.

[74] Gulzar Ahmad, Muhammad Adnan Khan, Sagheer Abbas, Atifa Athar, Bilal Shoaib Khan, and Muhammad Shoukat Aslam. Automated diagnosis of

hepatitis b using multilayer mamdani fuzzy inference system. *Journal of health-care engineering*, 2019, 2019.

[75] Patrick Lucey, Jeffrey F Cohn, Kenneth M Prkachin, Patricia E Solomon, and Iain Matthews. Painful data: The unbc-mcmaster shoulder pain expression archive database. In *2011 IEEE International Conference on Automatic Face & Gesture Recognition (FG)*, pages 57–64. IEEE, 2011.

[76] Frank E Pollick. In search of the uncanny valley. In *International Conference on User Centric Media*, pages 69–78. Springer, 2009.

[77] Rachel Gockley, Reid Simmons, Jue Wang, Didac Busquets, Carl DiSalvo, Kevin Caffrey, Stephanie Rosenthal, Jessica Mink, Scott Thomas, William Adams, et al. Grace and george: Social robots at aaai. In *Proceedings of AAAI*, volume 4, pages 15–20, 2004.

[78] Taakaki Kuratate, Yosuke Matsusaka, Brennand Pierce, and Gordon Cheng. "mask-bot": A life-size robot head using talking head animation for human-robot communication. In *2011 11th IEEE-RAS International Conference on Humanoid Robots*, pages 99–104. IEEE, 2011.

[79] Masahiro Mori, Karl F MacDorman, and Norri Kageki. The uncanny valley [from the field]. *IEEE Robotics & Automation Magazine*, 19(2):98–100, 2012.

[80] Mingzhe Jiang, Riitta Mieronkoski, Elise Syrjälä, Arman Anzanpour, Virpi Terävä, Amir M Rahmani, Sanna Salanterä, Riku Aantaa, Nora Hagelberg, and Pasi Liljeberg. Acute pain intensity monitoring with the classification of multiple physiological parameters. *Journal of clinical monitoring and computing*, 33(3):493–507, 2019.

[81] Mohammad A Haque, Ruben B Bautista, Fatemeh Noroozi, Kaustubh Kulkarni, Christian B Laursen, Ramin Irani, Marco Bellantonio, Sergio Escalera, Golamreza Anbarjafari, Kamal Nasrollahi, et al. Deep multimodal pain recognition: a database and comparison of spatio-temporal visual modalities. In *2018 13th*

IEEE International Conference on Automatic Face & Gesture Recognition (FG 2018), pages 250–257. IEEE, 2018.

[82] Kenneth M Prkachin. The consistency of facial expressions of pain: a comparison across modalities. *Pain*, 51(3):297–306, 1992.

[83] Paul Ekman, W Friesen, and J Hager. Facial action coding system: Research nexus network research information. *Salt Lake City, UT*, 2002.

[84] Ghazal Bargshady, Xujuan Zhou, Ravinesh C Deo, Jeffrey Soar, Frank Whittaker, and Hua Wang. Enhanced deep learning algorithm development to detect pain intensity from facial expression images. *Expert Systems with Applications*, 149:113305, 2020.

[85] Jane Bromley, Isabelle Guyon, Yann LeCun, Eduard Säckinger, and Roopak Shah. Signature verification using a" siamese" time delay neural network. *Advances in neural information processing systems*, pages 737–737, 1994.

[86] Wassan Hayale, Pooran Negi, and Mohammad Mahoor. Facial expression recognition using deep siamese neural networks with a supervised loss function. In *2019 14th IEEE International Conference on Automatic Face & Gesture Recognition (FG 2019)*, pages 1–7. IEEE, 2019.

[87] Daizong Liu, Xi Ouyang, Shuangjie Xu, Pan Zhou, Kun He, and Shiping Wen. Saanet: Siamese action-units attention network for improving dynamic facial expression recognition. *Neurocomputing*, 413:145–157, 2020.

[88] Motaz Sabri and Takio Kurita. Facial expression intensity estimation using siamese and triplet networks. *Neurocomputing*, 313:143–154, 2018.

[89] Mohammad Shorfuzzaman and M Shamim Hossain. Metacovid: A siamese neural network framework with contrastive loss for n-shot diagnosis of covid-19 patients. *Pattern Recognition*, page 107700, 2020.

[90] Raia Hadsell, Sumit Chopra, and Yann LeCun. Dimensionality reduction by learning an invariant mapping. In *2006 IEEE Computer Society Conference*

on Computer Vision and Pattern Recognition (CVPR'06), volume 2, pages 1735–1742. IEEE, 2006.

[91] Christopher S Nielsen, Roland Staud, and Donald D Price. Individual differences in pain sensitivity: measurement, causation, and consequences. *The journal of pain*, 10(3):231–237, 2009.

[92] Anna Maria Carlsson. Assessment of chronic pain. i. aspects of the reliability and validity of the visual analogue scale. *Pain*, 16(1):87–101, 1983.

[93] Kashfia Sailunaz, Manmeet Dhaliwal, Jon Rokne, and Reda Alhajj. Emotion detection from text and speech: a survey. *Social Network Analysis and Mining*, 8(1):1–26, 2018.

[94] Martina Szabóová, Martin Sarnovský, Viera Maslej Krešňáková, and Kristína Machová. Emotion analysis in human–robot interaction. *Electronics*, 9(11):1761, 2020.

[95] Bella M DePaulo and Howard S Friedman. Nonverbal communication. 1998.

[96] Dhwani Mehta, Mohammad Faridul Haque Siddiqui, and Ahmad Y Javaid. Facial emotion recognition: A survey and real-world user experiences in mixed reality. *Sensors*, 18(2):416, 2018.

[97] Evangelos Sariyanidi, Hatice Gunes, and Andrea Cavallaro. Automatic analysis of facial affect: A survey of registration, representation, and recognition. *IEEE transactions on pattern analysis and machine intelligence*, 37(6):1113–1133, 2014.

[98] Davis E King. Dlib-ml: A machine learning toolkit. *The Journal of Machine Learning Research*, 10:1755–1758, 2009.

[99] Daniel Lundqvist and JE Litton. The averaged karolinska directed emotional faces. *Stockholm Q12*, 1998.

[100] Garima Sharma, Latika Singh, and Sumanlata Gautam. Automatic facial expression recognition using combined geometric features. *3D Research*, 10(2):14, 2019.

[101] E Friesen and Paul Ekman. Facial action coding system: a technique for the measurement of facial movement. *Palo Alto*, 3(2):5, 1978.

[102] Daniel Lundqvist, Anders Flykt, and Arne Öhman. The karolinska directed emotional faces (kdef). *CD ROM from Department of Clinical Neuroscience, Psychology section, Karolinska Institutet*, 91(630):2–2, 1998.

[103] Jong-Chan Park, Hyoung-Rock Kim, Young-Min Kim, and Dong-Soo Kwon. Robot's individual emotion generation model and action coloring according to the robot's personality. In *RO-MAN 2009-The 18th IEEE International Symposium on Robot and Human Interactive Communication*, pages 257–262. IEEE, 2009.

[104] Sajal Chandra Banik, Keigo Watanabe, Maki K Habib, and Kiyotaka Izumi. An emotion-based task sharing approach for a cooperative multiagent robotic system. In *2008 IEEE International Conference on Mechatronics and Automation*, pages 77–82. IEEE, 2008.

[105] Chika Itoh, Shohei Kato, and Hidenori Itoh. Mood-transition-based emotion generation model for the robot's personality. In *2009 IEEE International Conference on Systems, Man and Cybernetics*, pages 2878–2883. IEEE, 2009.

[106] Robert R McCrae and Paul T Costa. Validation of the five-factor model of personality across instruments and observers. *Journal of personality and social psychology*, 52(1):81, 1987.

[107] Ernest R Hilgard. Introduction to psychology. 1953.

[108] Michael Gurven, Christopher Von Rueden, Maxim Massenkoff, Hillard Kaplan, and Marino Lero Vie. How universal is the big five? testing the five-factor model of personality variation among forager–farmers in the bolivian amazon. *Journal of personality and social psychology*, 104(2):354, 2013.

[109] Albert Mehrabian. Analysis of the big-five personality factors in terms of the pad temperament model. *Australian journal of Psychology*, 48(2):86–92, 1996.

[110] Karsten Berns and Jochen Hirth. Control of facial expressions of the humanoid robot head roman. In *2006 IEEE/RSJ International Conference on Intelligent Robots and Systems*, pages 3119–3124. IEEE, 2006.

[111] Akinobu Maejima, Takaaki Kuratate, Brennand Pierce, Shigeo Morishima, and Gordon Cheng. Automatic face replacement for a humanoid robot with 3d face shape display. In *2012 12th IEEE-RAS International Conference on Humanoid Robots (Humanoids 2012)*, pages 469–474. IEEE, 2012.

[112] Takaaki Kuratate, Marcia Riley, and Gordon Cheng. Effects of 3d shape and texture on gender identification for a retro-projected face screen. *International Journal of Social Robotics*, 5(4):627–639, 2013.

[113] Brennand Pierce, Takaaki Kuratate, Christian Vogl, and Gordon Cheng. "maskbot 2i": An active customisable robotic head with interchangeable face. In *2012 12th IEEE-RAS International Conference on Humanoid Robots (Humanoids 2012)*, pages 520–525. IEEE, 2012.

Full list of publications

This doctoral dissertation is based on the following $^{\alpha}$several papers. Reprints are made with permission from the *IEEE Publishing*, *Frontiers Media SA*, and *Springer Nature*.

In Preparation

- $^{\alpha}$ **Miran Lee**, Dinh Tuan Tran, and Joo-Ho Lee. **2021**. "Robotic Emotion Transition with Personality based on Care Training Ability and Interaction Skill in Elderly Care Education Environment." *In preparation.*

- $^{\alpha}$ **Miran Lee**, Dinh Tuan Tran, and Joo-Ho Lee. **2021**. "CaTARo: Effect of Repetitive Care Training using Patient Robot with Musculoskeletal Symptom." *In preparation.*

Submitted and Revision

- **Miran Lee**, Joo-Ho Lee, and Deok-Hwan Kim. **2021**, "Gender Recognition using Optimal Gait Feature based on Recursive Feature Elimination in Normal Walking," *Expert with Systems and Applications*, *In Revision.*

Peer-Reviewed Journals

- **Miran Lee** and Joo-Ho Lee. **2021**. "A Robust Fusion Algorithm of LBP and IMF with Recursive Feature Elimination Based ECG Processing for QRS and Arrhythmia Detection." *Applied Intelligence*, pp.1-15, May, 2021.

- $^{\alpha}$ **Miran Lee**, Dinh Tuan Tran, and Joo-Ho Lee. **2021**. "3D Facial Pain Expression for a Care Training Assistant Robot in an Elderly Care Education Environment." *Frontiers in AI and Robotics*, vol. 8, no. 42, pp.1-15, Apr. 2021.

- [α] **<u>Miran Lee</u>**, Ko Ameyama, Hirotake Yamazoe, and Joo-Ho Lee. **2020**. "Necessity and Feasibility of Care Training Assistant Robot (CaTARo) as Shoulder Complex Joint with Multi-DOF in Elderly Care Education." *ROBOMECH Journal*, vol. 7, no. 12, pp.1-12, Mar. 2020.

- **<u>Miran Lee</u>**, Tae-Geon Song, and Joo-Ho Lee. **2020**. "Heartbeat Classification using Local Transform Pattern Feature and Hybrid Neural Fuzzy-Logic System based on Self-Organizing Map." *Biomedical Signal Processing and Control*, vol. 57, Issue 101690, pp.1-9, Mar. 2020.

- **<u>Miran Lee</u>**, Jaehwan Ryu, and Deok-Hwan Kim. **2020**. "Automated Epileptic Seizure Waveform Detection Method based on the Feature of the Mean Slope of Wavelet Coefficient Counts using a Hidden Markov Model and EEG Signals." *ETRI Journal*, vol. 42, no. 2, pp.217-29, Oct. 2019.

- [α] **<u>Miran Lee</u>**, Kodai Murata, Ko Ameyama, Hirotake Yamazoe, and Joo-Ho Lee. **2019**. "Development and Quantitative Assessment of an Elbow Joint Robot for Elderly Care Training." *Intelligent Service Robotics*, vol. 12, no. 4, pp.277-287, Oct. 2019.

- Jaehwan Ryu, **<u>Miran Lee</u>**, and Deok-Hwan Kim. **2019**. "EOG-based Eye Tracking Protocol using Baseline Drift Removal Algorithm for Long-Term Eye Movement Detection." *Expert Systems with Applications*, vol. 131, pp.275-87, Oct. 2019.

- **<u>Miran Lee</u>**, Dajeong Park, Suh-Yeon Dong, and Inchan Youn. **2018**. "A Novel R Peak Detection Method for Mobile Environments." *IEEE Access*, vol. 6, pp.51227-51237, Aug. 2018.

- Dajeong Park, **<u>Miran Lee</u>**, Sunghee E. Park, Joon-Kyung Seong, and Inchan Youn. **2018**. "Determination of Optimal Heart Rate Variability Features Based on SVM-Recursive Feature Elimination for Cumulative Stress Monitoring Using ECG Sensor." *Sensors*, vol. 18, no. 7, pp.2387-2401, Jul. 2018.

179

- Heesu Park, Suh-Yeon Dong, **<u>Miran Lee</u>**, and Inchan Youn. **2017**. "The Role of Heart-Rate Variability Parameters in Activity Recognition and Energy-Expenditure Estimation Using Wearable Sensors." *Sensors*, vol. 17, no. 7, pp.1698-1702, Jul. 2017.

Domestic Publications (South Korea)

- Byeong-Hyeon Lee, Jae-Hwan Ryu, **<u>Miran Lee</u>**, and Deok-Hwan Kim. **2016**. "Monophthong Recognition Optimizing Muscle Mixing Based on Facial Surface EMG Signals." *Journal of the Institute of Electronics and Information Engineers*, vol. 53, no. 3, pp.143-150, Mar. 2016.

- **<u>Miran Lee</u>**, Jae-Hwan Ryu, Sang-Ho Kim, and Deok-Hwan Kim. **2016**. "Gait Phase Recognition based on EMG Signal for Stairs Ascending and Stairs Descending." *Journal of the Institute of Electronics and Information Engineers*, vol. 52, no. 3, pp.181-189, Mar. 2015.

International Conference

- $^\alpha$ **<u>Miran Lee</u>**, Dinh Tuan Tran, and Joo-Ho Lee. **2021**. "Pain Expression-based Visual Feedback Method for Care Training Assistant Robot with Musculoskeletal Symptoms." In *2021 IEEE/RSJ International Conference on Intelligent Robots and Systems (IROS 2021)*, *Accepted*.

- $^\alpha$ **<u>Miran Lee</u>**, Dinh Tuan Tran, H. Yamazoe, and Joo-Ho Lee. **2021**. "Care Training Assistant Robot and Visual-based Feedback for Elderly Care Education Environment," In *2021 IEEE/SICE International Symposium on System Integration (SII 2021, IEEE)*, pp.572-577, Jan. 2021, *Oral Presentation*.

- **<u>Miran Lee</u>**, Joo-Ho Lee, and Deok-Hwan Kim. **2020**. "A Robust sEMG Feature Selection based on Recursive Feature Elimination for Gait Recognition." In *2020 6th International Conference on Next Generation Computing 2020 (ICNGC 2020)*, Accepted, *Oral Presentation*.

- [α] **<u>Miran Lee</u>**, H. Yamazoe, and Joo-Ho Lee. **2020**. "Fuzzy-Logic based Care Training Quantitative Assessment using Care Training Assistant Robot (CaTARo)." In *2020 17th International Conference on Ubiquitous Robots (UR 2020, IEEE)*, pp.602-607, Jun. 2020, *Oral Presentation*.

- [α] **<u>Miran Lee</u>**, Hirotake Yamazoe, and Joo-Ho Lee. **2019**. "Elderly Care Training using Real-Time Monitoring System with Care Training Assistant Elbow Robot (CaTARo-E)." In *2019 16th International Conference on Ubiquitous Robots (UR 2019, IEEE)*, pp.259-264, Jun. 2019, *Oral Presentation*.

- Suh-Yeon Dong, **<u>Miran Lee</u>**, Heesu Park, and Inchan Youn. **2018**. "Stress Resilience Measurement With Heart-Rate Variability During Mental And Physical Stress." In *2018 40th Annual International Conference of the IEEE Engineering in Medicine and Biology Society (EMBC 2018, IEEE)*, pp.5290-5293, Jul. 2018, *Oral Presentation*.

- **<u>Miran Lee</u>**, Inchan Youn, Jaehwan Ryu, and Deok-Hwan Kim. **2018**. "Classification of both Seizure and Non-seizure based on EEG Signals using Hidden Markov Model." In *2018 IEEE International Conference on Big Data and Smart Computing (BigComp 2018, IEEE)*, pp.469-474, Jan. 2018, *Oral Presentation*.

- Jaehwan Ryu, Byeong-Hyeon Lee, **<u>Miran Lee</u>**, Jeongpil Choi, and Hyunil Cho. **2017**. "Automatic Sensor Fault Detection and Sensor Reconstruction Algorithm for Emergency Recovery in Industrial Fields." In *2017 International Conference on Intelligent Informatics and Biomedical Sciences (ICIIBMS 2017, IEEE)*, pp.85-86, Nov. 2017, *Oral Presentation*.

- **<u>Miran Lee</u>**, Jaehwan Ryu, and Inchan Youn. **2017**. "Biometric personal identification based on gait analysis using surface EMG signals." In *IEEE International Conference on Computational Intelligence and Applications (ICCIA 2017, IEEE)*, pp.318-321, Sep. 2017, *Oral Presentation*.

- Jaehwan Ryu, Sang-Ho Kim, **<u>Miran Lee</u>**, and Deok-Hwan Kim. **2015**. "EMG Signal-Based Gait Phase Detection Using a EMG Signal Graph Matching(ESGM)

Algorithm." In *The 1st International Conference on Information and Convergence Technology for Smart Society, (ICICTS 2015, SCIR)*, Jan. 2015, *Oral Presentation*.

Domestic Conferences (Japan)

- 梶山 主税, 李 美蘭, チャン ディン トゥアン, 李 周浩. **2020**. "介護練習用ロボットの自然な痛み表現手法." 第21回計測自動制御学会システムインテグレーション部門講演会(SI2020), 計測自動制御学会, 2C2-14, 2020.12.17

- 梶山 主税、李 美蘭、山添 大大、李 周浩. **2020**. "介護練習用ロボットの為の表情による痛み再現システム." ロボティクス・メカトロニクス講演会 2020 (ROBOMECH 2020 in Kanazawa), 一般社団法人 日本機械学会 ロボティクス・メカトロニクス部門, 2P1-F08, 2020.05.29

Domestic Conferences (South Korea)

- Byeong-Hyeon Lee, Jaehwan Ryu, <u>**Miran Lee**</u>, Sang-Ho Kim, Md. Zia Uddin, and Deok-Hwan Kim. **2015**. "Monophthong Recognition using Feature and Muscle Selection based on Facial Surface EMG Signals." In *2015 Institute of Electronics and Information Engineers Summer Conference, (IEIE 2015)*, pp.933-936, Jun. 2015, *Oral Presentation*.

- <u>**Miran Lee**</u>, Jaehwan Ryu, and Deok-Hwan Kim. **2015**. "EMG Signal based Gait Phase Recognition using Feature Selection Adaptive to Muscles for Stairs Ascending and Stairs Descending." In *2015 Institute of Electronics and Information Engineers Summer Conference, (IEIE 2015)*, pp.586-589, Nov. 2015, *Oral Presentation*.

- <u>**Miran Lee**</u>, Jaehwan Ryu, and Deok-Hwan Kim. **2014**. "EMG Signal based Gait Phase Recognition using Feature Selection Adaptive to Muscles for Stairs

Ascending and Stairs Descending." In *2014 Institute of Electronics and Information Engineers Summer Conference, (IEIE 2014)*, pp.1061-1064, Jun. 2014, *Oral Presentation*.

- Sang-Ho Kim, Jaehwan Ryu, **Miran Lee**, and Deok-Hwan Kim. **2014**. "Human Identification based on Gait Cycle using EMG signal." In *2014 Institute of Electronics and Information Engineers Summer Conference, (IEIE 2014)*, pp.592-594, Jun. 2014, *Oral Presentation*.

- Jaehwan Ryu, Sang-Ho Kim, **Miran Lee**, and Deok-Hwan Kim. **2015**. "User adaptive classification based on sEMG and signal Gait phase prediction using linear interpolation." In *2014 Rehabilitation Engineering And Assistive Technology Society of Korea, (RESKO 2014)*, pp.337-340, Nov. 2014, *Oral Presentation*.

Patent

- (*South Korea*) "Method and Apparatus for EOG-Based Eye Tracking Protocol using Baseline Drift Removal Algorithm for Long-term Eye Movement Detection." **2021**, KR Patent, *Registration (Not determined yet)*.

- (*South Korea*) "Method and Apparatus for Automatic Detection of Epileptic Seizure Waveform based on Feature Extraction with Probabilistic Model and Machine Learning using Coefficient in Multi-frequency Bands from Electroencephalogram Signals." **2021**, KR Patent, *Registration (10-2256313)*.

- (*United States*) "Internet of Things-based Trespassing Situations Analysis System for Smart Security Window." **2020**, US Patent, *Registration (10,769,905 B2)*.

- (*South Korea*) "System for the Assessment of Lower Limb Activity and the Personalized Electrical Stimulation using Surface Electromyography and Motion Signals." **2020**, KR Patent, *Registration (10-2147099)*.

- (*South Korea*) "Method for Detecting R-peak of Electrocardiogram in Mobile Environment and System for Implementing The Same." **2020**, KR Patent, *Registration (10-2165205).*

- (*South Korea*) "A System of Detecting Epileptic Seizure Waveform based on Co-efficient in Multi-Frequency Bands from Electroencephalogram Signals, using Feature Extraction Method with Probabilistic Model and Machine Learning." **2020**, KR Patent, *Registration (10-2141185).*

- (*South Korea*) "Internet of Things-based Trespassing Situations Analysis System for Smart Security Window." **2019**, KR Patent, *Registration (10-1966198).*

- (*South Korea*) "Method of Monitoring Stress using Heart Rate Variability Parameter Selection in Daily Life." **2019**, KR Patent, *Registration (10-1998114).*

- (*South Korea*) "Method for Analyzing Stress using Biological and Exercising Signals." **2019**, KR Patent, *Registration (10-2053329).*

- (*South Korea*) "Method and Device for The Measurement of Energy." **2018**, KR Patent, *Registration (10-1870630).*

- (*South Korea*) "An EMG Signal-based Gait Phase Recognition Method using Feature Selection Adaptive to Muscles for Stairs Ascending and Stairs Descending." **2017**, KR Patent, *Registration (10-1705075).*

- (*South Korea*) "A Gait Phase Recognition Method based on EMG Signal for Stairs Ascending and Stairs Descending." **2017**, KR Patent, *Registration (10-1705082).*

Workshop

- [α] **Miran Lee**, Hirotake Yamazoe, and Joo-Ho Lee. **2019**. "Development and Quantitative Assessment of an Elbow Joint Robot for Elderly Care Training." *The Workshop on Machine Perception and Robotics (MPR 2019), Ritsuemikan University, Shiga, Japan*, Nov. 2019.

Appendix A. Financial support

Appendix B. Research ethical approval

All experiments for this dissertation were approved by the Institutional Review Board (IRB) at Ritsumeikan University.

1. BKC-2018-059

- 介護技術の定量的評価のための要介護者模擬ロボットの開発とそれを用いた学習支援

- BKC-人医-2018-059

- 2019/02/21-2021/12/31

2. BKC-2019-060

- 介護技術の定量的評価のための要介護者模擬ロボットの開発に向けた顔表情変化の研究

- BKC-人医-2019-060

- 2020/05/26-2022/12/31

Appendix C. Informed consent

In the experiment of this dissertation, all of participants agreed to participate by signing a consent form, while researchers observed to ensure their safety.

Further, some informed consent forms have been submitted to each university and institute to use the public databases.

- Among the subjects who participated in the experiments for this dissertation, several individuals have provided written consent to publish his/her likeness.

- To use the UNBC McMaster database[1] for research purposes in this thesis, an end-user license agreement, including portrait approval, has been submitted to the Affect Analysis Group at Pittsburgh[2].

- To use the AKDEF[3] and KDEF databases[4] for research purposes in this dissertation, the terms of use have been submitted to the KDEF website[5].

---

[1] Lucey, P., Cohn, J. F., Prkachin, K. M., Solomon, P. E., Matthews, I. (2011). Painful data: The UNBC-McMaster shoulder pain expression archive database. In 2011 IEEE International Conference on Automatic Face & Gesture Recognition, pp.57-64.

[2] http://www.jeffcohn.net/Resources/.

[3] Lundqvist, D., & Litton, J. E. (1998). The Averaged Karolinska Directed Emotional Faces-AKDEF, CD ROM from Department of Clinical Neuroscience, Psychology section, Karolinska Institutet, ISBN 91-630-7164-9.

[4] Lundqvist, D., Flykt, A., & Öhman, A. (1998). The Karolinska Directed Emotional Faces-KDEF, CD ROM from Department of Clinical Neuroscience, Psychology section, Karolinska Institutet, ISBN 91-630-7164-9.

[5] https://kdef.se/index.html.

Appendix D. Permission to reprint

Permission to reprint, from [*Mouri et al*., Development of robot hand for therapist education/training on rehabilitation, 2007 IEEE/RSJ International Conference on Intelligent Robots and Systems, and 10/2017 of publication]

Permission to reprint, from [*Fujisawa et al.*, Basic Research on the Upper Limb Patient Simulator, 2007 IEEE 10th International Conference on Rehabilitation Robotics, and 06/2017 of publication]

Permission to reprint, from [*Lee et al.*, Necessity and feasibility of care training assistant robot (CaTARo) as shoulder complex joint with multi-DOF in elderly care education, ROBOMECH Journal, and 03/2020 of publication]

Permission to reprint, from [*Lee et al*., Development and quantitative assessment of an elbow joint robot for elderly care training, Intelligent Service Robotics, and 07/2019 of publication]

Permission to reprint, from [*Bakker et al.*, Pleasure, Arousal, Dominance: Mehrabian and Russell revisited, Current Psychology, and 06/2014 of publication]